Investigating Holography: Traversable Wormholes and Closed Universes

SEAMUS FALLOWS

Investigating Holography: Traversable Wormholes and Closed Universes

Seamus Fallows

A Thesis presented for the degree of
Doctor of Philosophy

Centre for Particle Theory
Department of Mathematical Sciences
Durham University
United Kingdom

December 2022

Investigating Holography: Traversable Wormholes and Closed Universes

Seamus Fallows

Submitted for the degree of Doctor of Philosophy

December 2022

Abstract: In this thesis we study three recent and overlapping developments in the subject of holography: traversable wormholes, quantum extremal islands, and holographic models of closed universes.

We construct a traversable wormhole from a charged AdS black hole by adding a coupling between the two boundary theories. We investigate how the effect of this deformation behaves in the extremal limit of the black hole and show that under certain conditions the wormhole can be made traversable even in the extremal limit.

Next, we use braneworlds in three-dimensional multiboundary wormhole geometries as a model to study the appearance of entanglement islands when a closed universe with gravity is entangled with two non-gravitating quantum systems. We show that the entropy of the mixed state in the closed universe is bounded by half of the coarse-grained entropy of the effective theory on the braneworld.

For large values of the tension T, the worldvolume of a constant-tension brane inside a Schwarzschild-AdS$_{d+1}$ black hole is a closed FRW cosmology. However, for $d > 2$, having a smooth Euclidean solution where the brane does not self-intersect limits the brane tension to $T < T_*$, preventing us from realising a separation of scales between the brane and bulk curvature scales. We show that adding interface branes to this model does not relax the condition on the brane tension.

Declaration

The work in this thesis is based on research carried out in the Department of Mathematical Sciences at Durham University. The results are based on the following collaborative works:

- S. Fallows, S. F. Ross, *Making near-extremal wormholes traversable*, *JHEP* **12** (2020) 044 [2008.07946].
- S. Fallows, S. F. Ross, *Islands and mixed states in closed universes*, *JHEP* **07** (2021) 022 [2103.14364].
- S. Fallows, S. F. Ross, *Constraints on cosmologies inside black holes*, *JHEP* **05** (2022) 094 [2203.02523].

No part of this thesis has been submitted elsewhere for any degree or qualification.

Acknowledgements

First and foremost, I would like to thank my supervisor Prof. Simon Ross. Simon's breadth and depth of knowledge of physics is inspiring; the ability to throw basically any question at him and immediately receive a comprehensive and insightful answer has been a great academic privilege. Most importantly though, I feel incredibly lucky to have had such a kind and supportive supervisor as Simon. I wouldn't have made it through this PhD were it not for his continued patience and encouragement.

I would like to thank my Mum for buying me a microscope when I was a child and telling me that I should become a scientist when I wanted to be a 'daredevil'. Thank you Emily for helping me become the person I am today and Naomi for everything you've done for me.

Finally, thank you Nia for supporting me through such a difficult time in my life and giving me reason to be happy.

Contents

Chapter 1

Introduction

Holography is the idea that gravitational physics, in some sense, is massively redundant; a gravitational theory in $(d+1)$ dimensions can be exactly described by a non-gravitational theory in d dimensions. The idea that gravity is holographic was first inspired by the study of black holes. The Bekenstein-Hawking formula says that the entropy of a black hole is proportional to its area,

$$S_{\mathrm{BH}} = \frac{A_{\mathrm{hor}}}{4G_N}. \tag{1.0.1}$$

This is surprising, since if we think of entropy as counting the number of microstates of a system, we would expect this to scale with the volume of the system, not its area. What's more, as argued by Bekenstein, this is an upper bound on the entropy of a physical system. The maximum entropy associated with a given volume is that of a black hole with the same volume. Thus, the true number of microstates of any physical system should not scale more than with the area of a surface bounding it. Susskind [1] and 't Hooft [2] were the first to articulate these ideas as a general feature of quantum gravity.

Over the past few decades, it has become increasingly apparent that holography will be a crucial principle for developing a complete understanding of quantum gravity. In fact, holography in its most concrete realization as the AdS/CFT correspondence provides the only precise, non-perturbative definition of quantum gravity

that we know of [3–6]. The AdS/CFT correspondence is a truly remarkable discovery. Not only does it represent our best attempt at a theory of quantum gravity, the strong/weak nature of the duality also gives us a powerful tool to investigate strongly-coupled quantum field theories.

Perhaps one of the most important lessons to come from AdS/CFT is the extent to which quantum entanglement and classical spacetime geometry are fundamentally related. Starting with the Ryu-Takayanagi formula [7], we learned that the geometry of asymptotically AdS spacetimes can be encoded in the entanglement structure of certain quantum field theories. The Ryu-Takayanagi formula and its subsequent generalizations later inspired the ideas of subregion-subregion duality, the notion that a spatial subregion A in the boundary theory contains complete information about some subregion of the bulk [8,9]; entanglement wedge reconstruction, which says that this bulk region is the entire entanglement wedge of A [10]; and the quantum error correcting code interpretation of AdS/CFT, which says that the boundary encoding of the bulk physics can be understood as a quantum error correcting code that is robust against erasure errors in the boundary [11].

Recent developments have again highlighted the role of entanglement in understanding gravity [12–40]. These include traversable wormholes and quantum extremal islands, two topics that we will investigate in this thesis. Traversable wormholes provide a new insight into the relation between entanglement and spacetime in holographic theories: the passage of a bulk observer through the wormhole can be understood as quantum teleportation in the dual theory, using the entanglement of the dual state as a resource and using the coupling to communicate the needed classical information from one theory to the other. The discovery of quantum extremal islands [23–25], which arise when a quantum system is entangled with a gravitational system, has allowed us to tackle the black hole information loss paradox and explicitly show that the entropy of radiation of evaporating black holes follows the Page curve [41, 42].

In this section we will review the background material that motivates and un-

derpins the later work in this thesis. We will introduce the key concepts of the AdS/CFT correspondence, covering the relation between bulk and boundary operators, thermofield double states as the dual of charged and uncharged black holes, the connection between entanglement and geometry through the various holographic entanglement entropy formulas, and the dual interpretation of BCFTs as asymptotically AdS geometries terminating on dynamical branes. We will also review the recently discovered *island rule* as a method for calculating the entropy of radiation of an evaporating black hole.

In chapter 2, we extend the work of [12] to construct a traversable wormhole from a charged AdS black hole by adding a coupling between the two boundary theories. We investigate how the effect of this deformation behaves in the extremal limit of the black hole. The black holes have finite entropy but an infinitely long throat in the extremal limit. We argue that it is still possible to make the throat traversable even in the extremal limit, but this requires either tuning the field for which we add a boundary coupling close to an instability threshold or scaling the strength of the coupling inversely with the temperature. In the latter case we show that the amount of information that can be sent through the wormhole scales with the entropy.

In chapter 3, we investigate the appearance of islands when a closed universe with gravity is entangled with a non-gravitating quantum system. We use braneworlds in three-dimensional multiboundary wormhole geometries as a model to explore what happens when the non-gravitating system has several components. The braneworld can be either completely contained in the entanglement wedge of one of the non-gravitating systems or split between them. In the former case, entanglement with the other system leads to a mixed state in the closed universe, unlike in simpler setups with a single quantum system, where the closed universe was necessarily in a pure state. We show that the entropy of this mixed state is bounded by half of the coarse-grained entropy of the effective theory on the braneworld.

In chapter 4, we study an approach proposed in [43] (and further developed in [44–47]) to understand closed universes with big-bang/big-crunch cosmologies

holographically. This construction comprises an asymptotically AdS_{d+1} black hole spacetime with a co-dimension one, constant-tension, dynamical end of the world brane behind the horizon. The brane worldvolume is a closed FRW spacetime. In $d = 2$ dimensions, the brane can be taken close to the conformal boundary by increasing the tension, producing an effective closed cosmology on the braneworld. However, in dimensions $d > 2$, having a smooth Euclidean solution where the brane does not self-intersect limits the brane tension to $T < T_*$, preventing us from realising a separation of scales between the brane and bulk curvature scales. We investigate a solution to the self-intersection problem suggested by [47] in which an interface brane is introduced to the spacetime; the idea being that this might allow the end of the world brane to be multiply wound on one side of the interface brane relative to the original spacetime. We find that this does not resolve the self-intersection problem. The brane tension cannot be taken greater than T_* without the two branes colliding with each other.

1.1 The AdS/CFT correspondence

The AdS/CFT correspondence is a conjecture that any theory of quantum gravity that is asymptotically Anti-de Sitter is equivalent to a conformal field theory living on its conformal boundary[1]. The first example of this correspondence was discovered by Maldacena in the context of string theory [3], who demonstrated an equivalence between type IIB supergravity, the classical limit of type IIB string theory, on $\mathrm{AdS}_5 \times S^5$ and a particular limit of $\mathcal{N} = 4$ super Yang-Mills (SYM) on $\mathbb{R} \times S^3$ with an $\mathrm{SU}(N)$ gauge group. The free parameters of the two theories are related via:

$$g_{\mathrm{YM}}^2 = 4\pi g_s, \qquad g_{\mathrm{YM}}^2 N = \left(\frac{\ell}{\ell_s}\right)^4, \tag{1.1.1}$$

where g_{YM} is the Yang-Mills coupling, N is the rank of the gauge group, g_s is the string coupling, ℓ_s is the string length, and ℓ is the AdS radius. The quantity $\lambda \equiv g_{\mathrm{YM}}^2 N$ is

[1] We will often omit the word 'conformal' and simply refer to the 'boundary'.

called the *'t Hooft coupling*. The classical supergravity limit corresponds to taking $g_s \ll 1$ and $\ell/\ell_s \gg 1$ in which quantum gravitational and stringy corrections can be neglected. From (1.1.1), this translates to the following limit in the boundary theory

$$N \gg \lambda \gg 1. \tag{1.1.2}$$

This is an example of a strong/weak duality: when the field theory is strongly coupled (large λ) and has many degrees of freedom (large N), it is fully described by classical general relativity. The large N limit, with fixed λ, is a special case in which the structure of the perturbative expansion of the boundary theory simplifies; non-planar diagrams are suppressed and the sub-dominant diagrams arrange according to their topology.

While the correspondence was first discovered in a particular limiting case, the modern view is that it should hold for all possible values of the parameters of the theory. There should exist a mapping between any statement in the bulk to a corresponding statement in the boundary. This is referred to as the AdS/CFT dictionary. The most basic way to view the duality is as an isomorphism of Hilbert spaces $\mathcal{H}_{\text{bulk}} \cong \mathcal{H}_{\text{CFT}}$ and operator algebras $\mathscr{A}_{\text{bulk}} \cong \mathscr{A}_{\text{CFT}}$. In particular, the spectrum of the Hamiltonian is the same on both sides, and the states decompose into the same irreducible representations of $\mathrm{SO}(d,2)$. The conformal symmetry of the CFT_d corresponds to the asymptotic isometry group of AdS_{d+1}.

A particularly useful formulation of AdS/CFT is in terms of the bulk and boundary partition functions. For a theory of quantum gravity with a set of fields Φ_a (including the metric) on an asymptotically $\mathrm{AdS}_{d+1} \times \mathcal{C}$ manifold $\mathcal{M}$, with $\mathcal{C}$ some (possibly trivial) compact manifold, dual to a CFT on the conformal boundary $\partial\mathcal{M}$, we have

$$Z_{\text{bulk}}\left[\lim_{r\to\infty} r^{\Delta_a - d}\Phi_a(r,x) = J_a(x)\right] = Z_{\text{CFT}}[J_a] \tag{1.1.3}$$

$$= \left\langle \exp i \int_{\partial\mathcal{M}} \mathrm{d}^d x \sum_a J_a(x)\mathcal{O}_a(x) \right\rangle_{\text{CFT}}, \tag{1.1.4}$$

where Δ_a is the scaling dimension of the CFT primary operator $\mathcal{O}_a$ and r is an asymptotically AdS radial coordinate. This says that the boundary values of the bulk fields, once stripped of a divergent r-dependant factor, are identified with sources that couple to dual boundary operators. The left side of (1.1.3) is meant to represent the complete quantum-gravitational partition function (of course this is not something we know how to independently define). Without knowing the full partition function it is useful to work in the leading saddlepoint approximation, corresponding to a large-N limit in the CFT, where this relation becomes

$$iS_{\text{bulk}}\left[\Phi_a^{\text{c}}\right] = \ln Z_{\text{CFT}}[J_a]. \tag{1.1.5}$$

The left-hand-side is the classical gravitational action[1] evaluated on solutions to the classical equations of motion Φ_a^{c}.

To provide some motivation for the form of (1.1.3) and give an illustration as to how the correspondence can be applied, we will consider a free scalar field $\phi(z, x)$ of mass m propagating on a fixed AdS_{d+1} background $\mathcal{M}$. The action is given by

$$S = -\frac{1}{2}\int_{\mathcal{M}} \mathrm{d}^{d+1}x\sqrt{-g}\left(g^{\mu\nu}\partial_\mu\phi\partial_\nu\phi + m^2\phi^2\right), \tag{1.1.6}$$

where $g_{\mu\nu}$ is the AdS_{d+1} metric. From this we get the equation of motion

$$\left(\nabla^2 - m^2\right)\phi = \frac{1}{\sqrt{-g}}\partial_\mu(\sqrt{-g}g^{\mu\nu}\partial_\nu\phi) - m^2\phi = 0. \tag{1.1.7}$$

We use coordinates that put the metric into the form

$$\mathrm{d}s^2 = \frac{\ell^2}{z^2}(\mathrm{d}z^2 + \eta_{ab}\mathrm{d}x^a\mathrm{d}x^b) \tag{1.1.8}$$

where η_{ab} is the d-dimensional Minkowski metric, with $x^a \in \mathbb{R}^d$, $z \in (0, \infty)$. These coordinates cover a subset of AdS known as the *Poincaré patch*. The asymptotic boundary of the Poincaré patch is at $z \to 0$, and has topology $\mathbb{R}^d$. The induced metric on a constant z-slice is just an overall constant times η_{ab}, so the conformal boundary is d-dimensional Minkowski space. In Poincaré coordinates the equation

[1] Both quantum and stringy corrections are neglected.

of motion becomes

$$\left(z^2\partial_z^2 - (d-1)z\partial_z + z^2\partial^a\partial_a + m^2\ell^2\right)\phi = 0. \tag{1.1.9}$$

We want to investigate the asymptotic $z \to 0$ behaviour of the solutions; choosing a separable ansatz $\phi(z,x) = z^\Delta\phi(x)$ and dropping subleading terms, we get two independent near-boundary solutions

$$\phi(z,x) \sim (\phi_+(x) + \mathcal{O}(z^2))z^{\Delta_+} + (\phi_-(x) + \mathcal{O}(z^2))z^{\Delta_-}, \tag{1.1.10}$$

with the exponents given by

$$\Delta_\pm = \frac{d}{2} \pm \sqrt{\frac{d^2}{4} + m^2\ell^2} \equiv \frac{d}{2} \pm \nu. \tag{1.1.11}$$

In Minkowski space we would require a positive mass squared term, $m^2 \geq 0$, for stability of the vacuum. In AdS, however, it is possible to have a stable vacuum with $m^2 < 0$ provided it is no less than the *Breitenlohner-Freedman (BF) bound*[1],

$$m^2\ell^2 \geq -\frac{d^2}{4}. \tag{1.1.12}$$

This is because the total energy receives a positive contribution from the kinetic term which compensates for the negative contribution from the mass term. As a result, the total energy can be positive. Going forward, we assume the BF bound is not saturated, $m^2 > m^2_{\mathrm{BF}}$. The modes $\phi_\pm(x)z^{\Delta_\pm}$ can be classified according to an appropriate norm on the solution space. A natural inner product for solutions of the Klein-Gordon equation in curved space is given by

$$(\phi_1,\phi_2)_{\mathrm{KG}} \equiv \frac{i}{2}\int_\Sigma \mathrm{d}^d x\sqrt{h}n^\mu\left(\phi_1^*\partial_\mu\phi_2 - \phi_2\partial_\mu\phi_1^*\right), \tag{1.1.13}$$

where Σ is a spacelike surface, which we will take to be a surface of constant t and n^μ is the past-pointing unit normal to Σ. Evaluating the norm defined by this inner product on a solution with asymptotic behaviour $\phi(z,x) \sim \phi(x)z^\Delta$, we see that the

[1]Saturating the BF bound corresponds to the degenerate case $\Delta_+ = \Delta_- = d/2$ in which the asymptotic solution (1.1.10) contains a logarithmic term $\phi(z,x) \sim \phi_{\mathrm{BF}}(x)z^{d/2}\ln\mu z$, where μ is some scale required to define the logarithm.

integrand behaves near $z = 0$ as

$$\sqrt{h}\sqrt{g^{tt}}\phi\partial_t\phi \sim z^{2\Delta-d+1}, \tag{1.1.14}$$

which leads to a convergent integral if $2\Delta - d + 2 > 0$. For the subleading mode, with $\Delta = \Delta_+$, this condition becomes $\nu + 1 > 0$, which is always satisfied. This mode is always normalizable and upon quantization defines a state in the bulk Hilbert space; in accordance with AdS/CFT, this corresponds to a state in the boundary theory. The leading mode, with $\Delta = \Delta_-$, is non-normalizable for $\nu \geq 1$ or equivalently $m^2 \geq m^2_{\text{BF}} + 1/\ell^2$. Non-normalizable modes are not elements of the bulk Hilbert space. Instead, as we will further justify, they correspond to sources in the boundary theory. Interestingly, for masses in the range $m^2_{\text{BF}} \leq m^2 < m^2_{\text{BF}} + 1/\ell^2$ both modes are normalizable and give rise to different bulk Hilbert spaces dual to physically different boundary theories.

AdS is not globally hyperbolic; the equation of motion plus initial data on a Cauchy surface do not uniquely specify the evolution of $\phi(z, x)$. In order to have well-defined dynamics we need to impose boundary conditions at $z \to 0$[1]. We will consider the standard boundary conditions given by fixing the leading mode $\phi_-(x)$ to be some fixed function on the boundary

$$\phi_-(x) = J(x), \qquad \text{for } x \in \partial\mathcal{M} \tag{1.1.15}$$

Let us consider the following bulk isometry

$$D : (z, x^a) \to (\lambda z, \lambda x^a)\,, \tag{1.1.16}$$

which reduces to a dilatation on the boundary

$$D|_{\partial\mathcal{M}} : x^a \to \lambda x^a. \tag{1.1.17}$$

Since $\phi(z, x)$ is a coordinate scalar, under this isometry $\phi_-(x)$ and $\phi_+(x)$ must scale

[1]One way to see this is that a null ray can leave the centre of AdS at $z = \infty$ and reach the asymptotic boundary $z = 0$ in a finite proper time for a timelike observer at the centre.

so as to cancel the transformations of z^{Δ_-} and z^{Δ_+}. This implies that under the induced dilatation in the boundary, $\phi_-(x) = J(x)$ and $\phi_+(x)$ transform as objects with scaling dimensions Δ_- and Δ_+, respectively. Notice, $\Delta_- = d - \Delta_+$ is the correct dimension of a source J to couple to an operator of dimension Δ_+ in d dimensions, in agreement with (1.1.3) (the two radial coordinates are related near the boundary via $z = 1/r$).

The full bulk field $\phi(z, x)$ can be constructed from the boundary configuration $\phi_-(x)$ via a Greens function solution [4, 5, 48], so that

$$\phi(z, x) = \int \mathrm{d}^d x' K_{\Delta_+}(z, x, x')\phi_-(x'). \tag{1.1.18}$$

The bulk-to-boundary propagator $K_{\Delta_+}(z, x, x')$ is defined such that it satisfies the bulk equation of motion in the unprimed arguments and its leading behaviour near the boundary is a delta function,

$$(\nabla^2 - m^2)K_{\Delta_+}(z, x, x') = 0, \qquad \lim_{z\to 0} z^{-\Delta_-} K_{\Delta_+}(z, x, x') = -i\delta^d(x - x'). \tag{1.1.19}$$

It is given by[1]

$$K_{\Delta_+}(z, x, x') = C_{\Delta_+}\left(\frac{z}{z^2 + (x - x')^2}\right)^{\Delta_+}, \qquad C_{\Delta_+} = \frac{\Gamma(\Delta_+)}{\pi^{\frac{d}{2}}\Gamma(\Delta_+ - d/2)}. \tag{1.1.20}$$

Expanding the solution (1.1.18) near $z = 0$, we find the subleading mode $\phi_+(x)$ as a functional of the leading mode $\phi_-(x)$:

$$\phi_+(x) = C_{\Delta_+} \int \mathrm{d}^d x' \frac{\phi_-(x')}{|x - x'|^{2\Delta_+}}. \tag{1.1.21}$$

A non-trivial test of the AdS/CFT dictionary is that it can be used to generate CFT correlation functions from an entirely bulk calculation. However, in order to do this we must first address an apparent problem with the saddlepoint formulation in (1.1.5): the bulk on-shell action is divergent. To see how this happens, we introduce a regulator in the form of a radial cutoff $z = \varepsilon \ll \ell$. Integrating the action by parts,

[1] Since we are in Lorentzian signature, the bulk-to-boundary propagator carries an implicit epsilon prescription for avoiding the lightcone pole: $(t - t')^2 \to (t - t')^2 - i\epsilon$.

we get

$$S = \frac{1}{2}\int_{z\geq\varepsilon} \mathrm{d}^{d+1}x\sqrt{-g}\phi\left(\nabla^2 - m^2\right)\phi - \frac{1}{2}\int_{z=\varepsilon}\mathrm{d}^d x\sqrt{-h}\phi n^\mu\partial_\mu\phi, \tag{1.1.22}$$

where h_{ab} is the induced metric, and n^μ is the outward pointing unit normal to the surface. The first term vanishes on-shell, $\phi = \phi_\mathrm{c}$, but plugging in the asymptotic solution, and using $\sqrt{-h} = (\ell/z)^d$, $n^\mu\partial_\mu = -(z/\ell)\partial_z$, the second term gives

$$S[\phi_\mathrm{c}] = \frac{\ell^{d-1}}{2}\int \mathrm{d}^d x\left(\Delta_-\phi_-^2\varepsilon^{-2\nu} + d\phi_-\phi_+ + \Delta_+\phi_+^2\varepsilon^{2\nu}\right). \tag{1.1.23}$$

The first term is singular in the limit $\varepsilon \to 0$. While this might seem initially concerning, the appearance of a near-boundary divergence in the action is actually to be expected; radial transformations in the bulk are associated with scale transformations in the CFT, so this small z (large r) divergence is just the bulk-manifestation of the short-distance, ultraviolet divergence of the boundary field theory. The action can be renormalised by introducing suitable counterterms such that the action is finite on shell and stationary under variations that preserve the boundary conditions. This procedure is known as *holographic renormalisation*. In our case, this is achieved by the renormalised action [49]:

$$S_\mathrm{re} = S - \frac{\Delta_-}{2\ell}\int_{\partial\mathcal{M}}\mathrm{d}^d x\sqrt{-h}\phi^2. \tag{1.1.24}$$

Evaluated on-shell, the divergence of this new boundary term cancels the divergence from the bulk action, leaving the finite result:

$$S_\mathrm{re}[\phi_\mathrm{c}] = \nu\ell^{d-1}\int_{\partial\mathcal{M}}\mathrm{d}^d x\,\phi_-\phi_+. \tag{1.1.25}$$

Now consider varying the field $\phi \to \phi + \delta\phi$, which induces variations $\delta\phi_-$ and $\delta\phi_+$. The variation of the renormalised action is given by

$$\delta S_\mathrm{re}[\phi_\mathrm{c}] = \int_{\mathcal{M}}\mathrm{d}^{d+1}x\sqrt{-g}\left(\nabla^2\phi_\mathrm{c} - m^2\phi_\mathrm{c}\right)\delta\phi + 2\nu\ell^{d-1}\int_{\partial\mathcal{M}}\mathrm{d}^d x\,\delta\phi_-\phi_+, \tag{1.1.26}$$

which vanishes when ϕ_- is fixed on the boundary, as in boundary condition (1.1.15), so S_re does indeed satisfy the conditions required of it.

We can now calculate correlation functions for the CFT primary $\mathcal{O}$ dual to ϕ. In the presence of a source J, the one-point function can be defined as the functional derivative of the CFT partition function with respect to the source,

$$\langle \mathcal{O}(x) \rangle_J = \frac{1}{i} \frac{\delta}{\delta J(x)} \ln Z_{\mathrm{CFT}}[J]. \tag{1.1.27}$$

Using the correspondence (1.1.3) this is equivalent to

$$\begin{aligned} \langle \mathcal{O}(x) \rangle_J = \left. \frac{\delta S_{\mathrm{re}}[\phi_{\mathrm{c}}]}{\delta \phi_-(x)} \right|_{\phi_-=J} &= 2\nu \ell^{d-1} \phi_+(x) \\ &= 2\nu C_{\Delta_+} \ell^{d-1} \int \mathrm{d}^d x' \frac{J(x')}{|x-x'|^{2\Delta_+}}. \end{aligned} \tag{1.1.28}$$

This tells us that, just as the leading term ϕ_- corresponds to the source for the dual operator, the subleading term ϕ_+ corresponds to its expectation value; it is the response to turning on the leading mode. Setting the source $J = 0$, gives us a bulk derivation of the simple fact that CFT one-point functions vanish

$$\langle \mathcal{O}(x) \rangle = 0. \tag{1.1.29}$$

Taking two derivatives, we get the two-point function

$$\langle \mathcal{O}(x_1) \mathcal{O}(x_2) \rangle = -i \left. \frac{\delta S_{\mathrm{re}}[\phi_{\mathrm{c}}]}{\delta \phi_-(x_1) \delta \phi_-(x_2)} \right|_{\phi_-=0} = \frac{-2i\nu C_{\Delta_+} \ell^{d-1}}{|x_1 - x_2|^{2\Delta_+}}, \tag{1.1.30}$$

in agreement with the standard CFT result derived via symmetry considerations. Likewise, considering an interaction term of the form $\lambda_n \phi^n$ in the bulk action, one can calculate connected n-point CFT correlation functions,

$$\langle \mathcal{O}(x_1) \dots \mathcal{O}(x_n) \rangle = (-i)^{n-1} \left. \frac{\delta S_{\mathrm{re}}[\phi_{\mathrm{c}}]}{\delta \phi_-(x_1) \dots \delta \phi_-(x_n)} \right|_{\phi_-=0}. \tag{1.1.31}$$

Bulk duals for operators with scaling dimensions as small as $\Delta = d/2$ can be found by taking m^2 down to the BF bound. Generically, CFTs can have operators with scaling dimensions as small as the unitary bound $\Delta \geq d/2 - 1$. It turns out that these operators can also be realized from the bulk dual. As mentioned previously,

for the restricted range of m^2,

$$m^2_{\rm BF} < m^2 \leq m^2_{\rm BF} + 1, \tag{1.1.32}$$

both asymptotic modes are normalizable, so different boundary conditions can be chosen such that $\phi_+(x) = J(x)$ and $\phi_-(x)$ is dynamical. This is known as the *alternate* boundary condition and requires altering the holographic counterterm. The alternate action is given by

$$S_{\rm alt} = S + \int_{\partial\mathcal{M}} d^dx\sqrt{-h}\,\phi\left(n^\mu\partial_\mu + \frac{\Delta_+}{2\ell}\right)\phi. \tag{1.1.33}$$

With alternate boundary conditions, the one-point function in the presence of a source is given by

$$\langle\mathcal{O}_{\rm alt}(x)\rangle_J = \left.\frac{\delta S_{\rm alt}}{\delta\phi_+(x)}\right|_{\beta=J} = -2\nu\ell^{d-1}\phi_-(x). \tag{1.1.34}$$

Thus, the dual operator $\mathcal{O}_{\rm alt}$ has scaling dimension Δ_-, which hits the unitary bound at $m^2 = m^2_{\rm BF} + 1$.

1.1.1 Mixed states and entanglement

Before jumping into a discussion of black holes and their holographic dual states, it will be useful to give a recap of mixed states and entanglement. Entanglement is one of the primary features distinguishing quantum from classical mechanics and is an incredibly important concept in holography; it has deep connections to the emergence of classical gravitational spacetime and is central to the black hole information paradox. This section largely draws from [50] (see also [51–53]).

Consider a Hilbert space $\mathcal{H}$ for a system which can be decomposed into a subsystem A and its complement $\bar{A}$ as

$$\mathcal{H} = \mathcal{H}_A \otimes \mathcal{H}_{\bar{A}}. \tag{1.1.35}$$

Given a state $|\Psi\rangle \in \mathcal{H}$ of the full system, it is natural to ask if there exists a state $|\psi_A\rangle \in \mathcal{H}_A$ that fully describes the subsystem A. More precisely, is there a state

$|\psi_A\rangle \in \mathcal{H}_A$ such that for all operators $\mathcal{O}_A \in \mathrm{End}(\mathcal{H}_A)$ acting only on $\mathcal{H}_A$ we have

$$\langle\psi_A|\mathcal{O}_A|\psi_A\rangle = \langle\Psi|\mathcal{O}_A \otimes \mathbb{I}_{\bar{A}}|\Psi\rangle? \tag{1.1.36}$$

The answer of course for general $|\Psi\rangle$ is no; the state $|\Psi\rangle$ is said to be entangled when (1.1.36) fails to hold.

To properly formulate a theory of quantum mechanical subsystems, one needs to introduce the idea of ensembles of states, otherwise known as *mixed states*. An ensemble $\{|\psi^i\rangle, p_i\}$ is a collection of orthogonal states and associated probabilities. The ensemble expectation value of an operator $\mathcal{O}$ is defined as the sum of the expectation values for the individual states weighted by the associated probabilities,

$$\langle\mathcal{O}\rangle_{ensemble} \equiv \sum_i p_i \langle\psi^i|\mathcal{O}|\psi^i\rangle. \tag{1.1.37}$$

The probabilities can be thought of as representing some classical uncertainty about the state of the system.

For any state $|\Psi\rangle \in \mathcal{H}_A \otimes \mathcal{H}_{\bar{A}}$ describing a composite system, the *Schmidt decomposition theorem* says that there exist orthonormal states $|\psi^i_A\rangle \in \mathcal{H}_A$ and orthonormal states $|\psi^j_{\bar{A}}\rangle \in \mathcal{H}_{\bar{A}}$, such that

$$|\Psi\rangle = \sum_i \sqrt{p_i}|\psi^i_A\rangle \otimes |\psi^i_{\bar{A}}\rangle, \tag{1.1.38}$$

where p_i are positive real numbers satisfying $\sum_i p_i = 1$ [52]. Evaluating the expectation value of an operator $\mathcal{O}_A$ acting only on subsystem A gives

$$\langle\Psi|\mathcal{O}_A \otimes \mathbb{I}_{\bar{A}}|\Psi\rangle = \sum_{i,j} \sqrt{p_i p_j}\langle\psi^i_A|\mathcal{O}|\psi^j_A\rangle\langle\psi^i_{\bar{A}}|\psi^j_{\bar{A}}\rangle = \sum_i p_i \langle\psi^i_A|\mathcal{O}|\psi^i_A\rangle. \tag{1.1.39}$$

We see that subsystems are examples of ensembles. A convenient means for describing mixed states is in the language of density matrices. A density matrix is a unit trace, positive semi-definite operator. For a mixed state $\{p_i, |\psi^i\rangle\}$, the density matrix ρ is defined by

$$\rho \equiv \sum_i p_i |\psi^i\rangle\langle\psi^i|. \tag{1.1.40}$$

Alternatively, one can take any unit trace, positive semi-definite operator to define a mixed state by taking $|\psi^i\rangle$ and p_i to be the orthogonal eigenvectors and eigenvalues of the operator. The expectation value of an operator is calculated by taking the trace against the density matrix:

$$\langle \mathcal{O} \rangle = \mathrm{Tr}(\mathcal{O}\rho) = \sum_i p_i \langle \psi^i | \mathcal{O} | \psi^i \rangle. \tag{1.1.41}$$

For a pure state $|\Psi\rangle \in \mathcal{H}$, the density matrix is simply $\rho = |\Psi\rangle\langle\Psi|$. A subsystem A is described by the *reduced* density matrix ρ_A defined by taking the partial trace over the complement,

$$\rho_A \equiv \mathrm{Tr}_{\bar{A}}(\rho) = \mathrm{Tr}_{\bar{A}}(|\Psi\rangle\langle\Psi|) \tag{1.1.42}$$

It is straightforward to show that the reduced density matrix satisfies

$$\langle \Psi | \mathcal{O}_A \otimes \mathbb{I}_{\bar{A}} | \Psi \rangle = \mathrm{Tr}((\mathcal{O}_A \otimes \mathbb{I}_{\bar{A}})\rho) = \mathrm{Tr}(\mathcal{O}_A \rho_A). \tag{1.1.43}$$

The eigenvalues p_i of a reduced density matrix ρ_A tell us about the entanglement between the subsystems. The states are separable and have zero entanglement if there is only a single non-zero eigenvalue $p_i = 1$, and they are maximally entangled if all eigenvalues are equal $p_i = 1/\min(\dim \mathcal{H}_A, \dim \mathcal{H}_{\bar{A}})$. We can define a measure for the degree of entanglement of a subsystem as the von Neumann (fine-grained) entropy of its reduced state,

$$S(\rho_A) \equiv -\mathrm{Tr}(\rho_A \log \rho_A). \tag{1.1.44}$$

It quantifies our ignorance about the precise quantum state of the system. For a pure bipartite state $\rho \in \mathcal{H}_A \otimes \mathcal{H}_{\bar{A}}$, the von Neumann entanglement entropy is the same for both subsystems, $S(\rho_A) = S(\rho_{\bar{A}})$. This follows straightforwardly from the Schmidt decomposition theorem. Von Neumann entropy has a number of important properties, including:

- $S(\rho) \geq 0$, with equality if and only if ρ is pure.
- $S(\rho) \leq \log(\dim \mathcal{H})$ with equality if and only if ρ is maximally mixed.

- $S(U^\dagger \rho U) = S(\rho)$ for any unitary operator U.
- $S(\rho_1 \otimes \rho_2) = S(\rho_1) + S(\rho_2)$, i.e. S is additive for independent systems.
- For any set of non-negative numbers λ_i obeying $\sum_i \lambda_i = 1$,

$$S\left(\sum_i \lambda_i \rho_i\right) \geq \sum_i \lambda_i S(\rho_i). \tag{1.1.45}$$

It will also be useful to introduce the notion of *coarse-grained* entropy. Coarse-grained entropy applies to cases where only a subset of observables are considered. For a system described by a density matrix ρ, the coarse-grained entropy associated with a subset of observables $\mathscr{O}$ is given by maximising the von Neumann entropy over all possible density matrices $\tilde{\rho}$ that produce the same expectation values for all observables in $\mathscr{O}$,

$$S_{\text{coarse}}(\rho) \equiv \max_{\tilde{\rho}} \left\{ -\operatorname{Tr}(\tilde{\rho} \log \tilde{\rho}) \mid \operatorname{Tr}(\tilde{\rho}\mathcal{O}_i) = \operatorname{Tr}(\rho \mathcal{O}_i),\ \forall \mathcal{O}_i \in \mathscr{O} \right\}. \tag{1.1.46}$$

A simple example of this is ordinary thermodynamic entropy. Unlike fine-grained entropy, which is invariant under unitary time evolution, coarse-grained entropy tends to increase over time. A simple consequence of this definition is that fine-grained entropy cannot be larger than coarse-grained entropy.

1.1.2 The thermofield double

In the previous section we saw that a subsystem A of a pure states can be described by a density matrix ρ_A. However, it is often useful to consider the inverse: starting from a mixed state $\rho_A \in \text{End}(\mathcal{H}_A)$, one can construct an entangled pure state belonging to an enlarged Hilbert space $|\psi\rangle \in \mathcal{H}_A \otimes \mathcal{H}_B$ such that the expectation values of operators restricted to the original system reproduce the statistical predictions in the original mixed state. The auxiliary Hilbert space $\mathcal{H}_B$, whose dimension is at least as large as the number of non-zero eigenvalues of ρ_A, is said to *purify* the mixed state. In general there are an infinite number of purifications of any mixed state. For a density matrix $\rho_A = \sum_i p_i |\psi_A^i\rangle\langle\psi_A^i|$, a general purification can be written as a

Schmidt decomposition

$$|\Psi\rangle = \sum_i \sqrt{p_i}|\psi_A^i\rangle \otimes |\psi_B^i\rangle \tag{1.1.47}$$

where $|\psi_B^i\rangle$ are orthogonal states belonging to $\mathcal{H}_B$. A simple calculation shows that this reduces to the original mixed state when traced over $\mathcal{H}_B$.

In the context of holography and black hole physics, a particularly important ensemble to consider is the canonical ensemble or thermal state of a system in which a system A is weakly coupled to a heat bath $\bar{A}$. The ensemble can be defined by maximising the entropy subject to the constraint that the expectation value for the energy of the subsystem is constant,

$$\mathrm{Tr}(H_A\rho_A) = E. \tag{1.1.48}$$

In terms of the energy eigenstates $|E_i\rangle$ of H_A, the ensemble is $\{|E_i\rangle, p_i = e^{-\beta E_i}/Z\}$ where $Z = \mathrm{Tr}_A\, e^{-\beta H_A}$ is the thermal partition function of inverse temperature β.

In [54], Maldacena argued using the AdS/CFT correspondence that the maximally extended AdS-Schwarzschild black hole is dual to a particular entangled state belonging to a pair of identical non-interacting CFTs, $\mathrm{CFT}_L \cong \mathrm{CFT}_R$, which live on each of the two asymptotic boundaries of the spacetime. This state, known as the thermofield double (TFD), is a symmetric purification of the canonical ensemble so that restricted to either boundary CFT, expectation values of local operators are thermal with the same temperature β^{-1}, equal to the Hawking temperature of the black hole. More precisely, this duality applies to so-called *big* AdS black holes. These are black holes that have positive specific heat and are the dominant saddle point of the Euclidean gravitational path integral.

Let $\mathcal{H} \equiv \mathcal{H}_L \otimes \mathcal{H}_R$ denote the full Hilbert space of the joint system $\mathrm{CFT}_L \otimes \mathrm{CFT}_R$. We can define an antiunitary time-reversal operator $\Theta : \mathcal{H}_L \to \mathcal{H}_R$ that implements the isomorphism $\mathcal{H}_L \cong \mathcal{H}_R$, with the Hamiltonians of the two CFTs related by $H_R = \Theta H_L \Theta^\dagger$. In terms of the energy eigenbases $|E_i\rangle_L$ and $|\tilde{E}_i\rangle_R \equiv \Theta|E_i\rangle_L$, the

thermofield double state is defined as

$$|TFD\rangle \equiv \frac{1}{\sqrt{Z(\beta)}} \sum_i e^{-\beta E_i/2} |E_i\rangle_L \otimes |\tilde{E}_i\rangle_R, \tag{1.1.49}$$

where $Z(\beta)$ is the thermal partition function of one copy of the CFT at temperature β^{-1}. The density matrix corresponding to this pure state is

$$\begin{aligned} \rho &= |TFD\rangle\langle TFD| \\ &= \frac{1}{Z(\beta)} \sum_{ij} e^{-\beta(E_i+E_j)/2} |E_i\rangle_{LL}\langle E_j| \otimes |\tilde{E}_i\rangle_{RR}\langle \tilde{E}_j|. \end{aligned} \tag{1.1.50}$$

This gives a thermal state when reduced to either subsystem $\rho_L = \mathrm{Tr}_R\, \rho = e^{-\beta H_L}/Z$ (and likewise for ρ_R).

The TFD is a natural candidate for the dual of maximally extended Schwarzschild-AdS; the AdS/CFT dictionary suggests that the bulk spacetime, having two disconnected asymptotically AdS boundaries, should be dual to a state in two CFTs. The boundary CFTs should be non-interacting since the two exterior regions are causally disconnected. The bulk $\mathbb{Z}_2$ reflection symmetry which exchanges the two exterior regions implies that the dual state should be identical when restricted to either factor in the Hilbert space $\mathcal{H}_L \otimes \mathcal{H}_R$. Additionally, it is a universal feature of quantum fields on black hole backgrounds that equilibrium states are thermal. Up to the insertion of possible phases, the TFD is the unique state in the product space $\mathcal{H}_L \otimes \mathcal{H}_R$ that reduces to the thermal state of temperature β^{-1} on either factor. For a free scalar field propagating in a static spacetime with a bifurcate Killing horizon with a regular bifurcation surface, it has been shown that there is at most one quantum state that is Killing-time independent and regular everywhere on the horizon [55]. In the case of Schwarzschild-AdS, this state is the Hartle-Hawking state and can be constructed via a path integral over half of the Euclidean section [56, 57]. Restricted to the conformal boundary, this becomes a Euclidean path integral over the cylinder $[0, \beta/2] \times S^{d-1}$ and should construct the TFD state. Equivalently, the TFD state defines a transition amplitude with boundary conditions ϕ_1 and ϕ_2 specified on either

end of the interval $[0, \beta/2]$. To confirm this consider the overlap

$$\left({}_L\langle\phi_1| \otimes {}_R\langle\tilde{\phi}_2|\right)|TFD\rangle = \frac{1}{\sqrt{Z(\beta)}}\sum_i e^{-\beta E_i/2}{}_L\langle\phi_1|E_i\rangle_L{}_R\langle\tilde{\phi}_2|\tilde{E}_i\rangle_R \tag{1.1.51}$$

$$= \frac{1}{\sqrt{Z(\beta)}}\sum_i {}_L\langle\phi_1|e^{-\beta H_L/2}|E_i\rangle_L{}_L\langle E_i|\phi_2\rangle_L \tag{1.1.52}$$

$$= \frac{1}{\sqrt{Z(\beta)}}{}_L\langle\phi_1|e^{-\beta H_L/2}|\phi_2\rangle_L, \tag{1.1.53}$$

where in the second line we used the antiunitary property $\langle\Theta x|\Theta y\rangle = \langle y|x\rangle$. This demonstrates that the TFD is prepared by a Euclidean path integral in which Euclidean time t_E runs over an interval of length $\beta/2$ [58]. Note also that the TFD state is invariant under time evolution generated by the Hamiltonian,

$$H_{tot} = H_L \otimes \mathbb{I}_R - \mathbb{I}_L \otimes H_R, \tag{1.1.54}$$

which has the natural interpretation of the dual to the bulk Hmailtonian that generates time evolution along the Schwarzschild isometry ∂_t; the Schwarzchild t coordinate runs in opposite directions on the left and right asymptotically AdS regions.

The TFD state serves as a paradigmatic example of the concept of *emergent spacetime* - the idea that classical spacetime is an emergent phenomena arising from the entanglement structure of underlying degrees of freedom. The TFD state is given by a sum over individual product states $|E_i\rangle_L \otimes |\tilde{E}_i\rangle_R$ (i.e. states with zero entanglement between the two subsystems). Since the CFTs are non-interacting, and there is zero entanglement, the natural interpretation is that a product state correspond to two completely independent physical systems. If $|E_i\rangle_L$ and $|\tilde{E}_i\rangle_R$ each correspond to an asymptotically AdS spacetime, then their product should correspond to a pair of disconnected asymptotically AdS spacetimes. However, taking the particular superposition of these states that constructs the TFD corresponds to an extended black hole with two asymptotically AdS regions connected by a smooth classical wormhole. This points towards a profound insight: the connectivity of classical spacetime is a consequence of (particular kinds of) entanglement in a more

fundamental quantum mechanical description. This perspective was emphasized in [59, 60] and is in line with the $ER = EPR$ proposal of Maldacena and Susskind [61]. They propose a more radical perspective; rather than simply claiming that entanglement underlies the connectivity of classical spacetime, as has been argued here, they claim that in a quantum theory of gravity *all* entangled systems, even individual entangled particles, are connected by a kind of Einstein-Rosen bridge, albeit not necessarily one that can be described by a classical geometry.

1.1.3 Charged black holes

Schwarzschild black holes and the TFD are a fundamental example of the relation of entanglement and geometry. It's interesting to see how this generalises; a natural, simple extension is to consider charged black holes, which are dual to an ensemble with chemical potential, purified by a generalisation of the TFD state.

In this section we will consider the case of a charged black hole in an asymptotically AdS_{d+1} spacetime. This bulk geometry arises from Einstein gravity with a negative cosmological constant, $\Lambda = -\frac{d(d-1)}{2\ell^2}$, coupled to a U(1) gauge field. The action is given by

$$S = \frac{1}{2\kappa^2}\int \mathrm{d}^{d+1}x\sqrt{-g}\left[(R-2\Lambda) - \frac{\ell^2}{g_F^2}F^2\right], \tag{1.1.55}$$

where g_F is an effective dimensionless gauge coupling. We are interested in the spherically symmetric AdS Reissner-Nördstrom black hole solution with the metric and gauge field given by

$$\mathrm{d}s^2 = -f(r)\mathrm{d}t^2 + \frac{\mathrm{d}r^2}{f(r)} + r^2\mathrm{d}\Omega_{d-1}^2, \qquad A = \mu\left(1 - \frac{r_+^{d-2}}{r^{d-2}}\right)\mathrm{d}t, \tag{1.1.56}$$

where $\mathrm{d}\Omega_{d-1}^2$ is the round metric on S^{d-1} and

$$f(r) \equiv 1 - \frac{M}{r^{d-2}} + \frac{Q^2}{r^{2d-4}} + \frac{r^2}{\ell^2}. \tag{1.1.57}$$

The constants Q and M are proportional to the charge and ADM mass of the black

hole respectively and the constant μ is given by

$$\mu = \sqrt{\frac{d-1}{2(d-2)}} \frac{g_F Q}{\ell r_+^{d-2}}. \tag{1.1.58}$$

For fixed mass M, there is an open interval $Q \in (0, Q_*)$ for which the metric function $f(r)$ has two distinct positive roots $f(r_-) = f(r_+) = 0$, corresponding to the inner and outer horizons of the black hole. As Q approaches the extremal charge Q_*, these two roots converge and $f(r)$ develops a double root at $r_* = r_+ = r_-$. For $Q > Q_*$, the metric function has no positive roots and no black hole solution exists. It will be useful to express the mass and charge parameters in terms of the inner and outer radii [44]:

$$M = \frac{\ell^2 \left[r_+^{2(d-2)} - r_-^{2(d-2)} \right] + r_+^{2(d-1)} - r_-^{2(d-1)}}{\ell^2 \left(r_+^{d-2} - r_-^{d-2} \right)}, \tag{1.1.59}$$

$$Q^2 = r_+^{d-2} r_-^{d-2} \left[\frac{\ell^2 \left(r_+^{d-2} - r_-^{d-2} \right) + r_+^d - r_-^d}{\ell^2 \left(r_+^{d-2} - r_-^{d-2} \right)} \right]. \tag{1.1.60}$$

In the extremal limit these become

$$\begin{aligned} M_* &= 2 r_*^{d-2} \left(1 + \frac{(d-1) r_*^2}{(d-2)\ell^2} \right), \\ Q_*^2 &= r_*^{2(d-2)} \left(1 + \frac{d r_*^2}{(d-2)\ell^2} \right). \end{aligned} \tag{1.1.61}$$

To calculate the black hole temperature, we can analytically continue to the Euclidean solution and impose a periodicity β in Euclidean time so as to remove the conical singularity at the outer horizon. This periodicity is the inverse temperature of the Lorentzian black hole. One finds the black hole temperature

$$T = \frac{d-2}{4\pi r_+} \left[\frac{2 r_+^2}{(d-2)\ell^2} + \frac{M}{r_+^{d-2}} - \frac{2Q^2}{r_+^{2d-4}} \right]. \tag{1.1.62}$$

Evaluating this expression in the extremal limit using (1.1.61), we see that the extremal limit $Q \to Q_*$ corresponds to the limit of zero temperature, $T \to 0$. In the grand canonical ensemble with fixed μ, zero temperature is only reached if

$$\mu^2 > \mu_c^2 \equiv \frac{2(d-2)\ell^2}{(d-1) g_F^2}, \tag{1.1.63}$$

as can be seen by eliminating the mass parameter and expressing the temperature in terms of μ:

$$T = \frac{d-2}{4\pi r_+}\left[1 + \frac{dr_+^2}{(d-2)\ell^2} - \mu^2 \frac{2(d-2)\ell^2}{(d-1)g_F^2}\right]. \tag{1.1.64}$$

As mentioned previously, in the extremal limit the metric develops a double pole at the horizon $f(r) \propto (r-r_*)^2 + \mathcal{O}(r-r_*)^3$. This implies a peculiar feature of extremal black holes: on a constant-t hypersurface, the horizon is an infinite proper distance away from any other radial point. Explicitly, the proper distance from any point r to the horizon $r_+ \to r_*$ is logarithmically divergent,

$$\int_{r_+}^{r} \frac{\mathrm{d}r'}{\sqrt{f(r')}} \sim \ln\left(\frac{r-r_*}{r_+-r_*}\right). \tag{1.1.65}$$

Curiously, extremal charged black holes also retain a non-zero Bekenstein-Hawking entropy, $S_* = \frac{A(r_*)}{4G_N}$, indicating non-zero entanglement in the dual state. These two facts motivate our study in chapter 2 of near-extremal AdS black holes in the context of traversable wormholes. The non-zero entanglement in the dual state suggests the possibility of constructing a traversable wormhole solution along the lines of [12] via introducing a simple coupling between the two boundaries; however, the divergence in the length of the wormhole's throat implies that correlation functions of operators on different boundaries vanishes in the extremal limit (unless the field dual to the operator is tuned to the threshold of an instability [62]), suggesting that the effect of the boundary coupling on the bulk geometry may also vanish in this limit. This begs the question: can we make these infinite wormholes traversable, enabling communication between the two CFTs through the bulk? We will find in chapter 2 that the answer to this question is yes! Aside from taking the bulk field to be at the threshold of an instability, this can be achieved provided we take the coupling between the two boundaries to scale to infinity as an inverse power of the temperature. If we accept this tuning of the coupling, we can communicate an amount of information that scales with the entropy of the black hole through the wormhole in the bulk.

We now wish to consider the holographic dual of the Reissner-Nördstrom AdS

geometry. We know that the gauge field A_t is dual to a conserved current J_t in the boundary theory corresponding to a global U(1) symmetry. According to the holographic dictionary, the boundary value of the gauge field, $\mu = A_t(r \to \infty)$, is equal to the source of the conserved current, i.e. μ is the chemical potential in the field theory. Thus, we expect the dual state to be a generalization of the TFD state to the grand canonical ensemble. That is, we include a chemical potential μ in the Boltzmann weights and define the charged TFD (CTFD) state to be [62]

$$|CTFD\rangle = \frac{1}{\sqrt{Z(\beta,\mu)}} \sum_i e^{-\beta(E_i+\mu Q_i)/2} |E_i, Q_i\rangle_L \otimes |\tilde{E}_i, -Q_i\rangle_R, \tag{1.1.66}$$

where Q_i are eigenvalues of the global conserved $U(1)$ charge conjugate to μ and $Z(\beta,\mu)$ is the grand canonical partition function. Here, the antiunitary Θ is taken to also implement charge conjugation, $|\tilde{E}_i, -Q_i\rangle_R \equiv \Theta|E_i, Q_i\rangle_L$. This state, as with the uncharged case, can also be constructed via a Euclidean path integral over a cylinder $[0, \beta/2] \times S^{d-1}$, but now we couple the charge Q to a background U(1) gauge field $A = -i\mu \mathrm{d}t_E$. The AdS Reissner-Nördstrom black hole is the dominant saddle point in the grand-canonical ensemble for all temperatures provided $\mu > \mu_c$ [63], so it provides the bulk dual of the CTFD state. Note that the form of (1.1.66) tells us that the CTFD is equivalent to the uncharged TFD state defined by the deformed Hamiltonians $H'_{L,R} \equiv H_{L,R} \pm \mu Q$.

In order for the CTFD state to have a well-defined zero-temperature limit $\beta \to \infty$, the spectrum of the deformed Hamiltonians $E'_{L,Ri} = E_i \pm \mu Q_i$ must be bounded from below. In the zero-temperature limit, the reduced density matrices on either CFT approximate projection operators onto the states which minimize E'_L, E'_R. The non-zero entropy of the black hole in the extremal, zero-temperature limit, implies an approximate degeneracy in the states at minimal E'_L,E'_R. This ground-state entanglement gives us the required entanglement for quantum teleportation, the dual interpretation of bulk wormhole traversability.

1.1.4 Holographic entanglement entropy

Building on the work of Bekenstein, Hawking showed that black holes are thermal objects with an entropy given by one quarter the area of their event horizon in Planck units. This famous result hints at a deep relationship between entropy and spacetime geometry. The study of holography has allowed us to gain remarkable insight into this relationship, most notably in the form of the Hubeny-Rangamani-Takayanagi (HRT) conjecture and its subsequent generalizations, which relate the entanglement entropy of a region in a holographic CFT to the area of certain co-dimension two surfaces in the bulk. This represents a large generalization of the black hole entropy formula; in the context of holography we can associate entropy with a large class of extremal surfaces, not just black hole horizons. Holographic entanglement entropy has been used extensively to study both sides of the AdS/CFT correspondence and has played a crucial role in the recent understanding of the black hole information problem.

Consider a holographic CFT_d on a manifold $\partial\mathcal{M}$ which is the conformal boundary of some asymptotically AdS_{d+1} spacetime $\mathcal{M}$ and let $\partial\Sigma \subset \partial\mathcal{M}$ be some boundary Cauchy slice. The Hubeny-Rangamani-Takayanagi conjecture says that for any subregion $R \subset \partial\Sigma$, and any appropriate state $\rho \in \mathcal{H}_{CFT}$ which is dual to semiclassical Einstein gravity in the bulk, the von Neumann entropy of the reduced density matrix ρ_R on R is given by

$$S(\rho_R) = \min_{\gamma_R} \operatorname{ext}_{\gamma_R} \left[\frac{\text{Area}(\gamma_R)}{4G_N} \right], \tag{1.1.67}$$

to leading order in G_N [64]. The extremum (and minimum if the extremum is not unique) is taken over co-dimension two manifolds γ_R anchored to R, i.e. $\partial\gamma_R = \partial R$, that are homologous to R, meaning there exists a spatial surface Σ_R such that $\partial\Sigma_R = \gamma_R \cup R$. The extremal surface γ_R is called the HRT surface. In the special case where the spacetime possesses a time-reflection symmetry under which the boundary spatial region R is invariant, this reduces to the original conjecture of Ryu and Takayanagi (RT) [65]. The original RT formulation applies to states with

this time-reflection symmetry e.g. a constant time slice of a static spacetime, and the RT surface is defined as the minimal area surface on this time slice. The HRT conjecture serves as a covariant generalization of RT which can accommodate general time-dependant states.

The RT/HRT formulae have been extensively tested in the literature, having been applied to a wide variety of different spacetimes and passing a number of non-trivial checks. For example, the RT proposal produces the correct universal formula for the entanglement entropy of an interval of length L for the vacuum state of a two-dimensional CFT. The holographic dual to the vacuum state of a CFT on $\mathbb{R}^2$ is the Poincaré patch of AdS_3 whose metric on a constant timeslice is

$$\mathrm{d}s^2 = \frac{\ell^2}{z^2}(\mathrm{d}z^2 + \mathrm{d}x^2). \tag{1.1.68}$$

The minimal surfaces in this space are easily found to be coordinate semi-circles centred on the boundary, with the minimal surface associated with the interval $x \in [-\frac{L}{2}, \frac{L}{2}]$ given by

$$x^2 + z^2 = \left(\frac{L}{2}\right)^2. \tag{1.1.69}$$

To regulate the divergence associated with the infinite distance to the AdS boundary, we calculate the area of the surface in the region $z > \epsilon$ with $\epsilon \ll L$. The RT prescription then gives

$$S_L = \frac{\text{Area}}{4G_N} = \frac{\ell}{2G_N} \ln\left(\frac{L}{\epsilon}\right). \tag{1.1.70}$$

Now, let us compare this to a direct calculation of the entanglement entropy in the CFT. In terms of the central charge c and UV cutoff $1/\epsilon$, the result is

$$S_L = \frac{c}{3} \ln\left(\frac{L}{\epsilon}\right) \tag{1.1.71}$$

We see that not only does the RT formula produce the correct logarithmic divergence but it also allows us to read off the Brown-Henneaux formula relating the central

charge of a two-dimensional holographic CFT to the bulk AdS_3 parameters [66],

$$c = \frac{3\ell}{2G_N}. \tag{1.1.72}$$

Notice that on the CFT side, the divergence in the entanglement entropy originates from the UV, short-distance, entanglement across the boundaries of the interval; On the bulk side this corresponds to the divergence of the AdS metric near the boundary as $z \to 0$, demonstrating the correspondence between boundary RG flow and the bulk radial direction.

The RT prescription also obeys all known properties of entanglement entropy, including an infinite set of inequalities [67]. For example, RT obeys the property of strong subadditivity. In fact, the proof of this is remarkably simple compared to the standard quantum-information-theoretic proof of the strong subadditivity of entanglement entropy. For a tripartite Hilbert space $\mathcal{H} \equiv \mathcal{H}_A \otimes \mathcal{H}_B \otimes \mathcal{H}_C$, strong subadditivity says that for any state $\rho_{ABC} \in \text{End}(\mathcal{H})$, the following inequality holds

$$S(\rho_{ABC}) + S(\rho_B) \leq S(\rho_{AB}) + S(\rho_{BC}). \tag{1.1.73}$$

To show that this is obeyed by the RT formula, consider three boundary regions A, B, C, on a constant timeslice of a holographic CFT. Let $\gamma_{A\cup B}$, $\gamma_{B\cup C}$ be the RT surfaces corresponding to the regions $A \cup B$ and $B \cup C$, respectively. The key to the proof is to notice that the union $\gamma_{A\cup B} \cup \gamma_{B\cup C}$ always defines homology regions $\Sigma_{A\cup B\cup C}$ and Σ_B, therefore it is always a candidate for the union of RT surfaces $\gamma_{A\cup B\cup C} \cup \gamma_B$. Since RT surfaces have minimal area, we have

$$\begin{aligned} \text{Area}(\gamma_{A\cup B}) + \text{Area}(\gamma_{B\cup C}) &= \text{Area}(\gamma_{A\cup B} \cup \gamma_{B\cup C}) && (1.1.74)\\ &\geq \text{Area}(\gamma_{A\cup B\cup C} \cup \gamma_B) && (1.1.75)\\ &= \text{Area}(\gamma_{\text{A}\cup\text{B}\cup\text{C}}) + \text{Area}(\gamma_B), && (1.1.76) \end{aligned}$$

which confirms (1.1.73). This argument crucially relies on the fact that RT surfaces are defined to minimise the area functional. In contrast, HRT surfaces are defined to extremise the area functional, so this argument cannot be easily generalised to

prove the strong subadditivity of HRT surfaces. In fact, this remained unproven for seven years until it was finally proven by Wall in [68].

Wall put forward an alternate definition of the HRT surface γ_R, known as the *maximin* construction. Maximin surfaces are defined operationally in the following way: given a boundary subregion R, consider all bulk Cauchy slices containing ∂R[1]. For a each Cauchy slice Σ, find the minimal area surface homologous to R, denoted $\min(\Sigma, R)$. The maximin surface $M(R)$ is then defined as the maximal area $\min(\Sigma, R)$ when varying over all possible Σ. Under certain general assumptions about the bulk spacetime, such as it being smooth, locally asymptotically AdS, and obeying the null curvature condition ($R_{ab}k^a k^b \geq 0$ for any null vector k^a), Wall proved that maximin and HRT surfaces are equivalent. Wall then used this construction to prove various results about HRT surfaces, including the strong subadditivity condition.

Additionally both RT and HRT have been derived from first principles assuming only basic elements of the AdS/CFT dictionary. Lewkowycz and Maldacena derived the RT prescription by mapping the replica construction used to compute entanglement entropy in quantum field theories to the Euclidean quantum gravity path integral [70]. This was extended in [71] to derive the HRT prescription.

A number of generalizations have appeared in the literature since the HRT prescription was first introduced. These extend the prescriptions to account for higher derivative theories of bulk gravity and to include higher order quantum effects in the bulk. In particular, the quantum extensions of HRT have led to considerable progress in our understanding of the black hole information problem through the quantum extremal island phenomenon, as will be discussed in section 1.3.

From the low-energy effective field theory view of Einstein gravity, it is natural to ask how the holographic entanglement entropy formula is modified by higher curvature corrections. In the black hole context the analogous question was answered

[1] In [69], they showed that this is equivalent to a restricted maximin proposal in which one varies over Cauchy slices with a fixed boundary $\partial\Sigma \supset R$ when the restricted maximin surface lies in a smooth region of spacetime.

by Wald who proposed the following entropy formula in $(d+1)$ dimensions [72–74]:

$$S_{\text{Wald}} = -2\pi \int_{\mathcal{B}} \mathrm{d}x^{d-1}\sqrt{h}\frac{\delta\mathcal{L}}{\delta R_{\mu\nu\rho\sigma}}\varepsilon_{\mu\nu}\varepsilon_{\rho\sigma}, \tag{1.1.77}$$

where h_{ab} is the induced metric on the black hole horizon $\mathcal{B}$, $\varepsilon_{\mu\nu}$ is the binormal to the horizon normalized by $\varepsilon_{\mu\nu}\varepsilon^{\mu\nu} = -2$, and $\mathcal{L}$ is the gravitational Lagrangian. This reduces to the Bekenstein-Hawking area formula in the case of Einstein gravity. One might guess that Wald's formula can simply be carried over to give the prescription for the holographic entanglement entropy for theories dual to higher derivative gravity. However, as pointed out by Hung, Myers and Smolkin [75], this does not give the correct universal logarithmic term in the entanglement entropy for CFTs when the bulk entanglement surface has non-zero extrinsic curvature. In [76], using a generalization of the Lewkowycz-Maldacena derivation of RT, Dong derived an expression for entanglement entropy for general higher derivative gravity theories with a Lagrangian $\mathcal{L}(R_{\mu\nu\rho\sigma})$ built from arbitrary contractions of the Reimann tensor. This was extended in [77] to also include derivatives of the curvature. These more general functionals consist of a term corresponding to Wald's formula plus corrections involving the extrinsic curvature. The prescription then for higher derivative classical gravity is that the holographic entanglement entropy associated with a boundary spatial region R is given by

$$S(\rho_R) = \min_{\gamma_R} \operatorname*{ext}_{\gamma_R} \left[\frac{\mathcal{A}(\gamma_R)}{4G_N}\right], \tag{1.1.78}$$

where $\mathcal{A}$ is the appropriate generalised functional which reduces to the area in the Einstein gravity limit. For a Lovelock-type term in the action, the correction to the area functional takes a particularly simple form as the next lower Lovelock term applied to the surface [75,78]. For example, a Gauss-Bonnet term in the gravitational action adds an Einstein-Hilbert term to the area functional.

Moving away from the classical limit, the HRT formula should receive additional higher order corrections. At order G_N^0 , or equivalently order N^0 in the boundary theory, Faulkner, Lewkowycz, and Maldacena (FLM) argued that the correction is

given by the bulk entanglement entropy of the homology surface Σ_R [79]:

$$S(\rho_R) = \min_{\gamma_R} \operatorname{ext}_{\gamma_R} \left[\frac{\mathcal{A}(\gamma_R)}{4G_N} \right] + S_{bulk}(\rho_{\Sigma_R}). \tag{1.1.79}$$

This correction arises from a semi-classical treatment in which the bulk fields and metric perturbations are considered quantum fields propagating on a fixed background. The entanglement entropy $S_{bulk}(\rho_{\Sigma_R})$, therefore, is a standard quantum field theory entanglement entropy[1].

The modern form of the HRT prescription is an all orders generalization of FLM, conjectured by Engelhardt and Wall, known as the *quantum extremal surface* (QES) prescription [80]. It states that the entanglement entropy of a boundary state ρ_R supported on a boundary subregion R is given by

$$S(\rho_R) = \min_{\gamma_R} \operatorname{ext}_{\gamma_R} \left[\frac{\mathcal{A}(\gamma_R)}{4G_N} + S_{bulk}(\rho_{\Sigma_R}) \right]. \tag{1.1.80}$$

The sum of the two terms inside the brackets is known as the *generalised entropy* and the minimal surface that extremises the generalised entropy is called the quantum extremal surface. The QES should also satisfy the same homology condition required of HRT surfaces. The QES surface prescription has since also been derived from basic elements of the AdS/CFT dictionary [81].

The quantum extremal surface formula has led to a number of important results. For example, it implies a feature of AdS/CFT known as subregion-subregion duality holds between the boundary subregion R and the bulk domain of dependence of the quantum extremal homology surface, also known as the entanglement wedge $W_R \equiv D[\Sigma_R]$. That is, it suggests that W_R is entirely encoded in R. Assuming the QES formula, this was proven using general information-theoretic arguments in [82]. They showed that all bulk operators in W_R have a representation in the dual CFT as operators supported only on R, which is referred to as *entanglement wedge reconstruction*. This result both made use of and helped develop the quantum error

[1]Strictly speaking, (1.1.79) is ill-defined since $S_{bulk}(\rho_{\Sigma_R})$ is UV divergent, however it can be renormalized by including appropriate local counterterms in the action, so we should think of (1.1.79) as containing the renormalized bulk entanglement entropy.

correcting code interpretation of AdS/CFT [11, 83, 84].

1.2 AdS/BCFT

1.2.1 Boundary states

An interesting extension of conformal field theory is to consider manifolds with boundary; we can define a theory on a manifold with boundary by choosing boundary conditions for the fields, and possibly adding boundary degrees of freedom coupled to the bulk fields. When the boundary conditions preserve a maximal subset of the conformal symmetry, the theory is called a *boundary conformal field theory* (BCFT). This is a subject with an extensive literature; below we will give a brief review based on [46, 85].

To be concrete, consider a Euclidean CFT defined on the half-space $\mathcal{M} \equiv \mathbb{R}^{d-1} \times \mathbb{R}_+$ with Cartesian coordinates (τ, x^i) such that the boundary $\partial\mathcal{M} = \mathbb{R}^{d-1}$ is located at $\tau = 0$. This theory is a BCFT when the choice of boundary physics preserves the subset of the conformal group mapping the half-space to itself, $\mathrm{SO}(d,1) \subset \mathrm{SO}(d+1,1)$. We will investigate how correlation functions transform under infinitesimal conformal transformations that map the half-space to itself $f_\varepsilon : \mathcal{M} \to \mathcal{M}$,

$$f_\varepsilon : x^\mu \to x'^\mu = x^\mu + \varepsilon^\mu(x), \qquad \varepsilon^\tau(0, \mathbf{x}) = 0. \tag{1.2.1}$$

Using a path integral formulation, conformal invariance of correlation functions gives

$$\delta_\varepsilon \langle X \rangle = \int \mathcal{D}\Phi \, e^{-S[\Phi]} \left(\delta_\epsilon X + X \int_{\mathcal{M}} \mathrm{d}^d x T^{\mu\nu} \partial_\mu \varepsilon_\nu \right) = 0 \tag{1.2.2}$$

where we take X to be some product of local operators

$$X = \prod_i \mathcal{O}(x_i). \tag{1.2.3}$$

After integrating by parts we arrive at

$$\langle \delta_\varepsilon X \rangle = \int_{\mathcal{M}} \mathrm{d}^d x \, \varepsilon_\nu \partial_\mu \langle T^{\mu\nu}(x) X \rangle - \int_{\partial\mathcal{M}} \mathrm{d}^{d-1} x \, \varepsilon_\nu n_\mu \langle T^{\mu\nu}(x) X \rangle \,. \tag{1.2.4}$$

The first term is the familiar condition that the stress tensor is conserved away from the insertion points of other fields. The second term leads us to the Cardy boundary condition $T_{\tau i}(\tau = 0, \mathbf{x}) = 0$, i.e. momentum flow vanishes at the boundary. This is a necessary condition for boundary conformal field theories.

The presence of a boundary modifies a theory's correlation functions. For example, consider the one point function of a local operator. For a CFT without boundary, the one point function of a primary operator is required to vanish by translation invariance. This symmetry is broken in a BCFT. The remaining conformal symmetry requires the one point function takes the form

$$\langle \mathcal{O}(\tau, \mathbf{x}) \rangle_{\mathcal{M}} = \frac{A_{\mathcal{O}}}{\tau^{\Delta}}, \tag{1.2.5}$$

where $A_{\mathcal{O}}$ is determined by the details of the theory and the boundary state. For a two-point function we have

$$\langle \mathcal{O}_1(x_1)\mathcal{O}_2(x_2) \rangle_{\mathcal{M}} = \frac{F(\xi)}{\tau_1^{\Delta_1}\tau_2^{\Delta_2}}, \tag{1.2.6}$$

where $F(\xi)$ is some function of the conformal invariant

$$\xi = \frac{(x_1 - x_2)^2}{\tau_1 \tau_2} \tag{1.2.7}$$

that is not fixed by conformal symmetry.

Using the correspondence between states and path integrals with an unspecified boundary condition, we can formally define a boundary state $|b\rangle$ associated with boundary condition b. The wavefunctional $\langle \phi_0 | b, \tau_0 \rangle$ is defined by a Euclidean path integral for the CFT on a cylinder of height τ_0, with boundary condition b at Euclidean time $\tau = -\tau_0$ and CFT field configuration ϕ_0 at $\tau = 0$. The boundary state $|b\rangle$ is then defined by

$$|b\rangle = \lim_{\tau_0 \to 0} |b, \tau_0\rangle. \tag{1.2.8}$$

Alternatively, we can think of the state $|b, \tau_0\rangle$ as arising from a Euclidean time

evolution of the boundary state

$$|b, \tau_0\rangle = e^{-\tau_0 H}|b\rangle. \tag{1.2.9}$$

The boundary state itself has infinite energy expectation value. However, the Euclidean time evolution suppresses the high energy components so that $|b, \tau_0\rangle$ is a finite energy state.

In two dimensions, an important quantity is the overlap of the boundary state with the vacuum $\mathfrak{g} \equiv \langle 0|b\rangle$, computed via a path integral on a semi-infinite cylinder. This can mapped to the disk via a conformal transformation, so is equivalent to the disk partition function. The parameter $\mathfrak{g}$ can be understood as the boundary analogue of the central charge; it has been shown that $\mathfrak{g}$ is strictly decreasing along boundary RG flows [86]. The parameter $\mathfrak{g}$ also appears in the expression for the vacuum entanglement entropy for a CFT on a half line. The entanglement entropy for an interval of length L including the boundary is given by

$$S(L) = \frac{c}{6}\log\left(\frac{L}{\epsilon}\right) + \log \mathfrak{g}. \tag{1.2.10}$$

The second term is known as the *boundary entropy*.

1.2.2 End of the world branes

In [65], Takayanagi proposed a remarkably simple holographic dual to BCFTs from a bottom-up perspective. He argued that for a BCFT defined on a d-dimensional manifold M with boundary ∂M, the holographic dual is given by a $(d+1)$-dimensional asymptotically AdS space N so that $\partial N = M \cup Q$, where Q is a d-dimensional manifold satisfying $\partial Q = \partial M$ (see fig. 1.1). We think of the co-dimension one surface Q as the worldvolume of a brane which we will often refer to as the *end of the world* (ETW) brane. In particular, he proposes imposing Neumann boundary conditions on the bulk metric at Q (and the standard Dirichlet boundary conditions at M). Using this he is able to successfully calculate the boundary entropy in two-dimensional BCFTs and find agreement with the finite part of the holographic entanglement

entropy as well as derive a holographic g-theorem. Alternative prescriptions have since been considered in the literature [87–89]; however, in this thesis we will only consider Takayanagi's prescription using Neumann boundary conditions.

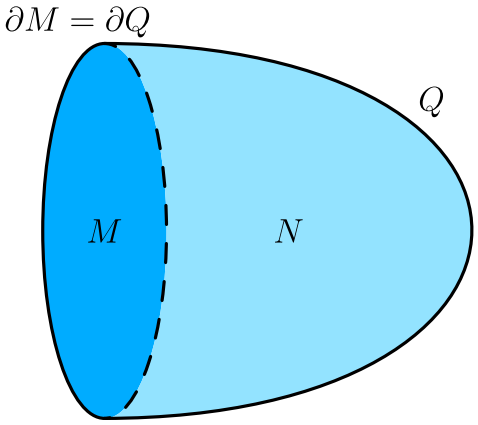

Figure 1.1: A depiction of the holographic dual of a BCFT defined on a manifold M with boundary ∂M. Its gravity dual is denoted by N and is bounded by M and a surface Q.

Consider the Einstein-Hilbert action including Gibbons-Hawking boundary terms (taking $16\pi G = 1$)

$$I = \int_N \sqrt{-g}(R - 2\Lambda) + 2\int_Q \sqrt{-h}K + 2\int_M \sqrt{-\gamma}K + 2\int_P \sqrt{-\sigma}\theta, \tag{1.2.11}$$

where $P \equiv \partial M = \partial Q$ is the codimension two submanifold where M and Q meet; the induced metrics on Q, M, and P are denoted h_{ab}, γ_{ij}, and $\sigma_{\alpha\beta}$ respectively; $\theta = \arccos(n^Q \cdot n^M)$ is the supplementary angle between the boundaries M and Q, calculated using the outward pointing unit normals n^Q, n^M; and $K = h^{ab}K_{ab}$ (or $K = \gamma^{ij}K_{ij}$) is the trace of the extrinsic curvature on Q (or M). The extrinsic curvature K_{ab} is defined by

$$K_{ab} = h_a{}^c h_b{}^d \nabla_c n^Q_d. \tag{1.2.12}$$

The final term in (1.2.11) is necessary for a well defined variational principle in the presence of a cusp-like singularity where Q and M are joined non-smoothly at P[1] [91].

[1]This boundary term is often omitted since many physical quantities are left unchanged by its exclusion; one exception is the boundary energy momentum tensor [90].

Considering the variation of the on-shell action, we have

$$\delta I = -\int_Q \sqrt{-h}(K^{ab} - Kh^{ab})\delta h_{ab} - \int_M \sqrt{-g}(K^{ij} - Kg^{ij})\delta g_{ij} + \int_P \sqrt{-\sigma}\theta\sigma^{\alpha\beta}\delta\sigma_{\alpha\beta}. \tag{1.2.13}$$

Takayangi's prescription is to impose Dirichlet boundary conditions on M and P, $\delta g_{ij}|_M = \delta\sigma_{\alpha\beta}|_P = 0$, but Neumann boundary conditions on Q. This leads to a dynamical brane worldvolume whose position is determined by

$$K_{ab} - Kh_{ab} = 0. \tag{1.2.14}$$

This can be generalized by including matter fields localized on Q. Adding a boundary matter term to the action,

$$I_Q^{mat} = \int_Q \sqrt{-h}L_Q, \tag{1.2.15}$$

our equation of motion for Q becomes

$$K_{ab} - Kh_{ab} = T_{ab}^Q, \tag{1.2.16}$$

where we define

$$T^{Qab} = \frac{2}{\sqrt{-h}}\frac{\delta I_Q^{mat}}{\delta h_{ab}} \tag{1.2.17}$$

In this thesis we will only be interested in the case where the boundary matter Lagrangian L_Q is a constant

$$L_Q = -(d-1)T. \tag{1.2.18}$$

The constant T can be interpreted as the tension of the brane. The boundary condition for this case reads

$$K_{ab} = (K - (d-1)T)h_{ab}, \tag{1.2.19}$$

and taking the trace we obtain

$$K = dT. \tag{1.2.20}$$

As mentioned previously, the boundary we consider breaks the $\mathrm{SO}(2,d)$ symmetry

of the CFT to $\mathrm{SO}(2, d-1)$. This motivates the following ansatz for the bulk metric

$$\mathrm{d}s^2 = g_{\mu\nu}\mathrm{d}x^\mu \mathrm{d}x^\nu = \mathrm{d}\rho^2 + \cosh^2\left(\frac{\rho}{\ell}\right)\mathrm{d}s^2_{\mathrm{AdS}_d}. \tag{1.2.21}$$

If we let ρ take all values $\rho \in (-\infty, \infty)$, then (1.2.21) represents a foliation of AdS_{d+1} by AdS_d leaves given by surfaces of constant ρ; the isometry group of the AdS_d slices correspond to the unbroken $\mathrm{SO}(2, d-1)$ conformal symmetries. To see that (1.2.21) is equivalent to the AdS_{d+1} metric, take the Poincaré metric for AdS_d,

$$\mathrm{d}s^2_{\mathrm{AdS}_d} = \frac{\ell^2}{y^2}(\mathrm{d}y^2 + \eta_{ab}\mathrm{d}x^a\mathrm{d}x^b), \tag{1.2.22}$$

where η_{ab} is the d-dimensional Minkowski metric, and define new coordinates

$$z = \frac{y}{\cosh\frac{\rho}{\ell}} \qquad u = y\tanh\frac{\rho}{\ell}. \tag{1.2.23}$$

This gives the Poincaré metric for AdS_{d+1}

$$\mathrm{d}s^2 = \frac{\ell^2}{z^2}(\mathrm{d}z^2 + \mathrm{d}u^2 + \eta_{ab}\mathrm{d}x^a\mathrm{d}x^b). \tag{1.2.24}$$

To realize a gravity dual to a BCFT we restrict this space to the region $\rho \in (-\infty, \rho_*)$, placing the boundary Q at $\rho = \rho_*$. The BCFT in this case is defined on the half-space $M = \mathbb{R}^{d-1} \times \mathbb{R}_-$, given by $u \leq 0$. The metric (1.2.21) is in a Gaussian normal coordinate system, i.e. it takes the form

$$\mathrm{d}s^2 = \mathrm{d}\rho^2 + h_{ab}\mathrm{d}x^a\mathrm{d}x^b, \tag{1.2.25}$$

so the extrinsic curvature on Q can be straightforwardly calculated via

$$K_{ab} = \frac{1}{2}\left.\frac{\partial h_{ab}}{\partial\rho}\right|_{\rho=\rho_*}. \tag{1.2.26}$$

We find

$$K_{ab} = \frac{1}{\ell}\tanh\left(\frac{\rho_*}{\ell}\right)h_{ab}(\rho_*). \tag{1.2.27}$$

This satisfies the boundary condition (1.2.19) provided

$$T = \frac{1}{\ell}\tanh\frac{\rho_*}{\ell}, \tag{1.2.28}$$

which leads to the constraint $-1 \leq T\ell \leq 1$.

1.2.3 Branes behind horizons

In this thesis we will be interested in eternal Schwarzschild geometries in which one asymptotic region terminates in an end of the world brane. These geometries are dual to pure states of the CFT living on the single asymptotic boundary. These states were first suggested in [92] and further explored in [43]. To describe these states let us first consider the thermofield double state of two CFTs on S^d,

$$|\Psi^{\beta}_{TFD}\rangle = \frac{1}{\sqrt{Z_\beta}} \sum_n e^{-\frac{\beta E_n}{2}} |E_n\rangle_L \otimes |E_n\rangle_R. \tag{1.2.29}$$

For sufficiently high temperatures, this is dual to a maximally extended large AdS-Schwarzchild black hole. If we project this state onto a particular pure state $|B\rangle$ of the left CFT, the result is a pure state of the right CFT given by

$$|\hat{\Psi}^{\beta}_{B}\rangle = \frac{1}{\sqrt{Z_\beta}} \sum_n e^{-\frac{\beta E_n}{2}} \langle B|E_n\rangle |E_n\rangle. \tag{1.2.30}$$

This state can be thought of as arising from a measurement of the state of the left CFT. Projecting onto a generic state $|B\rangle \in \mathcal{H}_L$, we would expect the bulk dual of the resulting state $|\hat{\Psi}^{\beta}_{B}\rangle \in \mathcal{H}_R$ not to contain a significant portion of the left asymptotic region. In order to retain a significant portion of the left asymptotic region, we consider only states $|B\rangle$ with no long-range entanglement. This is due to the duality between boundary RG flows and the bulk radial direction; avoiding states with long-range (IR) correlations should avoid modifying the geometry deep in the bulk.

Let us consider the time reversed state $|\Psi^{\beta}_{B}\rangle \equiv \mathcal{T}|\hat{\Psi}^{\beta}_{B}\rangle$, where $\mathcal{T}$ the anti-linear and anti-unitary time-reversal operator. We have

$$\begin{aligned} |\Psi^{\beta}_{B}\rangle &\equiv \mathcal{T}|\hat{\Psi}^{\beta}_{B}\rangle \\ &= \frac{1}{\sqrt{Z_\beta}} \sum_n e^{-\frac{\beta E_n}{2}} \langle E_n|B\rangle |E_n\rangle \end{aligned}$$

$$= \frac{1}{\sqrt{Z_\beta}} \sum_n e^{-\frac{\beta E_n}{2}} |E_n\rangle\langle E_n|B\rangle$$
$$= \frac{1}{\sqrt{Z_\beta}} e^{-\frac{\beta H}{2}} |B\rangle. \tag{1.2.31}$$

Thus, we see that the states $|\Psi_B^\beta\rangle$ correspond to a state $|B\rangle$ evolved in Euclidean time by an amount $\beta/2$. These states are naturally defined by a Euclidean path integral on a cylinder of height $\beta/2$. We will consider states that are symmetric under time-reversal, $|\Psi_B^\beta\rangle = |\hat{\Psi}_B^\beta\rangle$, so that (1.2.31) and (1.2.30) are equivalent definitions.

1.3 Islands

For the past half-century, Hawking's black hole information problem has posed a serious challenge to consistently combining gravity and quantum mechanics. Using semi-classical techniques, Hawking showed that when coupled to quantum fields, black holes will evaporate, losing their mass to thermal radiation [93, 94]. When a black hole forms, the horizon divides the spacetime into two regions, the region inside the black hole and the region outside. We can imagine a black hole forming form an initial pure quantum state. On a full Cauchy slice, unitarity requires that the quantum fields are still in a pure state after the black hole has formed, but restricting to either region gives a mixed state due to the short-range entanglement in the state of the fields across the horizon. It is this entanglement that is responsible for the thermal nature of the radiation. The mixed state of the radiation is purified by the interior of the black hole. This means that the fine-grained entropy of the black hole is equal to the fine-grained entropy of the radiation, $S_{\text{black hole}}(t) = S_{\text{rad}}(t)$.

According to Hawking's calculation, however, the von Neumann entropy of the radiation increases linearly in time. This implies that eventually the fine-grained entropy of the radiation would exceed the coarse-grained Bekenstein-Hawking entropy of the black hole S_{BH}. After this point, the fine-grained entropy of the black hole and the radiation can no longer be equal, since $S_{\text{black hole}} \leq S_{\text{BH}} < S_{\text{rad}}$, meaning that the radiation cannot be purified by the interior and the state on the entire Cauchy

slice is now mixed. This violates unitarity; a pure state has evolved into a mixed state and information about the original pure state has been lost.

The fine-grained entropy of any subsystem is bounded from above by the coarse-grained entropy of the smaller subsystem and when the subsystems are macroscopic this bound is approximately saturated. Therefore, unitarity would predict the following evolution of the fine-grained entropy $S_{\text{rad}}(t)$. At early times, when the radiation is the smaller of the two subsystems, $S_{\text{rad}}(t)$ is given by the growing thermal entropy of the radiation (as calculated by Hawking), $S_{\text{rad}}(t) = S_{\text{thermal}}(t)$. At late times, however, when the black hole is the smaller of the two subsystems, $S_{\text{rad}}(t)$ is given by the decreasing Bekenstein-Hawking entropy of the black hole, $S_{\text{rad}}(t) = S_{BH}(t)$, tending to zero as the black hole evaporates completely. This trajectory of $S_{\text{rad}}(t)$ is called the Page curve and the time at which $S_{\text{BH}}(t_{\text{Page}}) = S_{\text{thermal}}(t_{\text{Page}})$ is known as the Page time [41, 42]. The black hole information problem can be encapsulated as the semi-classical predicted departure of $S_{\text{rad}}(t)$ from the Page curve.

Assuming unitarity, there must be a flaw in Hawking's calculation. However, it is very difficult to see what this might be. The calculation can be done far from the singularity, where quantum-gravitational effects are negligible, and the problem emerges at the Page time, well before the black hole's size has become comparable to the Planck length where we expect the semi-classical gravity description to break down. This is a puzzling situation: is quantum gravity a unitary theory? And if so how did Hawking's calculation go wrong?

The discovery of the AdS/CFT correspondence strongly favours unitarity and shows that at least in the case of asymptotically AdS black holes, Hawking's calculation must be wrong. This is because a small black hole (with negative specific heat) in AdS can evaporate via Hawking radiation and, according to the correspondence, this process should be dual to a manifestly unitary evolution of the non-gravitational boundary quantum system. While this answers the question of whether AdS black hole evaporation is unitary, it does not illuminate our understanding of how unitarity is preserved from the gravitational perspective and how to correctly calculate the

entropy of the radiation, nor does it decisively answer the unitarity question for black holes in non-asymptotically AdS spacetimes.

In recent years, significant progress has been made in resolving the information loss problem. This was triggered by new insights gained from applying the recently developed quantum extremal surface prescription for entanglement entropy to various holographic models of black hole evaporation and has resulted in a new rule for computing the von Neumann entropy of a quantum mechanical system entangled with a gravitational system, known as the *Island rule* [23–25]. When applied to the Hawking radiation of an evaporating black hole, this new rule has been shown to reproduce the Page curve, confirming unitarity. The island rule says that the von Neumann entropy of some subsystem A of a quantum system that is entangled with a gravitational system that has a semi-classical, effective description is given by

$$S(A) = \min_{\mathcal{I}} \operatorname*{ext}_{\mathcal{I}} S_{\text{gen}}(A \cup \mathcal{I}), \tag{1.3.1}$$

where $\mathcal{I}$ is the *island*, some spatial subregion of the spacetime the gravitational system lives in, and S_{gen} is the generalised entropy. If the semi-classical theory is Einstein gravity coupled to matter, the island formula is given by

$$S(A) = \min_{\mathcal{I}} \operatorname*{ext}_{\mathcal{I}} \left[\frac{\text{Area}(\partial \mathcal{I})}{4G_N} + S_{\text{eff}}(A \cup \mathcal{I}) \right], \tag{1.3.2}$$

where S_{eff} is the von Neumann entropy of the effective semi-classical state of A together with the fields in the island. The minimal spatial subregion that extremises S_{gen} is called a quantum extremal island; the boundary of the island $\partial\mathcal{I}$ is the quantum extremal surface.

The classic information paradox is difficult to directly study in AdS/CFT; small black holes are subdominant in the Euclidean path integral and large black holes do not evaporate. Large black holes will reach thermal equilibrium, reabsorbing radiation reflected back from the AdS boundary. To realize the classic version of the information paradox in AdS, one can couple AdS to an auxiliary system R that absorbs the radiation, allowing a large black hole in the bulk to evaporate. In [23, 24],

the authors considered a setup in which the auxiliary system is constructed by gluing half of non-gravitating Minkowski space along the AdS boundary with absorbing boundary conditions[1]. Using this construction, they studied the time-evolution of the fine-grained entropy of the black hole, $S_{\text{black hole}}$. Since the radiation is collected in the auxiliary reservoir R, the fine-grained entropy of the black hole is simply the entanglement between the entire AdS boundary and R. The QES prescription gives

$$S_{\text{black hole}} = \min_{Q} \operatorname*{ext}_{Q} \left[\frac{\text{Area}(Q)}{4G_N} + S_{\text{eff}}(\Sigma_Q) \right], \tag{1.3.3}$$

where Q is the quantum extremal surface and Σ_Q is the region between Q and the AdS boundary. They found that at exactly the Page time, there was a phase transition in the minimal QES. At very early times, before the radiation can escape the AdS region, the quantum extremal surface is the empty surface with zero area, in agreement with the classical extremal surface. Assuming the black hole formed from a pure state, the initial entropy is zero, $S_{\text{black hole}}(0) = 0$. Once the radiation starts to escape the AdS region, the von Neumann entropy starts to increase linearly as the number of quanta in the reservoir that are entangled with the interior of the black hole increases. This is the initial phase of the Page curve. However, shortly after the radiation begins to escape, another candidate QES appears. This second surface lies inside the black hole, close to the horizon and has generalized entropy approximately equal to the Bekenstein-Hawking entropy of the black hole. At early times this is much larger than the generalised entropy of the empty surface, so this second surface does not contribute to the fine-grained entropy of the black hole. At the Page time this ceases to be true and the fine-grained entropy is calculated using

[1]There are two differences between analysis of [23] and [24] that are worth mentioning. The first is that [23] considered a single-sided black hole formed from collapse, whereas [24] considered an eternal two-sided black hole with initially reflecting boundary conditions that become transparent at some fixed time. Secondly, the fine-grained entropy that [24] considered was the entropy of the single AdS boundary coupled to the reservoir. Even before the radiation is allowed to escape the AdS region, the state on this boundary is mixed with the QES coinciding with the bifurcation surface and having non-zero generalised entropy. Our discussion more closely follows [23], tracking the entropy of an initially pure state. In either case, the qualitative behaviour of the Page curve of the black hole is the same.

the non-vanishing QES,

$$S_{\text{black hole}}(t) \approx \frac{\text{Area}(\text{horizon}(t))}{4G_N}, \qquad t \geq t_{\text{Page}}, \tag{1.3.4}$$

where the contribution from the bulk quantum fields $S_{\text{eff}}(\Sigma_Q)$ is negligible since Σ_Q now contains only a very small portion of the black hole interior. The precise location of the non-vanishing extremal surface depends on the amount of radiation that has escaped and therefore on the boundary time t. It was shown to move outward in a spacelike direction, asymptotic to the black hole horizon. Since the area of the black hole decreases as it evaporates, this extremal surface gives a decreasing fine-grained entropy, in agreement with the Page curve.

Note that this calculation of the fine-grained entropy *of the black hole*, $S_{\text{black hole}}(t)$, does not resolve the information loss paradox. A resolution of the information loss paradox would involve a calculation of the fine-grained entropy *of the radiation*, $S_{\text{rad}}(t)$, that agrees with the Page curve and is consistent with unitarity. However, it does suggest a precise alternate prescription for calculating $S_{\text{rad}}(t)$. Let $\Sigma = \Sigma(t)$ be a Cauchy slice of the full AdS plus Minkowski space, passing through the AdS boundary at some time $t > t_{\text{Page}}$. This can be decomposed into three disjoint regions,

$$\Sigma \equiv \mathcal{I} \cup \Sigma_Q \cup \Sigma_R, \tag{1.3.5}$$

where Σ_R is the region contained in the auxiliary system, R; Σ_Q is the region bounded by the non-vanishing QES, Q, and the AdS boundary; and $\mathcal{I}$ is the remaining portion behind the horizon of the black hole. The fine-grained entropy of the black hole receives a contribution from the state of the fields only on Σ_Q. Assuming unitarity, the full state on Σ is pure. This implies that in order for the von Neumann entropy of the radiation to follow the Page curve, $S_{\text{rad}} = S_{\text{black hole}}$, it must receive contributions both from the region Σ_R containing the radiation and the region $\mathcal{I}$ behind the horizon. In particular it should be given by a variation of the usual QES prescription, in

which the extremal surfaces can bound disconnected 'islands' in the bulk,

$$S_{\text{rad}} = \min_{\mathcal{I}} \operatorname*{ext}_{\mathcal{I}} \left[\frac{\text{Area}(\partial\mathcal{I})}{4G_N} + S_{\text{eff}}(\Sigma_R \cup \mathcal{I}) \right]. \tag{1.3.6}$$

An island is only included in the generalised entropy if there is sufficient entanglement between the radiation and the spacetime in the semi-classical state to compensate for the large contribution to S_{gen} from the area term. Then $S_{\text{rad}} < S_{\text{eff}}(\Sigma_R)$, and the true fine-grained entropy of the radiation, calculated according to this prescription, is smaller than the effective entropy. This formula is telling us that the radiation and the interior of the black hole contained within the island are not really distinct systems. The effective semi-classical state in the island region is encoded in the radiation; semi-classically it looks like we have a separate Hilbert space $\mathcal{H}_{\mathcal{I}}$ of the quantum fields on the island, but in fact this is encoded as a code subspace in the Hilbert space $\mathcal{H}_R$ of the radiation.

Arriving at (1.3.6), we are begging the question with regards to the information loss paradox, since it was only justified on the assumption of unitarity. However, it does tell us what to aim for in a unitary theory. With this in mind, [25] constructed an ingenious *doubly holographic* setup in which an evaporating AdS_2 black hole in Jackiw-Teitelboim (JT) gravity was embedded into a holographic theory in one higher dimension. In this setting, they were able to derive the Page curve *for the radiation*, from purely geometric RT holographic entanglement calculations in the ambient AdS_3 space, in precise agreement with (1.3.6). This led them to conjecture the general formulation of the island rule (1.3.1) for any quantum system entangled with a gravitational system.

While initially the island rule was discovered in the context of holographic, low dimensional theories, it has since been derived directly from the Euclidean gravitational path integral [26, 27], so it is believed to apply more generally. The island rule has now been studied in a wide range of higher-dimensional and non-holographic contexts [30, 31, 38, 95–100].

1.3.1 The doubly holographic picture

It will be useful for chapter 3 for us to elucidate the doubly holographic view first presented in [25] and further developed by [30, 101–104]. These models essentially consist of some holographic CFT_d coupled to a co-dimension one conformal defect. This is dual to some asymptotically AdS_{d+1} geometry containing a co-dimension one dynamical brane supporting a copy of the same CFT_d, which intersects the AdS boundary at the location of the conformal defect. The interesting feature of these models is that in addition to the usual AdS_{d+1} bulk and boundary CFT_d descriptions of the physics, one can also consider an intermediate effective description, where we integrate over the bulk spacetime to obtain an effective gravity theory on the brane coupled to the holographic CFT. This is known as the *brane perspective*; there is a non-gravitational CFT_d on the rigid AdS_{d+1} boundary joined across an interface to the same CFT_d coupled to the brane gravity theory.

The advantage of this is that it allows us to relate the prima-facie surprising appearance of quantum extremal islands in the effective brane gravity perspective to the usual, entirely geometric, RT prescription for evaluating holographic entanglement entropy in the higher-dimensional bulk perspective. An island in the brane perspective corresponds to an RT surface in the bulk intersecting the brane; from the lower dimensional point of view, the island and the subregion in the fixed CFT for which we are calculating the entanglement entropy are disconnected, but they are connected through the additional holographic dimension.

For example, let us consider the model in [25]. They study the evaporation of an AdS_2 black hole in JT gravity coupled to a holographic CFT_2. The action for JT gravity is

$$I_{\mathrm{JT}} = \frac{1}{16\pi G_N^{(2)}} \int_{\mathcal{M}} \mathrm{d}x^2 \sqrt{-g}\phi\,(R+\Lambda) + \frac{1}{8\pi G_N^{(2)}} \int_{\partial\mathcal{M}} \mathrm{d}y \sqrt{-h}\phi\,(K-1)\,, \qquad (1.3.7)$$

where ϕ is the dilaton field. They allow the black hole to evaporate by coupling the AdS_2 boundary to a half-line supporting the same holographic CFT_2 but without gravity. The AdS_2 black hole is holographically dual to a (0+1)-dimensional quantum

system on its boundary; from the boundary perspective coupling the AdS_2 gravity theory to the bath CFT gives a CFT_2 on a half-line coupled to a quantum mechanical system on its boundary. Additionally, because the CFT_2 matter is holographic, the joint system is dual to an asymptotically AdS_3 spacetime with the JT gravity theory defined on a dynamical ETW brane and the non-gravitating CFT_2 supported on the rigid AdS_3 boundary.

Let us define a coordinate w running along the brane and bath, such that $w < 0$ corresponds to points in the brane, and $w > 0$ corresponds to points in the bath. We can summarise the three alternate descriptions of this setup as follows:

- **Boundary:** A two-dimensional CFT on a half-line, $w > 0$, with some quantum-mechanical system on its boundary, $w = 0$.
- **Bulk:** A three-dimensional asymptotically AdS_3 gravity with a dynamical ETW brane.
- **Brane:** A two-dimensional gravity-plus-matter theory on $w < 0$ joined across and interface to a two dimensional CFT living on a half-line, $w > 0$.

In the two-dimensional gravity theory, we can compute the fine-grained entropy of its quantum mechanical boundary theory using the prescription of extremizing the generalized entropy $S_{\text{black hole}} = \min_x \text{ext}_x S_{\text{gen}}(x)$, where

$$S_{\text{gen}}(x) = \frac{\phi(x)}{4G_N^{(2)}} + S_{2d-\text{eff}}(\Sigma_x). \tag{1.3.8}$$

Here, x is a point in the two-dimensional bulk and Σ_x is an interval from the point x to the AdS_2 boundary. The quantity $S_{2d-\text{eff}}(\Sigma_x)$ is the von Nuemann entropy of the semi-classical state on this interval. Note that the value of the dilaton $\phi(x)$ is the zero-dimensional analogue of the area, $\phi(x) = \text{Area}^{(2)}(x)$; in two dimensions, the area of a point is the coefficient of the curvature term in the action.

Assuming the CFT_2 has a large number of degrees of freedom, the contribution to $S_{2d-\text{eff}}(\Sigma_x)$ from the CFT matter fields dominates that of fluctuations of the dilaton and AdS_2 metric. Therefore, since the CFT_2 has a holographic dual, $S_{2d-\text{eff}}(\Sigma_x)$

can be computed to leading order using the RT/HRT formula in the AdS_3 bulk as proportional to the area of a minimal (or an extremal) co-dimension two surface Γ_x in the three-dimensional geometry homologous to Σ_x. We have

$$S_{\text{gen}} \approx \frac{\phi(x)}{4G_N^{(2)}} + \frac{\text{Area}^{(3)}(\Gamma_x)}{4G_N^{(3)}}. \tag{1.3.9}$$

Extremising the generalised entropy in the two-dimensional brane perspective is equivalent to the RT/HRT prescription in three dimensions with a dynamical brane. As argued in [101], when the brane supports an intrinsic gravitational action, the three-dimensional RT/HRT prescription should also include an area contribution from the region where the RT/HRT surface intersects the brane.

Now, calculating entropy of the radiation in the bath (after the Page time) is incredibly straightforward from the bulk/boundary perspectives. It is the entropy of the boundary region $w > 0$, excluding the quantum mechanical degrees of freedom at $w = 0$, which we calculate holographically using RT/HRT in AdS_3. Since this region is just the complement of the region considered above, the extremal surface is identical and the entropies are equal, $S_{\text{rad}} = S_{\text{black hole}}$. The homology surface of the bath is the complement of the homology surface of Σ_x in the AdS_3 bulk. In particular this includes the portion of the dynamical brane outside of Σ_x; part of the AdS_2 black hole is contained in the entanglement wedge of the radiation. This is the appearance of a quantum extremal island from the two-dimensional brane gravity perspective.

Chapter 2

Making Near-Extremal Wormholes Traversable

Time-independent black hole solutions have a wormhole, or Einstein-Rosen bridge, connecting two asymptotic regions. In holography, these solutions are related to entangled states in two copies of the dual CFT [54]. In the classical solution, this wormhole is not traversable; the two asymptotic regions are causally disconnected. In the holographic theory, this is a consequence of the fact that the two copies of the CFT are not coupled (only entangled), so no signal can propagate from one to the other. In [12], a simple coupling between the two boundaries was shown to make the wormhole traversable. In addition to realising the dreams of many science fiction authors, this provides a new insight into the relation between entanglement and spacetime in holographic theories: the passage of a bulk observer through the wormhole can be understood as quantum teleportation in the dual theory, using the entanglement of the dual state as a resource and using the coupling to communicate the needed classical information from one theory to the other [14, 15].

Much of the quantitative analysis of this phenomenon has focused on the simple example of the BTZ black hole in three dimensions, dual to a thermofield double (TFD) state in two copies of a two-dimensional CFT (although TFD states translated in time were considered in [16], and rotating BTZ was considered in [18]). It is

interesting to extend the discussion to more general cases: any entangled state can be used to realise quantum teleportation, but the bulk description in terms of a traversable wormhole may be special to particular forms of entanglement.

In this chapter, we take a step in this direction, by considering adding a boundary coupling to a charged Reissner-Nördstrom black hole in AdS_{d+1}, dual to a TFD state with a chemical potential for the charge in the CFT. The interest in this case is that the black holes have finite entropy (indicating finite entanglement in the dual state) but an infinitely long throat in the extremal limit. We would like to understand how difficult it is to make this infinite wormhole traversable, enabling communication between the two CFTs through the bulk. The divergence in the length of the throat implies that the correlation functions of operators on different boundaries vanishes in the extremal limit, unless the field dual to the operator is tuned to the threshold of an instability [62], suggesting that the effect of the boundary coupling on the bulk geometry may also vanish in this limit. Indeed, we find that unless we tune the bulk field to this instability threshold, we need to take the coupling between the two boundaries to scale to infinity as an inverse power of the temperature to have a finite effect on the bulk geometry in the extremal limit. If we accept this tuning of the coupling, however, we can communicate an amount of information that scales with the entropy of the black hole through the wormhole in the bulk. This is qualitatively different from the quotient construction of [19, 20], where the traversability of the wormhole traversable increased in the extremal limit. The key reason for this difference is that the double trace deformation we consider is a marginal or irrelevant deformation in the near-horizon AdS_2 region.

In section 2.1, we review the bulk solution, its extremal limit, and the dual CFT state. In section 2.2, we add a double-trace boundary coupling and consider the resulting bulk deformation. There are no analytic solutions for the propagator of bulk fields on the full black hole background, so in our analysis we focus on the near-horizon region, which in the extremal limit has an $AdS_2 \times S^{d-1}$ geometry. Boundary couplings on AdS_2 and traversable wormholes have been considered previously [13,

14, 17, 22], but our case is different as we emphasize the relation to the extremal limit of the asymptotic charged black hole geometry; we consider a charged field on the original near extremal black hole, which reduces to a charged field on AdS_2 with a uniform electric field background. We explicitly calculate the propagator for this charged field with the double-trace boundary condition.

We find that to obtain a non-trivial opening of the wormhole, we need to either consider the operators dual to fields at threshold, or take the strength of the coupling to infinity as we take the temperature to zero. We argue that the limit of infinite coupling remains under control, precisely because the distance between the two boundaries in the bulk diverges, so the back-reaction in the bulk remains finite. Under these conditions, the coupling leads to a traversable wormhole in the bulk. The timescale for travel through this wormhole is set by the temperature of the black hole.

We consider the back-reaction of a particle propagating through the wormhole in section 2.3, and infer bounds on the amount of information that can be transmitted through the wormhole. We find that the bound is related to the entropy of the black hole, as expected from the relation to quantum teleportation. This indicates that this entropy from the entanglement of ground states is "available" as a resource for teleportation using simple boundary couplings, just as the thermal entropy in the usual TFD state was.

It would be interesting to extend the calculations to consider other, general entangled states of the dual field theory where the two-point functions between the two boundaries are suppressed [105, 106]. The entanglement in such states in principle provides a resource for quantum teleportation, but it is not clear if this teleportation could have a bulk description as in [12]. It would also be interesting to consider states where the dual field theory has interacted with an environment, as in [29].

2.1 Bulk geometry and boundary CFT

2.1.1 RNAdS bulk solution

We consider Einstein-Maxwell gravity with a negative cosmological constant. The action is

$$S = \frac{1}{2\kappa^2}\int \mathrm{d}^{d+1}x\sqrt{-g}\left[(R-2\Lambda) - \frac{\ell^2}{g_F^2}F^2\right], \tag{2.1.1}$$

where g_F is an effective dimensionless gauge coupling and the cosmological constant is related to the AdS radius by

$$\Lambda = -\frac{d(d-1)}{2\ell^2}. \tag{2.1.2}$$

As discussed in section 1.1.3, this theory admits a spherically symmetric Reissner-Nördstrom AdS black solution with the metric and gauge field given by

$$\mathrm{d}s^2 = -f(r)\mathrm{d}t^2 + \frac{\mathrm{d}r^2}{f(r)} + r^2\mathrm{d}\Omega_{d-1}^2, \qquad A = \mu\left(1 - \frac{r_+^{d-2}}{r^{d-2}}\right)\mathrm{d}t, \tag{2.1.3}$$

where $\mathrm{d}\Omega_{d-1}^2$ is the round metric on S^{d-1} and r_+ is the largest root of the metric function

$$f(r) \equiv 1 - \frac{M}{r^{d-2}} + \frac{Q^2}{r^{2d-4}} + \frac{r^2}{\ell^2}. \tag{2.1.4}$$

The chemical potential μ is related to the other bulk quantities through

$$\mu = \sqrt{\frac{d-1}{2(d-2)}}\frac{g_F Q}{\ell r_+^{d-2}}. \tag{2.1.5}$$

The full black hole geometry has two asymptotic regions, connected by an Einstein-Rosen bridge. These coordinates cover one of the asymptotic regions. Our interest lies in the extremal limit, $Q \to Q_*$, $T \to 0$, which was described in detail in section 1.1.3. We recall that working in the grand canonical ensemble with fixed μ, zero temperature is only reached if $\mu^2 > \mu_c^2 = \frac{(d-1)g_F^2}{2(d-2)\ell^2}$

The Euclidean black hole geometry is a saddle-point for the dual CFT in an appropriate ensemble, and the Lorentzian black hole is a saddle-point for the TFD state obtained by slicing the Euclidean path integral defining the ensemble in half.

The TFD state for the grand canonical ensemble is [62]

$$|\psi\rangle = \frac{1}{\sqrt{Z}} \sum_i e^{-\beta(E_i+\mu Q_i)/2} |E_i, Q_i\rangle_1 \otimes |E_i, -Q_i\rangle_2. \tag{2.1.6}$$

This is a state in the Hilbert space of two copies of the CFT, $|\psi\rangle \in \mathcal{H}_1 \otimes \mathcal{H}_2$, corresponding to the two asymptotic boundaries in the full spacetime, where $|E_i, Q_i\rangle$ are a basis of eigenstates of the Hamiltonian and the $U(1)$ charge in the CFT Hilbert space. For this state to be well-defined at low temperatures, $\beta \to \infty$, $E+\mu Q$ must be bounded below. The black hole is the dominant saddle-point in the grand canonical ensemble for all temperatures if $\mu > \mu_c$ [63], so it provides the dual of this generalised TFD state. The finite entropy of the black hole in the extremal, zero-temperature limit implies an approximate degeneracy in the states at minimal $E + \mu Q$; in the extremal limit the TFD state remains entangled, with an entanglement entropy given by the black hole entropy.

2.1.2 Near horizon geometry

In the zero temperature limit the metric develops a double pole at the horizon $r = r_*$. This implies that the black hole develops an infinite throat; the horizon is an infinite proper distance away on constant t hypersurfaces. Taylor expanding,

$$f(r) = \frac{1}{2}(r - r_*)^2 f''(r_*) + \mathcal{O}(r - r_*)^3 \approx \frac{(r - r_*)^2}{\ell_2^2}, \tag{2.1.7}$$

where

$$\ell_2 \equiv \left[\frac{d(d-1)}{\ell^2} + \frac{(d-2)^2}{r_*^2} \right]^{-\frac{1}{2}}. \tag{2.1.8}$$

For a large black hole $r_* \gg \ell$ we have $\ell_2 \approx \ell/\sqrt{d(d-1)}$. If we introduce the coordinate

$$\zeta = \frac{\ell_2^2}{r - r_*}, \tag{2.1.9}$$

the extremal geometry for large ζ is approximately $\mathrm{AdS}_2 \times S^{d-1}$,

$$\mathrm{d}s^2 \approx \frac{\ell_2^2}{\zeta^2} \left(-\mathrm{d}t^2 + \mathrm{d}\zeta^2 \right) + r_*^2 \mathrm{d}\Omega_{d-1}^2, \qquad A \approx \frac{e_2}{\zeta} \mathrm{d}t, \tag{2.1.10}$$

where we have defined

$$e_2 \equiv (d-2)\frac{\ell_2^2}{r_*}\mu_* = \sqrt{(d-1)(d-2)}\frac{\ell_2^2 Q g_F}{\sqrt{2}\ell r_*^{d-1}}, \tag{2.1.11}$$

with $e_2 \approx g_F/\sqrt{2d(d-1)}$ for $r_* \gg \ell$. We see that ℓ_2 and r_* become the radii of AdS_2 and the $(d-1)$-sphere respectively. In this coordinate system the horizon is at $\zeta \to \infty$, and the geometry above is valid in a region of large ζ, $\zeta > \zeta_c$ where $\zeta_c \sim \ell_2^2/r_*$ is a cutoff where we patch onto the full geometry, which is small for $r_* \gg \ell$.

For near-extremal, finite temperature black holes, we in addition define

$$\zeta_0 \equiv \frac{\ell_2^2}{r_+ - r_*}. \tag{2.1.12}$$

Close to extremality $\zeta_0 \gg \zeta_c$, and the near-horizon geometry becomes an AdS_2 black hole,

$$\mathrm{d}s^2 = \frac{\ell_2^2}{\zeta^2}\left[-\left(1-\frac{\zeta^2}{\zeta_0^2}\right)\mathrm{d}t^2 + \frac{\mathrm{d}\zeta^2}{1-\frac{\zeta^2}{\zeta_0^2}}\right] + r_*^2\mathrm{d}\Omega_{d-1}^2, \qquad A = \frac{e_2}{\zeta}\left(1-\frac{\zeta}{\zeta_0}\right)\mathrm{d}t, \tag{2.1.13}$$

with inverse temperature $\beta = 2\pi\zeta_0$. The extremal limit is $\zeta_0 \to \infty$. Rescaling the coordinates $z = \zeta/\zeta_0$, $\tau = t/\zeta_0$, the AdS_2 metric becomes

$$\mathrm{d}s^2 = \frac{\ell_2^2}{z^2}\left[-(1-z^2)\mathrm{d}\tau^2 + \frac{\mathrm{d}z^2}{1-z^2}\right]. \tag{2.1.14}$$

with $\tilde{\beta} = 2\pi$ and cut-off $z_c = \zeta_c/\zeta_0$. This is the metric of AdS_2 in Rindler coordinates. There is a horizon at $z = 1$ and the conformal boundary is at $z = 0$. We see that in these coordinates the extremal limit $\zeta_0 \to \infty$ leaves the metric unchanged and acts to take the cut off $z_c \to 0$, reflecting the infinite length of the throat in the extremal limit.

These Rindler coordinates cover the right wedge of the spacetime. To discuss the full AdS_2 black hole region, we will also work in Kruskal coordinates on the AdS_2, which are related to the Rindler coordinates above by

$$U, V = \sqrt{\frac{1-z}{1+z}}e^{\pm\tau}. \tag{2.1.15}$$

In these coordinates, the metric and gauge field are

$$\mathrm{d}s^2 = \frac{4\ell_2^2 \mathrm{d}U\mathrm{d}V}{(1-UV)^2}, \quad A = e_2 \frac{V\mathrm{d}U - U\mathrm{d}V}{(1-UV)}. \tag{2.1.16}$$

The bifurcation surface of the Rindler horizon is at $U = V = 0$. The asymptotic boundaries are at $UV = 1$; the right boundary has $U, V > 0$ and the left boundary has $U, V < 0$. The near-horizon geometry is pictured in figure 2.1.

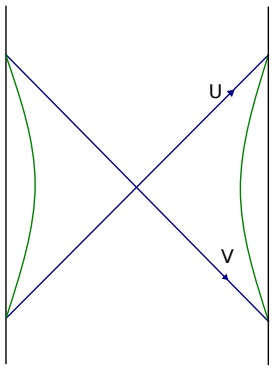

Figure 2.1: Near-horizon AdS_2 geometry of the near-extremal black hole, showing the cutoff boundaries and horizons. The coordinates U, V increase towards the right boundary.

It will also be useful later in discussing the back-reaction to write AdS_2 in terms of embedding coordinates (X_0, X_1, X_2) in $\mathbb{R}^{2,1}$, where AdS_2 is realised as the universal cover of the hyperboloid $-X_0^2 - X_1^2 + X_2^2 = -\ell_2^2$. The embedding coordinates are related to Kruskal coordinates by

$$(X_0, X_1, X_2) = \ell_2 \left(\frac{U-V}{1-UV}, \frac{1+UV}{1-UV}, \frac{U+V}{1-UV} \right). \tag{2.1.17}$$

If we define lightlike coordinates $X_\pm = X_0 \pm X_2$, the hyperboloid is $-X_+X_- - X_1^2 = -\ell_2^2$, and

$$(X_+, X_-, X_1) = \ell_2 \left(\frac{2U}{1-UV}, -\frac{2V}{1-UV}, \frac{1+UV}{1-UV} \right). \tag{2.1.18}$$

The near-horizon AdS_2 region is associated in the dual CFT description with a flow to a theory with an IR conformal symmetry acting just on the time direction [107]. This IR conformal symmetry is broken by the deviation away from AdS_2 in the full geometry, and we have a nearly AdS_2/ nearly CFT_1 duality in the IR [108–110].[1]

[1]The one-dimensional conformal symmetry of the fixed point is not related to the conformal

The dynamics of the Einstein-Mawxell theory in this near-horizon region of the RNAdS black hole reduces to JT gravity [111].

It is useful to organise bulk fields in the near-horizon region in terms of their scaling with respect to this IR conformal symmetry. Consider a bulk scalar field $\Phi(t, r, \Omega)$ of mass m and charge q on the full RNAdS background, dual to a local operator $\mathcal{O}(t, \Omega)$ in the UV boundary theory.

Expanding in spherical harmonics on the sphere,

$$\Phi(x) = \sum_{l,\mathbf{m}} \phi_{l\mathbf{m}}(t, \zeta) Y_{l\mathbf{m}}(\Omega), \qquad \int_{S^{d-1}_{r_*}} \mathrm{d}\Omega Y^*_{l\mathbf{m}} Y_{l'\mathbf{m}'} = \delta_{ll'}\delta_{\mathbf{m}\mathbf{m}'}, \tag{2.1.19}$$

the field modes $\phi_{l\mathbf{m}}$ are scalar fields on AdS_2 of mass

$$m_l^2 \equiv m^2 + \frac{l(l+d-2)}{r_*^2}. \tag{2.1.20}$$

The coupling to the gauge field implies these fields are dual to operators of scaling dimension [107]

$$\Delta = \frac{1}{2} + \sqrt{\frac{1}{4} + m_l^2 \ell_2^2 - q^2 e_2^2}. \tag{2.1.21}$$

If we take $q^2 e_2^2 > m^2 \ell_2^2 + \frac{1}{4}$, the scalar field is unstable to condensing in the near-horizon AdS_2 region [112, 113], and the RNAdS solution will become unstable sufficiently close to extremality. We will be interested in studying fields just below this instability threshold, corresponding to $\Delta \simeq \frac{1}{2}$.[1]

2.2 Wormhole construction

We want to consider the analogue of the traversable wormhole construction of [12] for this black hole. This involves turning on a double trace deformation coupling the two CFTs on the left and right cut-off boundaries with a time-dependant Hamiltonian

$$\delta H(t, \zeta_c) = -h(t)\mathcal{O}_L(-t, \zeta_c)\mathcal{O}_R(t, \zeta_c), \tag{2.2.1}$$

invariance of the ultraviolet CFT_d which is broken by the non-zero chemical potential.

[1] In AdS_2, we could obtain operators with $\Delta < \frac{1}{2}$ by considering the alternative quantization of the scalar field, but the near-horizon limit of the higher-dimensional solution gives us the standard quantization, so $\Delta \geq \frac{1}{2}$.

where $h(t)$ is a coupling which we take to vanish for $t < t_0$, and $\mathcal{O}$ is a boundary CFT operator dual to some bulk scalar field Φ on the RNAdS black hole. This coupling is dual to a modified boundary condition for the scalar Φ relating the fast fall-off part of the scalar at one asymptotic boundary to the slow fall-off part at the other and vice-versa. The idea of [12] is that introducing this coupling (with an appropriate choice of sign of h) produces a quantum stress tensor which violates the averaged null energy condition (ANEC) along the black hole horizon. That is, $\int dU \langle T_{UU} \rangle < 0$, where U is an affine parameter along the horizon. This ANEC violation means that the back-reaction of this quantum stress tensor can make the wormhole traversable; an observer crossing the horizon from one asymptotic region experiences a time advance due to the negative null energy (crossing the horizon moves them to an earlier time), and if they enter sufficiently early this enables them to escape into the other asymptotic region.

In [12], this calculation was carried out on the BTZ black hole, where it was possible to calculate the propagator for the scalar field with the modified boundary condition explicitly, at leading order in the coupling h, and hence to obtain the ANEC violating stress tensor on the horizon. We cannot do such a calculation explicitly in the full RNAdS black hole geometry, as the scalar propagator on this geometry is not known in closed form. We therefore focus on the calculation in the near-horizon AdS_2 region. We can see the essential physics of the extremal limit in this near-horizon region. In particular, we can study how the calculation is affected by the diverging length of the Einstein-Rosen bridge. As discussed in the previous section, in the Rindler coordinates of (2.1.14), this divergence is reflected in the cutoff approaching the boundary of the AdS_2 space, $z_c \to 0$.

We will consider one of the scalar modes $\phi_{l\mathbf{m}}$ on the AdS_2 space, and take a double-trace coupling of the form (2.2.1) on the cutoff boundary at $z = z_c$ in AdS_2. This is not precisely the same as taking this double-trace coupling on the boundary of the full AdS_{d+1} spacetime, but we assume that in the limit of large black holes $r_* \gg \ell$, the renormalization group flow from the AdS boundary to the near-horizon

region has a small effect.

As in [12], we then want to calculate the modified propagator for a charged scalar field on AdS_2 with these boundary conditions. Using the evolution operator $U(t,t_0) = \mathcal{T} e^{-i\int_{t_0}^{t} \mathrm{d}t \delta H(t,\zeta_c)}$ in the interaction picture the modified Wightman function is

$$\langle \phi_R^H(t,\zeta)\phi_R^{H\dagger}(t',\zeta')\rangle = \langle U^{-1}(t,t_0)\phi_R^I(t,\zeta)U(t,t_0)U^{-1}(t',t_0)\phi_R^{I\dagger}(t',\zeta')U(t',t_0)\rangle. \tag{2.2.2}$$

The superscripts H and I represent the Heisenberg and interaction picture respectively. To leading order in h this is (suppressing the ζ coordinate at intermediate steps and omitting I)

$$\begin{aligned} G_+^h \equiv & -i\int_{t_0}^{t} \mathrm{d}t_1 h(t_1)\langle[\mathcal{O}_L(-t_1)\mathcal{O}_R(t_1),\phi_R^\dagger(t)]\phi_R(t')\rangle \\ & \qquad -i\int_{t_0}^{t'} \mathrm{d}t_1 h(t_1)\langle\phi_R^\dagger(t)[\mathcal{O}_L(-t_1)\mathcal{O}_R(t_1),\phi_R(t')]\rangle \\ \approx & \, i\int_{t_0}^{t} \mathrm{d}t_1 h(t_1)\langle\phi_R(t')\mathcal{O}_L(-t_1)\rangle\langle[\phi_R^\dagger(t),\mathcal{O}_R(t_1)]\rangle \\ & \qquad +i\int_{t_0}^{t'} \mathrm{d}t_1 h(t_1)\langle\phi_R^\dagger(t)\mathcal{O}_L(-t_1)\rangle\langle[\phi_R(t'),\mathcal{O}_R(t_1)]\rangle \\ = & \, i\int_{t_0}^{t} \mathrm{d}t_1 h(t_1)\langle\phi_R(t')\mathcal{O}_R^\dagger(-t_1+i\beta/2)\rangle\langle[\phi_R^\dagger(t),\mathcal{O}_R(t_1)]\rangle \\ = & -\int_{t_0}^{t} \mathrm{d}t_1 h(t_1)\mathcal{G}_+(t',\zeta';-t_1+i\beta/2,\zeta_c)\mathcal{G}_{ret}^\dagger(t,\zeta;t_1,\zeta_c) \end{aligned} \tag{2.2.3}$$

where $\mathcal{G}_{+,ret}$ are the Wightman and retarded bulk-to-boundary propagators respectively, with the standard Dirichlet boundary conditions, and we have used analytic continuation to write $t_L = t_R + i\beta/2$. In the second line we used large N factorization and causality $[\mathcal{O}_L,\phi_R] = 0$. The second term in the second line is zero from $\langle\phi\phi\rangle = \langle\phi^\dagger\phi^\dagger\rangle = 0$.

This expression is written in terms of the t,ζ coordinates obtained from the near-horizon limit of the RNAdS black hole; to make the dependence on the extremal limit more explicit, it is useful to switch to the τ, z Rindler coordinates. We have

$$G_+^h = -\zeta_0^{1-2\Delta}\int_{\tau_0}^{\tau} \mathrm{d}\tau_1 h(\tau_1)\mathcal{G}_+(\tau',z';-\tau_1+i\pi,z_c)\mathcal{G}_{ret}^\dagger(\tau,z;\tau_1,z_c), \tag{2.2.4}$$

we see that this vanishes in the extremal limit $\zeta_0 \to \infty$, unless $\Delta = \frac{1}{2}$. The wormhole is becoming infinitely long in this limit, so the bulk-boundary two-point functions $\mathcal{G}$ go to zero as $\zeta_0^{-\Delta}$, and the effect of the change on the boundary conditions on the propagator between points in the interior of the geometry is going to zero. There is an exception for fields with $\Delta = \frac{1}{2}$, which correspond, as discussed at the end of the previous section, to scalars on the threshold of instability. For this case the effect remains finite in the extremal limit.

This discussion is assuming fixed coupling $h(t_1)$. We can instead take it to scale with the inverse temperature β. This source function has dimension $1 - 2\Delta$, so we can take the coupling to scale as

$$h(t_1) = h\left(\frac{2\pi}{\beta}\right)^{1-2\Delta} \theta\left(\frac{2\pi}{\beta}(t_1 - t_0)\right) = h\zeta_0^{2\Delta-1}\theta(\tau_1 - \tau_0), \tag{2.2.5}$$

where h is a dimensionless constant.[1] The scaling of the prefactor will then cancel the $\zeta_0^{1-2\Delta}$ term in G_+^h, giving us a finite result for $\Delta > \frac{1}{2}$. This requires a diverging boundary coupling in the extremal limit, but we see explicitly from the bulk propagator calculation that this has only a finite effect in the bulk.

We will be interested in evaluating G_+^h for bulk points on the Killing horizon. In the Kruskal coordinates, this corresponds to $V = V' = 0$ and some values U, U'. On the right boundary, the Kruskal coordinates U_1, V_1 are related to τ_1, z_c by (2.1.15), which for small z_c gives $1 - U_1V_1 \approx 2z_c$. On the left boundary, we have $(U_L, V_L) = -(V_R, U_R)$. Thus the modified propagator is

$$G_+^h = -\int_{U_0}^{U} \frac{\mathrm{d}U_1}{U_1} h\mathcal{G}_+(U', 0; -V_1, -U_1)\mathcal{G}_{ret}^{\dagger}(U, 0; U_1, V_1) \tag{2.2.6}$$

with $1 - U_1V_1 = 2z_c$.[2]

[1] This scaling of the coupling is introduced by hand to offset the behaviour of the propagator. There is an RG flow from the AdS_{d+1} boundary to the AdS_2 boundary, but this is unaffected by the extremal limit, as the matching surface remains at finite distance from points in the outside region in the extremal limit.

[2] The scaling of the boundary coupling assumed in (2.2.5) cancels against the explicit dependence on ζ_0 in the propagator, so even though the boundary coupling is growing in the extremal limit, the perturbative calculation of the propagator remains valid so long as the dimensionless constant h is small.

2.2.1 Charged scalar in AdS_2

To calculate G_+^h explicitly, we need to know the bulk-boundary propagators for a charged scalar field on AdS_2, with the standard Dirichlet boundary conditions. By symmetry, the propagator for a neutral scalar on AdS_{d+1} is a function only of the invariant distance between the two points. On AdS_2, the bulk-bulk Green's function is (see e.g. [114])

$$G(x,x') = C_\Delta \xi^\Delta {}_2F_1\left(\frac{\Delta}{2}, \frac{\Delta+1}{2}; \frac{2\Delta+1}{2}; \xi^2\right), \tag{2.2.7}$$

$$C_\Delta \equiv \frac{\Gamma(\Delta)}{2^\Delta \pi^{1/2}(2\Delta-1)\Gamma(\Delta-\frac{1}{2})}, \qquad \Delta = \frac{1}{2} + \sqrt{\frac{1}{4} + m^2\ell_2^2}, \tag{2.2.8}$$

where we represent the bulk points in terms of their embedding coordinates X, X', thinking of AdS_2 as the hyperboloid $-X_0^2 - X_1^2 + X_2^2 = -\ell_2^2$ in flat $\mathbb{R}^{2,1}$, and $\xi = -1/X\cdot X'$ is an $SL(2)$[1] invariant related to the invariant distance between the two points.

For a charged scalar, by contrast, the Green's function cannot be written purely as an $SL(2)$ invariant function of the coordinates. This is because the gauge field is not invariant under $SL(2)$ transformations, so the scalar equation of motion isn't either. However, as the field strength is invariant, the gauge field must only transform by some gauge transformation. The solution of the scalar equation of motion will then be some phase times an $SL(2)$ invariant function of the coordinates, $G(x,x') = e^{iqe_2\Lambda(x,x')}P(\xi)$. We can determine $P(\xi)$ by solving for G in the case where the source is at the bifurcation surface of the Rindler horizon, that is at $U' = V' = 0$ in the Kruskal coordinates of (2.1.16). The scalar equation of motion is

$$D^\mu D_\mu \phi - m^2\phi = 0, \tag{2.2.9}$$

where $D_\mu = \partial_\mu - iqA_\mu$. In this case $\xi = z$, and we expect the solution to be independent of τ by time-translation symmetry. Taking $\phi = P(\xi)$, the equation of

[1] We use the notation $SL(2) \equiv SL(2,\mathbb{R})$.

motion becomes

$$\xi^2\partial_\xi\left(\left(1-\xi^2\right)\partial_\xi P\right)-\left(m^2\ell_2^2-q^2e_2^2\frac{1-\xi}{1+\xi}\right)P=0. \tag{2.2.10}$$

Taking the solution that is normalizable at infinity we get

$$P(\xi)=C_\Delta\left(\frac{\xi}{1-\xi}\right)^\Delta\left(\frac{1+\xi}{1-\xi}\right)^{iqe_2}{}_2F_1\left(\Delta+iqe_2,\Delta+iqe_2;2\Delta;\frac{2\xi}{\xi-1}\right), \tag{2.2.11}$$

with Δ now given by expression (2.1.21). For $q=0$, this reduces to (2.2.7) by applying a transformation formula for the hypergeometric function.

In the gauge we have chosen for A, the phase factor Λ in the Green's function vanishes for a source on the bifurcation surface. To find Λ for a general point on the horizon we can move the source along the horizon using an SL(2) transformation. A basis for the Lie algebra $\mathfrak{sl}(2)$ in terms of the embedding coordinates $(X_\pm, X_1)$ is

$$Q^a=\frac{1}{2}\varepsilon^{abc}J_{bc}, \qquad\qquad J_{ab}=X_a\frac{\partial}{\partial X^b}-X_b\frac{\partial}{\partial X^a}. \tag{2.2.12}$$

Let us consider the killing vector

$$v=Q^+=X_-\partial_1-X_1\partial_-=\partial_U-V^2\partial_V, \tag{2.2.13}$$

we see that on the horizon v generates translations along the horizon, so it can be used to move the source off the bifurcation surface. Under the action of this vector field, the gauge field changes by $\mathcal{L}_vA=\mathrm{d}V$. This means that under an infinitesimal transformation $x'=x+\epsilon v$ the gauge transformation required to return A to the form in (2.1.16) is $\Lambda=-\epsilon V$. This suggests that for a source at position U' on the horizon we should make the ansatz $G(x,x')=e^{iq\Lambda(U',V)}P(\xi)$. Plugging this into (2.2.10) one finds that this is a solution provided

$$\Lambda=\ln(U'V-1). \tag{2.2.14}$$

Thus, the bulk-bulk propagator for a source on the horizon is

$$G(U',0,U,V)=(U'V-1)^{iqe_2}P(\xi), \tag{2.2.15}$$

where for a source point on the horizon,

$$\xi = \frac{1 - UV}{1 + UV - 2U'V}. \tag{2.2.16}$$

For a single propagator, the phase factor is not physical; one can always choose a gauge to set it to zero. However, the calculation for G^h_+ involves a product of propagators from the left and right boundaries to the horizon and it's not possible to chose a gauge which sets both of the phase factors to zero. The relative phase between the propagators is physical.

We now want to obtain the bulk-boundary propagator between a point on the horizon and points on the left and right boundaries. For the bulk-boundary propagator $\mathcal{G}_+$ between the left boundary and the horizon, let us consider a point on the horizon at $U' > 0$, so that the two points are spacelike separated. We can then simply take

$$\mathcal{G}_+(U', 0, -V_1, -U_1) = b_m z_c^{-\Delta} G(U', 0, -V_1, -U_1), \tag{2.2.17}$$

where the constant b_m relating the bulk-bulk and bulk-boundary propagators is

$$b_m = \begin{cases} 2\Delta - 1, & \Delta > \frac{1}{2}, \\ \frac{1}{2}, & \Delta = \frac{1}{2}. \end{cases} \tag{2.2.18}$$

In the limit as the bulk point approaches the boundary, $\xi \approx \frac{z_c}{1-U'V}$, so the propagator simplifies, as the hypergeometric function is simply one to leading order. Thus

$$\mathcal{G}_+(U', 0, -V_1, -U_1) = b_m C_\Delta e^{-\pi q e_2} \left(\frac{1}{1 + U'U_1}\right)^{\Delta - iqe_2}. \tag{2.2.19}$$

For the propagator to the right boundary, $\mathcal{G}^\dagger_{ret}(U, 0; U_1, V_1)$, there is an interesting subtlety; at finite cutoff, there is a region of the boundary with $U_1 \in (U(1 - 2z_c), U)$ which is connected to the point $(U, 0)$ by a timelike geodesic, as shown in figure 2.2. The structure of the propagator is different in this region. The size of this region goes to zero as $z_c \to 0$, but we need to check whether it makes a finite contribution to G^h_+. In this region, it is useful to make a change of variables $U_1 = U(1 - 2z_c x)$,

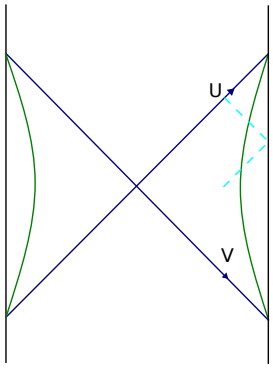

Figure 2.2: The portion of the cutoff boundary between the two dashed curves is connected to the point on the horizon by a geodesic.

with $x \in (0,1)$. Then

$$\frac{2\xi}{\xi-1} = \frac{(1-U_1V_1)}{V_1(U-U_1)} \approx \frac{1}{x}. \tag{2.2.20}$$

Thus, the bulk-bulk propagator does not simplify in this region. However, $P(\xi)$ is a function only of x, with no dependence on z_c at leading order, and the phase factor

$$(UV_1-1)^{iqe_2} \approx (2z_c(x-1))^{iqe_2}. \tag{2.2.21}$$

The bulk-boundary propagator is thus $\mathcal{G}^\dagger_{ret}(U,0;U_1,V_1) = b_m z_c^{-\Delta} G(U,0,U_1,V_1) \sim z_c^{-\Delta-iqe_2} f(x)$, so the contribution to G^h_+ from this region is

$$G^h_+ \sim \int_{U(1-2z_c)}^{U} \frac{\mathrm{d}U_1}{U_1} \mathcal{G}^\dagger_{ret}(U,0;U_1,V_1) \sim z_c^{1-\Delta-iqe_2} \int_0^1 \mathrm{d}x f(x), \tag{2.2.22}$$

so the contribution from this region vanishes in the limit as $z_c \to 0$ so long as $\Delta < 1$. We will henceforth assume that we consider operators with $\frac{1}{2} \leq \Delta < 1$.

In the region $U_1 \in (U_0, (1-2z_c)U)$, we have

$$\frac{2\xi}{\xi-1} \approx \frac{z_c}{UV_1-1}, \tag{2.2.23}$$

so

$$\mathcal{P} = b_m z_c^{-\Delta} P = b_m e^{-i\pi\Delta} (UV_1-1)^{-\Delta}, \tag{2.2.24}$$

and

$$\mathcal{G}_{ret,R} = (UV_1-1)^{iqe_2} 2\,\mathrm{Im}\,\mathcal{P} = -2b_m C_\Delta \sin(\pi\Delta) \left(\frac{U_1}{U-U1}\right)^{\Delta-iqe_2}. \tag{2.2.25}$$

We arrive at

$$G_+^h \approx -\frac{h\mathcal{C}_\Delta}{2}\int_{U_0}^{U}\frac{\mathrm{d}U_1}{U_1}\left(\frac{1}{1+U_1U'}\right)^{\Delta_q^*}\left(\frac{U_1}{U-U_1}\right)^{\Delta_q}$$
$$\equiv -\frac{h\mathcal{C}_\Delta}{2}\int_{U_0}^{U}\frac{\mathrm{d}U_1}{U_1}H(U,U',U_1), \tag{2.2.26}$$

where $\Delta_q \equiv \Delta + iqe_2$ and $\mathcal{C}_\Delta \equiv 4b_m^2 C_\Delta^2 e^{-\pi q e_2}\sin(\pi\Delta)$.

2.2.2 Calculation of the stress tensor on the horizon

We now calculate the quantum stress tensor on the horizon due to this boundary condition, showing that it leads to a violation of the ANEC. The stress tensor for a charged scalar is[1]

$$T_{\mu\nu} = (D_\mu\phi)(D_\nu\phi)^\dagger + (D_\nu\phi)(D_\mu\phi)^\dagger - g_{\mu\nu}g^{\rho\sigma}(D_\rho\phi)(D_\sigma\phi)^\dagger - g_{\mu\nu}m^2|\phi|^2. \tag{2.2.27}$$

In the original AdS_2 geometry $g_{UU} = A_U = 0$ on the horizon, so the terms involving the metric and gauge field drop out. The one-loop expectation value can then be related to the modified bulk propagator via point splitting,

$$\langle T_{UU}\rangle = 2\langle\partial_U\phi\partial_U\phi^\dagger\rangle = \lim_{U'\to U}\partial_{U'}\partial_U(G_+^h(U,U') + G_+^{h\dagger}(U,U')). \tag{2.2.28}$$

Evaluating the integral in (2.2.26) we find a closed form expression for the modified bulk propagator on the horizon[2]

$$G_+^h = \frac{h\mathcal{C}_\Delta}{2(\Delta_q-1)}\left(\frac{1}{1+U_0U'}\right)^{\Delta_q^*}\left(\frac{U_0}{U-U_0}\right)^{\Delta_q-1}$$
$$\times F_1\left(1;1-\Delta_q,\Delta_q^*;2-\Delta_q;1-\frac{U}{U_0},\frac{(U_0-U)U'}{1+U_0U'}\right), \tag{2.2.29}$$

where F_1 is the Appell hypergeometric function. Thus, from (2.2.27), we also have a closed form expression for the quantum stress tensor.

The wormhole is rendered traversable if the ANEC is violated on the horizon, so

[1] As the matter fields are charged, they will source a change in the electric field as well, which changes the Maxwell stress tensor at the same order, but because of the index structure this does not contribute to the null-null component of the stress tensor we consider below.

[2] Note that we have used a transformation formula for the Appell function to get G_+^h in this form.

we are interested in calculating the ANE given by

$$\mathcal{A}^{\infty}(U_0) = \int_{U_0}^{\infty} \mathrm{d}U \langle T_{UU} \rangle = 2 \int_{U_0}^{\infty} \mathrm{d}U \lim_{U' \to U} \partial_{U'} \partial_U \operatorname{Re} G_+^h, \tag{2.2.30}$$

where the superscript indicates that we are considering a source that is left on forever. Note that $\mathcal{A}^{\infty}$ has a simple relationship to the ANE for a source that is turned on for a finite interval (U_0, U_f),

$$\mathcal{A}(U_0, U_f) = \mathcal{A}^{\infty}(U_0) - \mathcal{A}^{\infty}(U_f). \tag{2.2.31}$$

Rather than attempting the daunting task of directly integrating the stress tensor, we choose a different tack; instead, we consider an instantaneous source function given by

$$h^{inst}(t_1) = h \left(\frac{2\pi}{\beta}\right)^{1-2\Delta} \delta\left(\frac{2\pi}{\beta}(t_1 - t_0)\right) = \frac{h}{\zeta_0^{1-2\Delta}} U_0 \delta(U_1 - U_0). \tag{2.2.32}$$

The ANE for this source is related to $\mathcal{A}^{\infty}$ by (see [21])

$$\mathcal{A}^{\infty}(U_0) = \int_{U_0}^{\infty} \frac{\mathrm{d}u}{u} \mathcal{A}^{inst}(u), \tag{2.2.33}$$

where the limits of integration are determined by $\mathcal{A}^{\infty}(\infty) = 0$, i.e. if the source is never turned on, nothing happens. The delta function source significantly simplifies the calculation. For an instantaneous source, the modified bulk propagator is simply

$$G_+^{inst} = -\frac{1}{2} h \mathcal{C}_{\Delta} H(U, U', U_0). \tag{2.2.34}$$

To calculate the ANE, however, it is better to start with the general expression (2.2.26) and take the derivatives before setting the source to a delta function. This gives closed form expressions for both ANEs

$$\mathcal{A}^{inst}(U_0) = \operatorname{Re}\left[\frac{h\mathcal{C}_{\Delta}\Gamma\left(1-\Delta_q\right)\Gamma\left(2\operatorname{Re}\Delta_q+1\right)}{\Gamma\left(\Delta_q^*\right)} \frac{U_0^{2\Delta_q+1}}{(1+U_0^2)^{2\operatorname{Re}\Delta_q+1}}\right], \tag{2.2.35}$$

$$\mathcal{A}^{\infty}(U_0) = \operatorname{Re}\left[\frac{h\mathcal{C}_{\Delta}\Gamma\left(1-\Delta_q\right)\Gamma\left(2\Delta_q+1\right)}{(2\Delta_q+1)\Gamma\left(\Delta_q\right)} \frac{{}_2F_1\left(\frac{1}{2}+\Delta_q, \frac{1}{2}-\Delta_q; \frac{3}{2}+\Delta_q; \frac{1}{1+U_0^2}\right)}{(1+U_0^2)^{\Delta_q+\frac{1}{2}}}\right]. \tag{2.2.36}$$

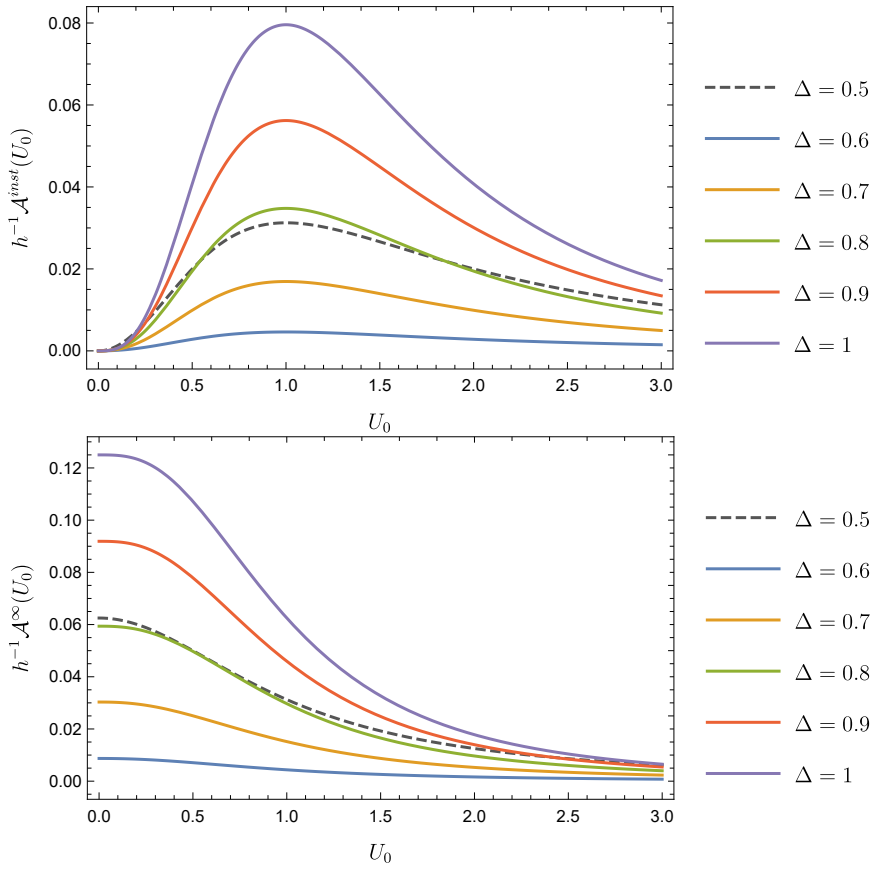

Figure 2.3: The ANE as a function of U_0 for $q = 0$.

It is interesting to note that if we considered an uncharged field, $q = 0$, our final expression has the same U_0 dependence as was found for the BTZ black hole in [12]. $\mathcal{A}^{inst}$ and $\mathcal{A}^{\infty}$ for $q = 0$ are plotted against U_0 for different values of Δ in figure 2.3. For the instantaneous source, maximal ANE is achieved when the non-local coupling is turned on at $U_0 = 1$ which corresponds to $t_R = t_L = 0$. Conversely, $\mathcal{A}^{\infty}$ is maximal when the coupling is turned on in the infinite past $U_0 = 0$ ($t_R = t_L = -\infty$). For $q = 0$ and $\Delta = \frac{1}{2}$, we have the simple expressions

$$\mathcal{A}^{inst}(U_0) = \frac{hU_0^2}{8\left(1 + U_0^2\right)^2} \tag{2.2.37}$$

$$\mathcal{A}^{\infty}(U_0) = \frac{h}{16\left(1 + U_0^2\right)}. \tag{2.2.38}$$

The ANE for $q > 0$ is plotted against U_0 in figure 2.4, and against Δ for representative values of U_0 in figure 2.5. We see that while it increases with Δ for $q = 0$, for $q > 0$ there is some maximum at an intermediate value $\Delta \in (\frac{1}{2}, 1)$.

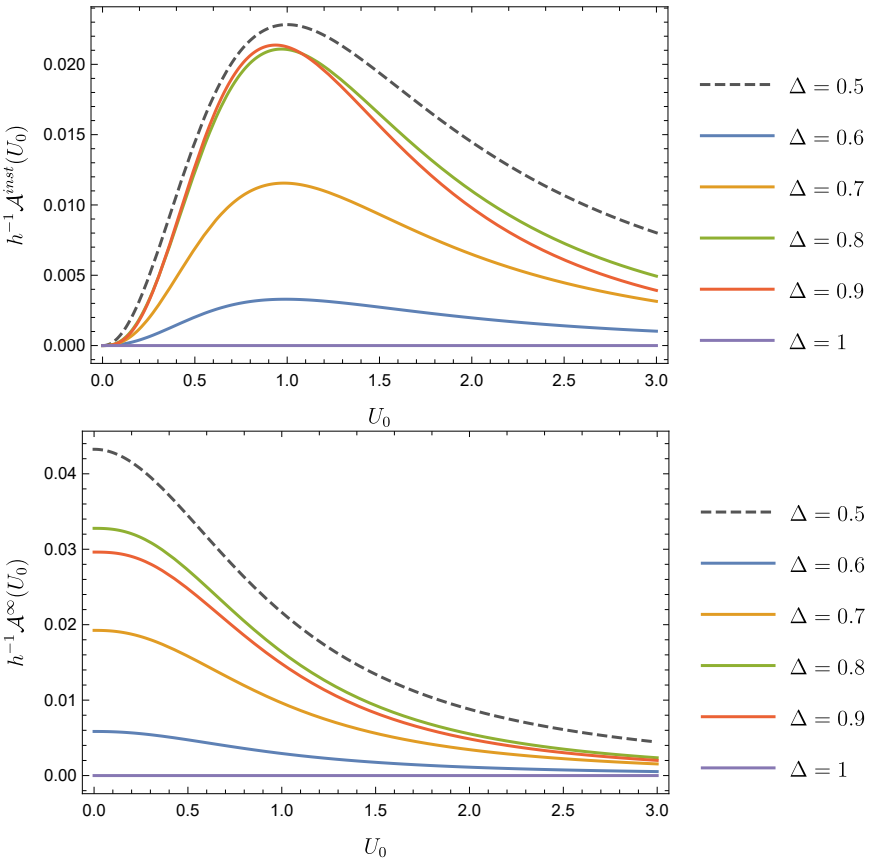

Figure 2.4: The ANE as a function of U_0 for non-zero $qe_2 = 0.1$.

2.3 Back-reaction and information bound

As discussed in the introduction, the back-reaction of this energy along the horizon will produce a time advance, making it possible for a message from the left boundary sent in at early times to reach the right boundary. This makes the Einstein-Rosen bridge in the black hole into a traversable wormhole. We would like to understand how much information can be transmitted through the wormhole, which requires taking into account the back-reaction of the message. In the AdS_2 context, these back-reaction questions can be easily addressed using a JT gravity description of the nearly-AdS_2 gravitational dynamics, as in [14] (see [109, 115] for further discussion). The result is the same as in [14], as the back-reaction only depends on the ANE along the horizon, which have seen above is qualitatively the same for uncharged or charged fields. Thus, introducing a double-trace coupling for a single field only allows us to communicate order one bits of information from one boundary to the

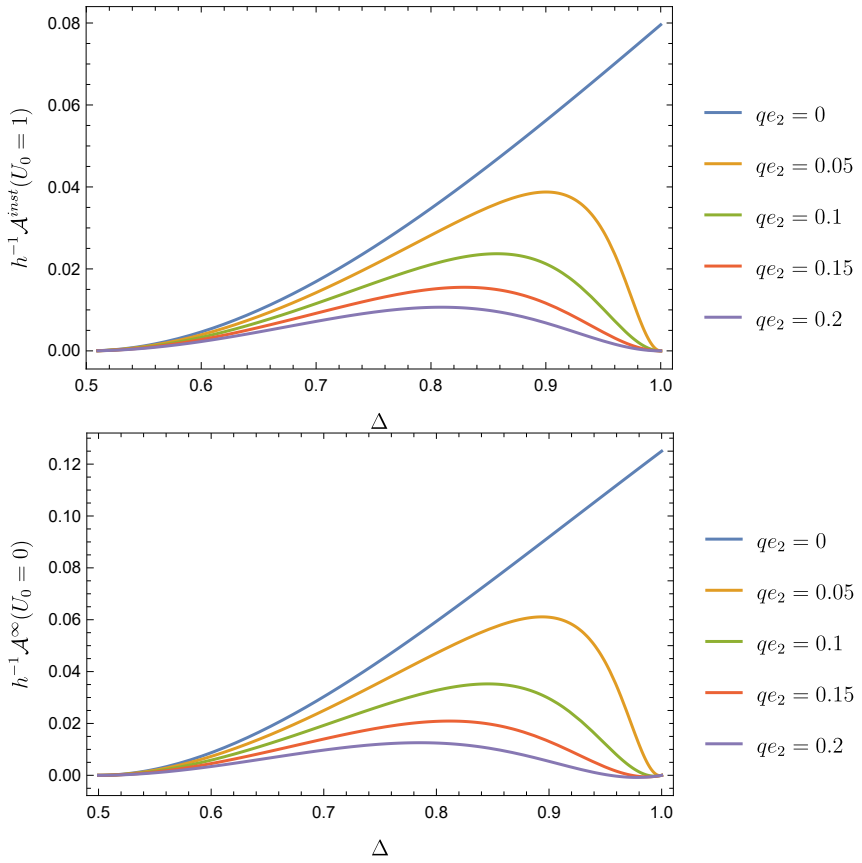

Figure 2.5: The ANE as a function of Δ. For $q > 0$, the ANE is suppressed at $\Delta = 1$ by the factor of $\sin(\pi\Delta)$ in $\mathcal{C}_\Delta$.

other.

We will describe the calculation here briefly for completeness. In the JT gravity description, we take the bulk geometry to be fixed to be AdS_2, and the position of the boundaries is the dynamical information. When some matter is emitted into the bulk from one of the boundaries, the back-reaction causes the boundary trajectory to change. This change is described in terms of the SL(2) charges associated with the trajectories of the boundary and the emitted particles.

In terms of the embedding coordinates X^a, the trajectories of the cutoff boundaries are described by $X \cdot Q = -2\Phi_b$, where Q^a is a vector in $\mathbb{R}^{2,1}$ which specifies the charges of the boundary trajectory under the SL(2) isometries of the bulk (we are thinking of the boundary as a particle moving in the bulk), and Φ_b is the boundary value of the dilaton. This equation gives a hyperbolic trajectory for the boundary, and the vector Q^a can also be thought of as specifying the center of this hyperboloid

$X^a = \bar{X}^a \propto Q^a$, that is, the point in the bulk which is light-like separated from the points where the trajectory meets the conformal boundary of AdS_2. For the near-horizon AdS_2 geometry described in (2.1.14), the boundaries lie at $X_1 \approx \ell_2/z_c$, whose center is the bifurcation surface at $U = V = 0$, that is $\bar{X}_\pm = 0, \bar{X}_1 = \ell_2$. This implies $X \cdot \bar{X} = -\ell_2^2/z_c$. For the right boundary, the SL(2) charge is $Q_R = Q$, and for the left boundary, $Q_L = -Q$, so that the total SL(2) charge vanishes, $Q_L + Q_R = 0$.

If we inject matter into the bulk it will also carry an SL(2) charge. Matter particles in the bulk follow geodesics, which can be described by trajectories $X \cdot Q_m = 0$, where Q_m is the SL(2) charge of the matter. The total SL(2) charge vanishes, $Q_L + Q_R + Q_m = 0$, so the addition of matter will change the trajectories of the boundaries. If say the left boundary emits some positive energy matter, the recoil pushes it away, increasing the distance between the two boundaries.

We are interested in two forms of back-reaction. First we consider the back-reaction of the bulk stress tensor due to the double-trace coupling. In the previous section, we calculated the null energy integrated along the horizon; this is precisely the charge

$$Q_{m,-} = \int \mathrm{d}U \langle T_{UU} \rangle. \tag{2.3.1}$$

This matter was emitted by the right boundary, so this shifts the right boundary trajectory by $Q_R \to Q_R - Q_m$. The negative $Q_{m,-}$ thus moves the center of the right boundary trajectory to negative V; the shift $\Delta V = CQ_{m,-}/2$, where C is a normalization factor depending on our conventions for the charges. This makes it possible for messages leaving the left boundary at early times, at small negative V, to reach the right boundary. Note that the message needs to enter the wormhole at some finite time in the past in the Rindler time coordinate τ; this implies that the time with respect to the asymptotic time $t = \zeta_0 \tau$ scales as the inverse temperature, so in the extremal limit the time it takes the message to go through the wormhole diverges.

Secondly, we consider the back-reaction on the left boundary of the emission of such a message. The message must be emitted at early times, so it is highly boosted

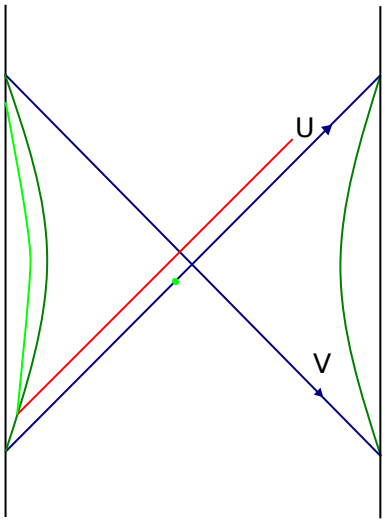

Figure 2.6: The emission of a null particle back-reacts on the trajectory of the left boundary, moving the center down along the horizon.

relative to our bulk coordinate system, and will follow a nearly null trajectory in the bulk, with some momentum $Q'_{m,+} = p_V$. The back-reaction of the message shifts the left boundary by $Q_L \to Q_L - Q'_m$, moving the two boundaries further apart and suppressing the effect of the double-trace coupling. The center of the left boundary trajectory shifts down by $\delta U = Cp_V/2$, as pictured in figure 2.6. This corresponds to transforming the boundary trajectory by a translation along the vector field v considered earlier.

This shift can thus be accounted for by a shift in the horizon coordinate in the calculation of the propagator from the left boundary to the horizon, so the integrand of the modified bulk propagator in the shockwave geometry is

$$H_\delta(U, U', U_1) = \left(\frac{1}{1 + U_1(U' + \delta U)}\right)^{\Delta_q^*} \left(\frac{U_1}{U - U_1}\right)^{\Delta_q}. \tag{2.3.2}$$

Repeating the same analysis as before we find

$$\mathcal{A}_\delta^{inst}(U_0) = \mathrm{Re}\left[\frac{h\mathcal{C}_\Delta \Gamma\left(1 - \Delta_q\right)\Gamma\left(2\,\mathrm{Re}\,\Delta_q + 1\right)}{\Gamma\left(\Delta_q^*\right)} \frac{U_0^{2\Delta_q+1}}{\left(1 + U_0^2\left(1 + \frac{\delta U}{U_0}\right)\right)^{2\,\mathrm{Re}\,\Delta_q+1}}\right]. \tag{2.3.3}$$

Comparing this expression to (2.2.35) we see that the probe approximation is valid for $\delta U/U_0 \ll 1$. This implies that the total momentum carried by the message is

bounded,

$$\frac{p_V^{total}}{2} < \frac{U_0}{C}. \tag{2.3.4}$$

A lower bound on the momentum carried by the individual particles making up the message can be found using the uncertainty principle,

$$p_V^{each} \gtrsim \frac{1}{\Delta V} = \frac{2}{C|\mathcal{A}|}. \tag{2.3.5}$$

Combining this with the probe approximation gives a bound on the number of bits that can be sent through the wormhole,

$$N = \frac{p_V^{total}}{p_V^{each}} < U_0|\mathcal{A}|. \tag{2.3.6}$$

We see from the discussion of the ANE in the previous section that the RHS takes values less than one.

Thus, coupling a single field in the AdS_2 region would only allow us to send less than one bit of information before the back-reaction of the message starts to close up the wormhole. It might seem surprising that this result is independent of the entropy of the black hole; but this is just because we have focused on coupling a particular spherical harmonic $\phi_{\ell\mathbf{m}}$ of a $(d+1)$-dimensional scalar field Φ. If we want to restrict attention to operators with $\Delta = \frac{1}{2}$, for which we can generate a traversable wormhole with a finite boundary coupling even in the extremal limit, we will only be able to consider the s-wave excitation of a scalar that saturates the instability threshold, and we will only be able to communicate less than a single bit for each field. However, if we allow consideration of operators with $\frac{1}{2} < \Delta < 1$ in the AdS_2 region, with a coupling that scales with the temperature, we get to consider a large number of spherical harmonics on the S^{d-1}: for $r_* \gg \ell$, we have K spherical harmonics with $\Delta < 1$ where

$$K \sim \frac{r_*^{d-1}}{\ell_2^{d-1}} \sim \frac{A}{\ell^{d-1}}, \tag{2.3.7}$$

so the number of fields we can introduce such a coupling for, and hence the number of bits we can send through the wormhole, scales as the area of the horizon in

AdS units, as in the BTZ analysis of [21]. As in [21], to make the number of bits scale like the area in Planck units, we would need to consider a large number of $(d+1)$-dimensional fields Φ.

Chapter 3

Islands and Mixed States in Closed Universes

3.1 Introduction

The Ryu-Takayanagi proposal [7] and its generalizations [64, 79, 80] have given us important insights into the description of spacetime in holographic theories of quantum gravity. This has recently been extended by the discovery of the island phenomenon [23–25]: when we consider entangling the holographic theory with another quantum system, the part of the spacetime described by the holographic dual can be bounded by a quantum extremal surface [80], and the spacetime region beyond this surface (the island) is encoded in the other system. These ideas were initially developed for holographic theories, but they can be derived from the Euclidean gravitational path integral [26, 27], so they are believed to apply more generally.

Consider a conventional quantum mechanical system (which could be a quantum field theory, or a simpler system, such as a spin chain) which is entangled with a gravitational system. The island rule is that given a semiclassical, effective description of the gravitational system, the *fine-grained* entropy of some subsystem A in the quantum system is given by

$$S(A) = \min_{\mathcal{I}} \operatorname{ext}_{\mathcal{I}} S_{\text{gen}}(A \cup \mathcal{I}), \tag{3.1.1}$$

where $\mathcal{I}$ is the *island*, some spatial subregion of the spacetime the gravitational system lives in, and S_{gen} is the generalised entropy. If the semiclassical theory is Einstein gravity coupled to matter, $S_{\text{gen}}(A \cup \mathcal{I}) = \frac{A_{\partial\mathcal{I}}}{4G} + S_{\text{eff}}(A \cup \mathcal{I})$, where $A_{\partial\mathcal{I}}$ is the area of the boundary of the island and S_{eff} is the von Neumann entropy of the effective semi-classical state of A together with the fields in the island. The spatial subregion that extremises S_{gen} is called a quantum extremal island; the surface $\partial\mathcal{I}$ is the quantum extremal surface. If there are multiple islands in the spacetime, we choose the one which minimizes the entropy.

We include an island in the spacetime if there is sufficient entanglement between A and the spacetime in the semi-classical state to compensate for the large contribution to S_{gen} from the area term. Then $S(A) < S_{\text{eff}}(A)$, and the true fine-grained entropy of A calculated according to this prescription is smaller than the effective entropy. The derivation of this formula from the path integral [26,27] tells us that the effective semi-classical state in the island region is encoded in A; semi-classically it looks like we have a seperate Hilbert space $\mathcal{H}_{\mathcal{I}}$ of the quantum fields on the island, but in fact this is encoded as a code subspace in the Hilbert space $\mathcal{H}_A$ of the quantum system A.

The path integral derivation suggests this prescription applies quite generally, and in particular we can consider its application to a closed universe. We do not have a good understanding of quantum gravity in closed universes, but we can still apply the island rule, as it only requires an understanding of the semi-classical state. In a closed universe U, if the gravitating system is entangled with A but otherwise in a pure state, then we can take the island to be the whole universe [25, 40].[1] Then there is no boundary term, and $S_{\text{gen}}(A \cup U) = S_{\text{eff}}(A \cup U)$. As soon as there is any entanglement between the closed universe and A, the whole closed universe is encoded in $\mathcal{H}_A$. In section 3.2, we review a simple doubly holographic model which illustrates this in a well-understood setting. Thus, entanglement allows us to recover some aspects of a theory of quantum gravity on a closed universe from this quantum

[1] For another perspective see [36, 37].

system, in a way which generalizes the holographic story.

This might seem surprising, as the semiclassical theory on U could have a Hilbert space $\mathcal{H}_U$ which is much larger than $\mathcal{H}_A$. However, we have so far considered only semi-classical states on U which have some entanglement with A but are otherwise pure. The purpose of the present work is to explore the extension to cases where the closed universe is in a mixed state. In the holographic context, even if individual pure states are encoded in a dual system, this encoding can break down when we consider mixtures of them; this is the essential issue underlying the original appearance of the islands in [23, 24]. To fully understand encoding of the semiclassical Hilbert space $\mathcal{H}_U$ in $\mathcal{H}_A$, we should ask how the encoding works when we consider mixed states in $\mathcal{H}_U$ with some entanglement with A. We can express this by considering a situation where U is entangled both with A and with some other quantum system B which acts as a purifier for the mixed state in $\mathcal{H}_U$. There is then clearly a competition between entanglement with A and entanglement with B, and we can have either $S_{\text{eff}}(A \cup U) < S_{\text{eff}}(A)$ or $S_{\text{eff}}(A \cup U) > S_{\text{eff}}(A)$; the whole universe is not always included in an island for A.

The qualitative picture is very similar to the holographic story mentioned above: if we start with a situation where the spacetime is encoded in a single quantum system, and add some additional entanglement of the semi-classical state on the spacetime with another system, initially this describes a mixed state of the quantum fields on the spacetime. When the entanglement with the new system gets large enough, a new island appears, and the spacetime is encoded partially or wholly in this second system. We will explore the limitations this imposes on the entropy of the mixed state we can consider in the context of our simple model.

We explore this issue in detail in a simple doubly holographic braneworld model, proposed in [43]. The original model, reviewed in section 3.2, has a bulk spacetime with two boundaries, where one boundary is a dynamical brane and the other boundary is an asymptotically AdS boundary. We take both boundaries to be closed spaces, and they are connected by a spatial wormhole (Einstein-Rosen bridge) in the bulk.

By integrating out the bulk spacetime, we can obtain a semi-classical description of this spacetime where we have a CFT coupled to gravity on the dynamical brane, and a second non-gravitating CFT on the asymptotic boundary, in an entangled state. Then according to the island formula, when we calculate the fine-grained entropy of the non-gravitating CFT, we include the whole of the other closed universe in an island. This corresponds simply to the bulk statement that the entanglement wedge for the CFT on the single asymptotically AdS boundary includes the whole of the bulk spacetime. Semi-classically we had an entangled state relating degrees of freedom on the brane and degrees of freedom on the boundary, but the microscopic theory is a field theory on the boundary; the semi-classical state is encoded in some subspace in this.

One approach to studying a brane entangled with multiple systems would be to simply subdivide the non-gravitating boundary in this model into several regions. The appearance of islands associated with subregions in this model was indeed already explored in [43]. We instead consider an extension of this model with a brane and multiple asymptotic regions, dual to several copies of a CFT. These different boundaries are connected by a multiboundary wormhole. We will focus on a wormhole with three asymptotic regions, one of which we cut off with a dynamical brane. This has a couple of advantages: since the two boundaries aren't coupled, the entanglement between them is time-independent and free of ultraviolet divergences. The lengths of the horizons associated with the different asymptotic regions are also all independent parameters.

We review the bulk wormhole geometry in section 3.3. We introduce the brane in section 3.4. In the semi-classical description, we have a CFT coupled to gravity on the brane, and non-gravitating CFTs on the asymptotic boundaries, in some entangled state $|\tilde{\Sigma}\rangle$. Microscopically, the whole spacetime, including the brane, is encoded in a state $|\Psi\rangle$ on the two asymptotic boundaries. To determine which of the CFTs the brane is encoded in, we determine the fine-grained entropies by comparing the different possible Ryu-Takayanagi (RT) surfaces in the bulk. The brane can be

fully encoded in one of the two systems or partially in each, with a quantum extremal surface dividing the two regions. The latter occurs if the entanglement between the brane and the other systems is large enough to compensate for the boundary term in S_{gen}.

We can treat one of the asymptotic boundaries as a reference system; tracing over this, we obtain a mixed state both semi-classically and microscopically. The semi-classical state will give a mixed state on the brane if it is entirely encoded in the other system, but still has some entanglement with the reference system. In this case we have a microscopic mixed state, part of whose entropy is associated with the semi-classical mixed state on the brane. When we consider multiboundary wormholes with long horizons, as in [116], we can split the microscopic entropy into a part associated semi-classically with entanglement between the reference system and the brane and a part associated with the entanglement between the reference system and the other system. We show that the entropy of the semi-classical mixed state on the brane has two bounds: it is always less than half the coarse-grained entropy of the fields on the brane in this semi-classical state (otherwise it would be favourable to have the brane entirely encoded in the reference system rather than the other boundary) and less than the contribution to the generalized entropy from boundaries of an island (otherwise it would be favourable to have an island on the brane). The simplicity of the latter bound is due to our model describing a particular kind of mixed state, where the reference system is entangled with a particular local region on the brane. We could certainly imagine entangling the brane with the reference system in more complicated ways, which could relax this bound. The first bound seems more universal.

We conclude with a brief discussion and consideration of future directions in section 3.5.

3.2 Braneworld model

The model we consider was proposed in [43]; this was further developed in [44–47]. It can be seen as an example of the doubly holographic setup of [25], which was applied to island calculations in [40]. The idea is to consider an end of the world brane in AdS which has a closed universe cosmology as its worldvolume, and seek insight into the quantum theory of the closed universe from the holographic dual CFT.

We will work with the simplest model of an end of the world brane, developed in [65, 117]. We consider a three-dimensional locally AdS_3 bulk, dual to a two-dimensional CFT, with a constant-tension end of the world brane in the bulk, holographically dual to some one-dimensional boundary degrees of freedom coupled to the CFT_2. The bulk three-dimensional theory has action

$$I = \frac{1}{16\pi G}\int_M d^3x\sqrt{-g}(R-2\Lambda)+\frac{1}{8\pi G}\int_{\partial M} d^2y\sqrt{-h}\,K-\frac{1}{8\pi G}\int_Q d^2y\sqrt{-h}\,\frac{T}{\ell} \quad (3.2.1)$$

where G is the three-dimensional Newton constant, $\Lambda = -\frac{1}{\ell^2}$ is a cosmological constant, K is the trace of the extrinsic curvature and T is the tension of the end of the world brane with worldvolume Q, which we take to be one component of the boundary ∂M of the spacetime, the other component(s) corresponding to asymptotically AdS boundary(ies). We will work in units where the AdS scale $\ell = 1$. The brane has a stress-energy tensor $8\pi G T_{ab} = -T h_{ab}$, and the action implies that the boundary condition for the bulk metric at Q is $K_{ab} - K h_{ab} = 8\pi G T_{ab} = -T h_{ab}$.

A simple solution of this theory is pure AdS_3 in Poincaré coordinates,

$$ds^2 = \frac{-dt^2 + dx^2 + dz^2}{z^2}, \quad (3.2.2)$$

with the end of the world brane Q along $x = z\tan\theta$ for $x > 0$, where $\theta = \sin^{-1}(T)$, so we have a solution for $T < 1$. For $T > 0$, the spacetime is the region between the AdS boundary at $z = 0$ for $x < 0$ and the brane worldvolume Q, as pictured in figure 3.1.[1] We obtain a useful insight into the interpretation of the tension by considering

[1] For $T < 0$, the brane has the same position but the spacetime is the wedge between the AdS

the entanglement entropy for a region A in the AdS boundary with $x \in (-L, 0)$. The bulk RT surface drawn in figure 3.1, cut off at $z = \epsilon$, gives

$$S(L) = \frac{c}{6} \ln\left(\frac{L}{\epsilon}\right) + \ln \mathfrak{g}, \tag{3.2.3}$$

where $c = \frac{3}{2G}$ is the central charge of the dual two-dimensional CFT, and

$$\ln \mathfrak{g} = \frac{1}{4G} \tanh^{-1} T. \tag{3.2.4}$$

The first contribution to the entropy comes from the part of the surface at $x < 0$, while the second part comes from the part at $x > 0$. The first contribution is the usual entanglement entropy for an interval of length L in a two-dimensional CFT, while the second term is the boundary entropy which appears in BCFTs.[1] Thus, $\ln \mathfrak{g}$ can be viewed as a boundary analogue of the central charge, and we see that T controls this central charge, analogously to the relation between ℓ and c.

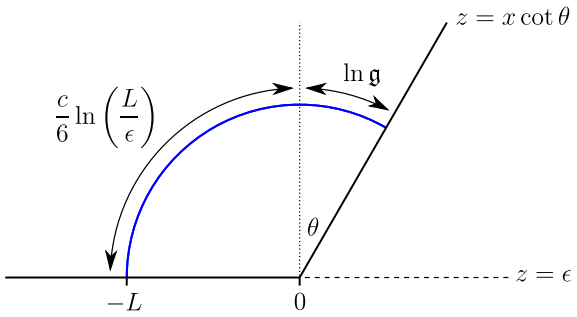

Figure 3.1: A constant-time slice of the geometry with an end of the world brane in Poincaré-AdS, showing the RT surface for a region $x \in (-L, 0)$ on the boundary

It is useful to consider the regime $T \approx 1$, when $\theta \approx \pi/2$, and the end of the world brane can be viewed as a cutoff version of the AdS boundary. This corresponds to a limit where the number of boundary degrees of freedom is large, $\ln \mathfrak{g} \gg c$. We can then obtain an effective gravitational theory on the brane by integrating over the bulk spacetime. In the higher-dimensional context, this gives a Karch-Randall theory, with an effective Einstein action on the brane [118–120]. In the present

boundary at $z = 0$ for $x > 0$ and the brane worldvolume Q.

[1] From the CFT perspective, there is a boundary state $|B\rangle$ associated to the boundary at $x = 0$, and $\mathfrak{g} = \langle 0|B\rangle$.

two-dimensional case, this gives a non-local gravity action [121], as discussed in [101]. This can be written in a local form by introducing an auxiliary scalar field; the brane gravity action is then a Polyakov action

$$I_{Poly} = \frac{1}{32\pi G}\int d^2y\sqrt{-h}\left[-\frac{1}{2}h^{ab}\nabla_a\phi\nabla_b\phi + \phi\,{}^{(2)}R - 2e^{-\phi}\right], \tag{3.2.5}$$

where ${}^{(2)}R$ is the Ricci scalar of the metric h_{ab} on the brane.

In earlier holographic analyses, attention focused on the relation between the bulk spacetime description, where we have Einstein gravity coupled to a constant-tension brane, and the boundary perspective, where we have the CFT dual to the bulk theory with some boundary state $|B\rangle$ at $x = 0$. The novelty in recent work, such as in [25], is to highlight an intermediate effective theory, where we integrate over the bulk spacetime to obtain an effective gravity theory on the brane; we then have a non-gravitational CFT for $x < 0$ joined across an interface to the same CFT coupled to the brane gravity theory (3.2.5) for $x > 0$. This is then a useful model to study the appearance of islands in the gravitational theory, by relating them to the classical RT surfaces in the bulk gravity. We can illustrate the idea by relating the entropy (3.2.3) to the brane gravity theory. For the Polyakov action (3.2.5), the generalized entropy is

$$S_{\rm gen}(\mathcal{I}) = \frac{\phi_{\partial\mathcal{I}}}{8G} + S_{\rm eff}(\mathcal{I}), \tag{3.2.6}$$

where $\phi_{\partial\mathcal{I}}$ is the value of the scalar at the boundary of $\mathcal{I}$ and $\phi_{\partial\mathcal{I}}/2$ is the zero-dimensional analogue of the area. In the solution we considered above, the brane has an AdS_2 geometry with ${}^{(2)}R = -2/\ell_2^2 = -2(1-T^2)$, and the auxiliary scalar is

$$\phi = \ln\left(-\frac{2}{{}^{(2)}R}\right) = -\ln(1-T^2) \approx 2\tanh^{-1}T. \tag{3.2.7}$$

Thus, we can re-interpret the $\ln\mathfrak{g}$ term in the entropy (3.2.3) as due to the boundary term in brane gravity,

$$S = \frac{\phi}{8G} \approx \ln\mathfrak{g}, \tag{3.2.8}$$

where this comes from the boundary of the region in the brane that is included as

an island for the region we consider in the boundary CFT.

To investigate gravity in closed universes, [43] considered a solution with a brane in one asymptotic region of an eternal black hole. We consider the simplest version, with a brane in a BTZ geometry. Considering first the Euclidean solution, we take the bulk metric to be

$$ds^2 = (r^2 - r_h^2)d\tau^2 + \frac{dr^2}{(r^2 - r_h^2)} + r^2 d\phi^2, \tag{3.2.9}$$

where τ is periodic with period $\beta = 2\pi/r_h$ to make the metric regular at $r = r_h$. We consider a brane which respects the $U(1)$ symmetry along ϕ, so the position of the brane is parametrized by $r(\tau)$. The trajectory of the brane is given by [43]

$$\sqrt{\frac{r^2}{r_h^2} - 1}\cos(r_h\tau) = \frac{T}{\sqrt{1-T^2}}. \tag{3.2.10}$$

The brane intersects the AdS boundary at $r \to \infty$ at $\tau = \pm\beta/4$, and reaches a minimum radius $r = r_0$ at $\tau = 0$, where

$$r_0 = \frac{r_h}{\sqrt{1-T^2}}. \tag{3.2.11}$$

For $T > 0$, the spacetime includes $r = r_h$, so the $\tau = 0$ slice includes the whole of one asymptotic region of the black hole, and a portion of the other region, up to $r = r_0$. In the boundary, the intersection of the brane with the asymptotic AdS boundary corresponds to a boundary state $|B\rangle$ for the CFT, and the Euclidean evolution defines a state $|\Psi\rangle = e^{-\beta H/4}|B\rangle$. In the regime where this bulk solution dominates the path integral with these boundary conditions, this state is dual to the bulk $\tau = 0$ time slice.

This time slice provides initial conditions for a Lorentzian evolution, which is just obtained by analytically continuing in time. The bulk metric is the Lorentzian BTZ black hole, and the brane now follows a trajectory given by

$$\sqrt{\frac{r^2}{r_h^2} - 1}\cosh(r_h t) = \frac{T}{\sqrt{1-T^2}}, \tag{3.2.12}$$

which reaches a maximum radius $r = r_0$ at $t = 0$, and falls into the black hole and

meets the singularity at $r \to 0$ in the past and future. Thus, the brane worldvolume is a closed universe undergoing a big-bang, big-crunch FRW cosmology.

Fundamentally, this bulk spacetime is described by the two-dimensional CFT in the state $|\Psi\rangle$, but we can also consider it from the intermediate perspective, where we integrate over the bulk spacetime to obtain an effective theory where we have a CFT coupled to gravity on the brane, entangled with the CFT on the AdS boundary. The appropriate semi-classical state is a deformation of the usual dual description of BTZ, in terms of an entangled thermofield double state [54],

$$|TFD\rangle = \sum_i e^{-\beta E_i/2} |i\rangle_L |i\rangle_R. \tag{3.2.13}$$

Considering the situation with an end of the world brane, at least for $T \approx 1$, can be understood as turning on gravity in one of the two copies with the effective action (3.2.5). So in the semi-classical picture, we have two copies of the CFT, one in a universe with dynamical gravity and one in a fixed background, in an entangled state which is a deformation of (3.2.13).

In this semi-classical effective theory, we apply the island rule to conclude that the entanglement in the semi-classical state implies that the whole of the gravitating universe is included in an island for the boundary CFT. From the fundamental microscopic point of view, this is just the statement that the whole spacetime, including the brane system, is encoded in the fundamental state $|\Psi\rangle$ of the dual CFT; fundamentally the brane is not something independent which is entangled with the CFT, but rather is a part of it. There is presumably some code subspace of states in the CFT built on $|\Psi\rangle$ which encodes excitations in the semi-classical Hilbert space in the closed universe on the brane.

3.3 Review of multiboundary wormholes

We want to generalize the previous model to a situation where the semi-classical theory has a gravitating brane entangled with several non-gravitating systems. We

will build this model by adding an end of the world brane to the multiboundary wormhole solutions discussed in [116, 122–127]. In this section we give a brief review of the multiboundary wormhole solutions in three-dimensional gravity, and their relation to the Euclidean path integral in the dual two-dimensional CFT.

We consider solutions of the action (3.2.1), so the bulk spacetime is locally AdS_3. We can obtain Lorentzian solutions with multiple asymptotic boundaries by considering quotients of AdS_3 by some discrete subgroup of its isometry group $SL(2,\mathbb{R})\times SL(2,\mathbb{R})$. We will describe the quotient using the $SL(2,\mathbb{R})$ representation of AdS_3, following [128]. A point in the spacetime is described by an $SL(2,\mathbb{R})$ matrix p, and the spacetime metric is $ds^2 = -\det(dp)$. We can parametrize p in terms of coordinates in an $\mathbb{R}^{2,2}$ embedding space,

$$p = \begin{pmatrix} X_0 + X_2 & X_3 - X_1 \\ X_3 + X_1 & X_0 - X_2 \end{pmatrix}. \tag{3.3.1}$$

This has $\det p = 1$ if the embedding space coordinates satisfy $-X_0^2 - X_1^2 + X_2^2 + X_3^2 = -1$. The global coordinates on AdS_3 are given by

$$X_0 = \cosh\chi\cos t, \qquad X_1 = \cosh\chi\sin t, \tag{3.3.2}$$

$$X_2 = \sinh\chi\cos\theta, \qquad X_3 = \sinh\chi\sin\theta. \tag{3.3.3}$$

The metric in global coordinates is

$$ds^2 = -\cosh^2\chi dt^2 + d\chi^2 + \sinh^2\chi d\theta^2. \tag{3.3.4}$$

The $SL(2,\mathbb{R})_L \times SL(2,\mathbb{R})_R$ isometries act as $p \to g_L p g_R^t$. We will focus on the diagonal subgroup acting as $p \to gpg^t$. This maps symmetric p to symmetric p, so it leaves the surface at $X_1 = 0$, corresponding to $t = 0$ in global coordinates, invariant. Thus, a quotient by a discrete subgroup Γ of this diagonal $SL(2,\mathbb{R})$ preserves the time-reflection symmetry about this surface, and we can define a Euclidean continuation which is the quotient of $\mathbb{H}^3$ by the same group Γ. We will largely focus on the action of the quotient on the surface $X_1 = 0$, which is described

in global coordinates as the Poincaré disc.

We will consider the geometry with three asymptotic boundaries, formed by a quotient by a subgroup Γ with two hyperbolic generators. We parametrize these generators as

$$g_1 = \begin{pmatrix} \cosh(\frac{\ell_1}{2}) & \sinh(\frac{\ell_1}{2}) \\ \sinh(\frac{\ell_1}{2}) & \cosh(\frac{\ell_1}{2}) \end{pmatrix}, \qquad g_2 = \begin{pmatrix} \cosh(\frac{\ell_2}{2}) & e^{\omega}\sinh(\frac{\ell_2}{2}) \\ e^{-\omega}\sinh(\frac{\ell_2}{2}) & \cosh(\frac{\ell_2}{2}) \end{pmatrix}. \tag{3.3.5}$$

The generator g_1 acts as a boost in the $X_0 - X_3$ plane in the embedding space. The generator g_2 can be written as a similar boost, up to conjugation,

$$g_2 = g_\omega \tilde{g}_2 g_\omega^{-1}, \quad g_\omega = \begin{pmatrix} e^{\omega/2} & 0 \\ 0 & e^{-\omega/2} \end{pmatrix}, \quad \tilde{g}_2 = \begin{pmatrix} \cosh(\frac{\ell_2}{2}) & \sinh(\frac{\ell_2}{2}) \\ \sinh(\frac{\ell_2}{2}) & \cosh(\frac{\ell_2}{2}) \end{pmatrix}. \tag{3.3.6}$$

The conjugating matrix g_ω acts as a boost in the $X_0 - X_2$ plane. If we considered just the quotient by the abelian group generated by g_1, the resulting spacetime would be the BTZ black hole (3.2.9) with $r_h = \ell_1/2\pi$. The BTZ coordinates are related to the embedding coordinates by

$$X_0 = \frac{r}{r_h}\cosh(r_h\phi), \qquad X_1 = \sqrt{\frac{r^2}{r_h^2} - 1}\sinh(r_h t) \tag{3.3.7}$$

$$X_3 = \frac{r}{r_h}\sinh(r_h\phi), \qquad X_2 = \pm\sqrt{\frac{r^2}{r_h^2} - 1}\cosh(r_h t). \tag{3.3.8}$$

The quotient by g_1 acts as translation in ϕ, $\phi \to \phi + 2\pi$. In the Poincaré disc representation, on the right in figure 3.2, a symmetric fundamental region for this identification is the region between the two blue geodesics, corresponding to $\phi = \pm\pi$. The horizon is the closed geodesic at $X_2 = 0$, of proper length ℓ_1. The other generator g_2 similarly identifies the two orange geodesics on the right of the picture, and the dotted curve connecting them is a closed geodesic of proper length ℓ_2, which is a horizon for the asymptotic region on the right. We restrict to $e^{\omega} > \coth\left(\frac{\ell_1}{4}\right)\coth\left(\frac{\ell_2}{4}\right)$, so that the orange and blue geodesics don't intersect [128]. The region bounded by these geodesics is a fundamental region for the quotient by the group Γ generated by g_1, g_2. The quotient geometry has three asymptotic regions,

each of which is isomorphic to the BTZ black hole outside a horizon. The horizon in the third asymptotic region is formed of the two minimal geodesics connecting the blue and orange surfaces in the right picture. The length ℓ_3 of this horizon is given by

$$\cosh\frac{\ell_3}{2} = \frac{1}{2}\operatorname{Tr} g_3 = -\frac{1}{2}\operatorname{Tr} g_1 g_2^{-1} = \cosh\omega \sinh\frac{\ell_1}{2}\sinh\frac{\ell_2}{2} - \cosh\frac{\ell_1}{2}\cosh\frac{\ell_2}{2}. \quad (3.3.9)$$

The region in between the three horizons is referred to as the causal shadow region, as no causal influence can propagate from this region to the asymptotic regions. The quotient of the surface $X_1 = 0$ is thus a surface Σ with the topology of a pair of pants, labelled by three parameters ℓ_1, ℓ_2, ℓ_3, as pictured on the left in figure 3.2. This is the simplest example of a multiboundary wormhole.

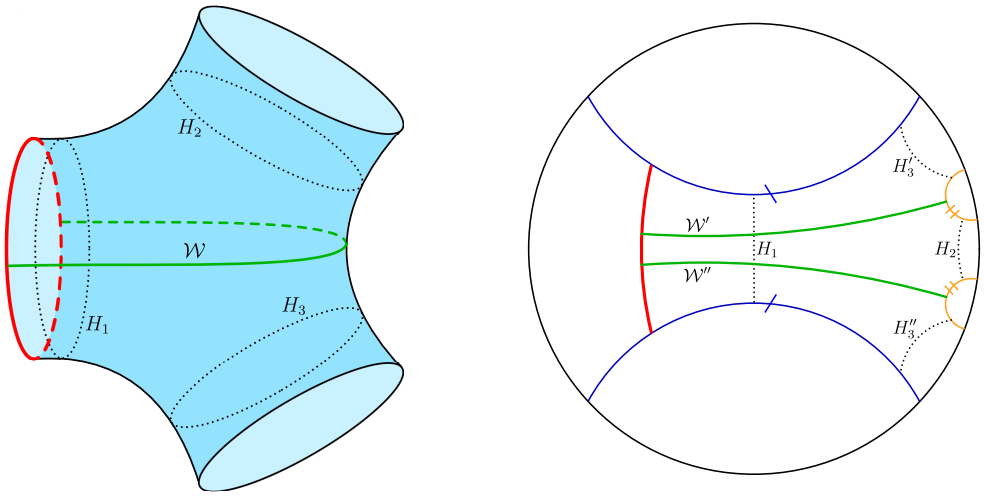

Figure 3.2: The pair of pants geometry with an end of the world brane (red) in one asymptotic region. On the left is a cartoon of the geometry of the $t = 0$ surface, and on the right is its description as a quotient of the Poincaré disc model. In the right picture the central region bounded by the blue and orange geodesics is a fundamental region for the identification. The geodesic $\mathcal{W} \equiv \mathcal{W}' \cup \mathcal{W}''$, which is the minimal geodesic anchored on the end of the world brane running in between the two asymptotic region, is shown in green. The horizon H_3 is similarly defined as $H_3 \equiv H_3' \cup H_3''$.

We can analytically continue the Lorentzian solution to a Euclidean spacetime with geometry

$$ds^2 = d\rho^2 + \cosh^2\rho\, d\Sigma^2. \quad (3.3.10)$$

Recall that the Euclidean BTZ black hole has the topology of solid torus with the

non-contractible cycle parameterised by Euclidean time. Its conformal boundary is a two-torus (a Riemann surface of genus one). Slicing the torus along a moment of time-reflection symmetry gives two cylinders as the conformal boundaries; the Euclidean path integral over one of these cylinders then defines the dual state at the moment of time-reflection symmetry in two copies of the Hilbert space of the CFT on S^1. Similarly, the conformal boundary of the Euclidean three-boundary wormhole is a Riemann surface of genus two formed by gluing together two copies of the surface Σ. The Euclidean path integral in the CFT on one copy of Σ defines an entangled state for the CFT in three copies of the Hilbert space of the CFT on S^1, $|\Sigma\rangle \in \mathcal{H}_1 \times \mathcal{H}_2 \times \mathcal{H}_3$. The bulk geometry provides a candidate bulk saddle-point dual to this Euclidean path integral; when this is the dominant bulk saddle-point, the bulk geometry on Σ is the dual of the CFT state $|\Sigma\rangle$. In the state $|\Sigma\rangle$, the reduced density matrix ρ_i on each copy of the CFT is not thermal, but one-point functions of local operators are determined by the geometry in the exterior region, so they take thermal values. In particular, the stress tensor of the CFT degrees of freedom will be a perfect fluid with coarse-grained entropy $S_i^{(c)} = \frac{\ell_i}{4G}$. The fine-grained entropy of ρ_i is $S_i = \frac{1}{4G}\min(\ell_i, \ell_j + \ell_k)$, so if one of the horizons is longer than the sum of the other two, the actual entropy of the density matrix in that region is less than the coarse-grained thermal value.

We will be particularly interested in the limit of large ℓ_1, ℓ_2, ℓ_3, with fixed ratios. In [116], the entanglement structure of $|\Sigma\rangle$ was shown to simplify in this limit. The essential point is that the causal shadow region has a constant negative curvature geometry bounded by geodesics, so its area is fixed by the Gauss-Bonnet theorem. Hence, as the horizons become long, the distance between them must become small. We can decompose the path integral over Σ defining the state $|\Sigma\rangle$ into an integral over the regions E_a outside the horizons, which are conformal to round cylinders, and the integral over the causal shadow region. The path integral over the causal shadow region then identifies the horizons locally. There are two different regimes, as pictured in figure 3.3: if one of the horizons is longer than the sum of the other

two, we have an "eyeglass" picture, where the whole of the two short horizons are identified with the long one, and the remaining parts of the long horizon are identified with each other. Otherwise, each horizon has a portion which is identified with each of the others. In the "eyeglass" regime, to leading order in c the state $|\Sigma\rangle$ only involves entanglement between the boundaries associated to the short horizons and the long one; there is no entanglement between the two boundaries associated to the short horizons.

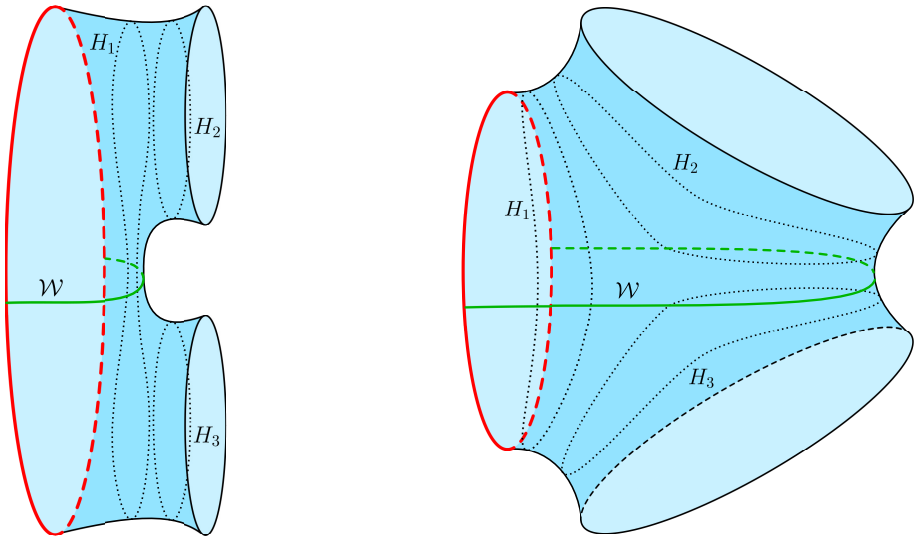

Figure 3.3: In the large ℓ_i limit, the horizons are locally identified. There are two cases: if one length is larger than the sum of the other two, $\ell_i > \ell_j + \ell_k$, we have an "eyeglass" picture, where the whole of the two short horizons are identified with the long one, and the remaining parts of the long horizon are identified with each other. Otherwise, each horizon has a portion which is identified with each of the others.

3.4 Islands on the braneworld

We now turn to the main point of this chapter: to add a brane to the multiboundary wormhole spacetime, to obtain a model where we can investigate the description of a closed universe entangled with a quantum system with two components. We simply consider inserting the same kind of brane considered above in one of the exterior BTZ regions in the $t = 0$ slice, as pictured in figure 3.2, at the maximum radius r_0 given by (3.2.11). We will call the asymptotic region that is cut off in this way

region 1. This initial data has a Euclidean continuation where the brane intersects the conformal boundary of the Euclidean wormhole spacetime (3.3.10). The brane intersects the Euclidean boundary at $\tau = \pm\beta/4$ in the BTZ coordinates. The path integral over half the Euclidean boundary, with the boundary state $|B\rangle$ dual to the end of the world brane inserted at $\tau = -\beta/4$, defines a state $|\Psi\rangle \in \mathcal{H}_2 \times \mathcal{H}_3$ dual to this bulk geometry.

At least when $r_0 \gg r_h$, this geometry can also be described in a semi-classical effective theory where we integrate out the bulk spacetime to obtain a CFT coupled to gravity living on the end of the world brane, entangled with the two other copies of the CFT. In this description, the semi-classical state of the theory is roughly the state $|\Sigma\rangle$ dual to the multiboundary wormhole, but with some deformation from coupling the CFT in boundary 1 to gravity; we will call this deformed state $|\tilde{\Sigma}\rangle$. The brane is embedded in a BTZ geometry, with horizon length ℓ_1. The effective stress tensor of the semi-classical theory on the brane is thus a perfect fluid, with a coarse-grained entropy $S_{coarse} = \frac{\ell_1}{4G}$.

In the state $|\tilde{\Sigma}\rangle$, we have some entanglement between the degrees of freedom in the closed universe and the two CFTs on boundaries 2 and 3. This entanglement is most easily characterised in the large ℓ_i limit, where the entanglement is approximately local; small regions in the brane form a thermofield double state with corresponding regions in one of the other systems (or with another region on the brane). We will explore the entanglement structure of $|\tilde{\Sigma}\rangle$ by considering RT surfaces in the bulk spacetime in figure 3.2. Before carrying out a quantitative analysis, we give a general qualitative description.

Since the microscopic state $|\Psi\rangle \in \mathcal{H}_2 \times \mathcal{H}_3$ is pure, the entropy of $\rho_2 = \mathrm{Tr}_3(|\Psi\rangle\langle\Psi|)$ is equal to the entropy of $\rho_3 = \mathrm{Tr}_2(|\Psi\rangle\langle\Psi|)$. There are three candidate RT surfaces for this entropy: the horizon H_2, of length ℓ_2, the horizon H_3, of length ℓ_3, or a geodesic with end points on the end of the world brane which separates the two boundaries, as pictured in figure 3.2. We call the minimal-length geodesic in this class $\mathcal{W}$. We take without loss of generality $\ell_2 \leq \ell_3$; then the RT surface is either

H_2 or $\mathcal{W}$.

When the RT surface is $\mathcal{W}$, the brane is partially encoded in $\mathcal{H}_2$ and partially in $\mathcal{H}_3$. This is the situation where the entanglement of the brane with boundaries 2 and 3 in $|\tilde{\Sigma}\rangle$ is big enough to overcome the cost of having a non-trivial island. In this situation the entropy $S = \frac{\ell_{\mathcal{W}}}{4G}$ is partially due to the geometric entropy on the brane, and partially due to entanglement between the degrees of freedom in system 2 together with the associated island on the brane and the rest.

When the RT surface is H_2, the brane is entirely encoded in $\mathcal{H}_3$. This is the regime which we are particularly interested in. If we treat $\mathcal{H}_2$ as a reference system, and trace over it, semi-classical entanglement between the brane and $\mathcal{H}_2$ gives us a mixed state on the brane, which is encoded microscopically in the mixed state ρ_3 of the CFT on the boundary. The fine-grained entropy is $S = \frac{\ell_2}{4G}$. Semi-classically, this can include both contributions from entanglement between the brane and boundary 2, and between boundary 3 and boundary 2. In the large ℓ_i limit, we can cleanly separate these two contributions, because of the local structure of the entanglement: the portion of H_2 which lies along H_1 represents entanglement between the brane and boundary 2 in the semi-classical state, so we identify the length of this portion with the entropy S_{brane} of the semi-classical state of the matter on the brane. There are three cases:

- If $\ell_1 > \ell_2 + \ell_3$, in $|\tilde{\Sigma}\rangle$ boundary 2 is entirely entangled with the brane, with no entanglement with boundary 3. The whole entropy $S_{brane} = S = \frac{\ell_2}{4G}$ can be thought of as entropy of the mixed state on the brane.

- If $\ell_3 > \ell_1 + \ell_2$, boundary 2 is entirely entangled with boundary 3, with no entanglement with the brane. The effective semi-classical state on the brane remains pure on tracing out boundary 2, as it's solely entangled with boundary 3.

- Otherwise, the entanglement is partially with the brane and partially with boundary 3. The entropy of the mixed state on the brane is determined by

the portion of H_2 that lies along H_1, which gives $S_{brane} = \frac{1}{8G}(\ell_1 + \ell_2 - \ell_3)$.

We see that $S_{brane} \leq S_{coarse}/2$, with equality when $\ell_2 = \ell_3 > \ell_1/2$.

3.4.1 The $\mathcal{W}$ geodesic

We now compute the length of the $\mathcal{W}$ geodesic, to compare it to the horizon H_2. By time reflection symmetry the geodesic lies in the $t = 0$ slice of the geometry. In the Poincaré disc model $\mathcal{W}$ corresponds to two geodesics $\mathcal{W}'$ and $\mathcal{W}''$, which hit the orange identification surfaces. There is a $\mathbb{Z}_2$ reflection symmetry about the $\theta = 0, \pi$ axis in the Poincaré disc, corresponding to the reflection symmetry about the plane of the page in the pair of pants geometry shown in figure 3.2. This $\mathbb{Z}_2$ symmetry implies that the two geodesics are identical and meet the identification surfaces orthogonally, so as to produce a smooth connected curve in the quotient space. The end of the world brane sits at constant r, and the geometry between the brane and the identification surface is locally BTZ, so if we consider connecting a fixed point on the identification surface to the end of the world brane, the the length is minimal when the curve lies at constant ϕ. The $\mathcal{W}'$ geodesic is then obtained by varying the point on the identification surface, to find the curve of constant ϕ which meets the identification surface orthogonally. The identification surfaces are geodesics in the Poincaré disc, given by

$$\tanh\chi\cos(\theta - \alpha) = \cos\psi, \tag{3.4.1}$$

in global coordinates. By finding the point where the normal to the identification surface $n \propto dr$, we find the angle θ_1 at which the geodesic hits the identification surface. It will be more convenient to define $\vartheta \equiv \theta - \alpha$. We get

$$\tan\vartheta_1 = \tan\alpha\tan^2\psi. \tag{3.4.2}$$

The geodesic distance between two spacelike separated points $s(X, X')$ is

$$\cosh s(X, X') = -X \cdot X'. \tag{3.4.3}$$

The length of $\mathcal{W}$ is then given by

$$\cosh\frac{1}{2}\ell_{\mathcal{W}} = \frac{\csc\psi}{\sqrt{1-T^2}}\left(\cos\alpha + \frac{T}{2}\sqrt{\cos 2\alpha + \cos 2\psi}\right). \tag{3.4.4}$$

To relate this to the horizon lengths, we need to relate the parameters α, ψ specifying the geodesics identified by g_2 to the horizon lengths. The geodesics identified by g_1 have $\tanh\chi\cos(\theta \pm \pi/2) = \cos\delta$, where

$$\cos\delta = \tanh\chi_{min} = \tanh\frac{\ell_1}{2} \Rightarrow \sin\delta = \operatorname{sech}\frac{\ell_1}{2}. \tag{3.4.5}$$

The geodesics identified by g_2 are similar, but conjugated by g_ω. That is, there is a conjugated Poincaré coordinate system with $\tilde{\alpha} = \pi/2$, $(\sin\tilde{\psi})^{-1} = \cosh\frac{\ell_2}{2}$. Conjugation by g_ω acts on the boundary coordinates by

$$\begin{pmatrix}\cos\frac{\theta}{2}\\ \sin\frac{\theta}{2}\end{pmatrix} \propto g_\omega \begin{pmatrix}\cos\frac{\tilde{\theta}}{2}\\ \sin\frac{\tilde{\theta}}{2}\end{pmatrix}. \tag{3.4.6}$$

This gives

$$\sin\alpha = \frac{1}{\sqrt{\cosh^2\omega - \sinh^2\omega\sin^2\tilde{\psi}}}, \qquad \sin\psi = \sin\tilde{\psi}\sin\alpha. \tag{3.4.7}$$

Thus,

$$\cosh\frac{\ell_2}{2} = \frac{1}{\sin\tilde{\psi}} = \frac{\sin\alpha}{\sin\psi}. \tag{3.4.8}$$

Using (3.3.9), we find

$$\tan\alpha = \frac{\sqrt{2}\cosh\frac{\ell_2}{2}\sinh\frac{\ell_1}{2}}{\sqrt{1+\cosh\ell_1+\cosh\ell_2+\cosh\ell_3+4\cosh\frac{\ell_1}{2}\cosh\frac{\ell_2}{2}\cosh\frac{\ell_3}{2}}}. \tag{3.4.9}$$

This gives an expression for the length of the $\mathcal{W}$ geodesic as a function of the horizon lengths and the tension T,

$$\cosh\frac{1}{2}\ell_{\mathcal{W}} = \frac{\operatorname{csch}\frac{\ell_1}{2}}{\sqrt{2(1-T^2)}}\left(\sqrt{1+\cosh\ell_1+\cosh\ell_2+\cosh\ell_3+4\cosh\frac{\ell_1}{2}\cosh\frac{\ell_2}{2}\cosh\frac{\ell_3}{2}}\right.$$
$$\left. + T\sqrt{2+\cosh\ell_2+\cosh\ell_3+4\cosh\frac{\ell_1}{2}\cosh\frac{\ell_2}{2}\cosh\frac{\ell_3}{2}}\right). \tag{3.4.10}$$

We can now compare this to the horizon lengths. Since we assume $\ell_2 \leq \ell_3$, we want to know whether $\ell_{\mathcal{W}}$ is bigger or smaller than ℓ_2.

The length $\ell_{\mathcal{W}}$ is monotonically decreasing in ℓ_1, and monotonically increasing in ℓ_2, ℓ_3. The former gives us a lower bound for the length: taking the large ℓ_1 limit at fixed ℓ_2, ℓ_3, $\lim_{\ell_1 \to \infty} \ell_{\mathcal{W}} = 2 \tanh^{-1} T$, so $\ell_{\mathcal{W}} \geq 2 \tanh^{-1} T$ for any values of the ℓ_i. Thus,

$$\ell_2 < 2 \tanh^{-1} T \quad \Rightarrow \quad \ell_{\mathcal{W}} > \ell_2; \tag{3.4.11}$$

for sufficiently small ℓ_2 the minimal geodesics is always H_2. Since $\ell_{\mathcal{W}}$ is monotonically increasing in ℓ_3, the minimum value for fixed ℓ_2 is at $\ell_2 = \ell_3$, where the formula simplifies to

$$\cosh \frac{1}{2} \ell_{\mathcal{W}} = \frac{\operatorname{csch} \frac{\ell_1}{4}}{\sqrt{1 - T^2}} \left(\sqrt{\cosh^2 \frac{\ell_2}{2} + \sinh^2 \frac{\ell_1}{4}} + T \cosh \frac{\ell_2}{2} \right). \tag{3.4.12}$$

Here it is interesting to note that

$$\ell_1 < 4 \sinh^{-1} \left(\sqrt{\frac{1+T}{1-T}} \right) \quad \Rightarrow \quad \ell_{\mathcal{W}} > \ell_2, \tag{3.4.13}$$

so also for sufficiently small ℓ_1 the minimal geodesic is always H_2. In figure 3.4, we plot the regions where $\ell_{\mathcal{W}} < \ell_2$ for $\ell_2 = \ell_3$ for various values of T.

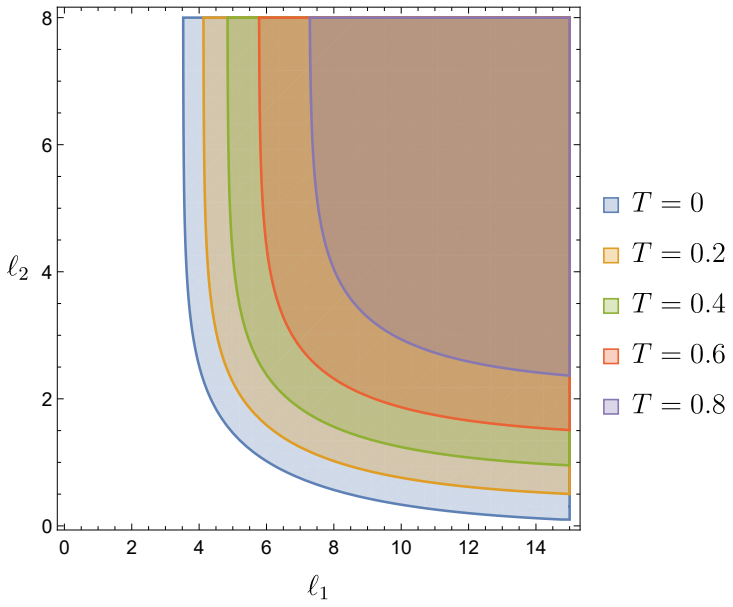

Figure 3.4: The regions where $\ell_{\mathcal{W}} < \ell_2$ for $\ell_2 = \ell_3$ for various values of T

We can simplify the expression by working in a regime where $\ell_{\mathcal{W}}$ is large — this is achieved either by considering large values of the ℓ_i, or $T \to 1$, or both. Let us first consider the limit $T \to 1$, for general ℓ_i. This corresponds to taking the brane towards the asymptotic boundary in region 1, so the $\mathcal{W}$ geodesic gets longer as it extends further out into this region. In this limit we can write

$$\ell_{\mathcal{W}} \approx \ell_S + \ln \frac{2}{1-T} \approx \ell_S + 2 \tanh^{-1} T, \tag{3.4.14}$$

where

$$e^{\frac{\ell_S}{2}} = \frac{\operatorname{csch} \frac{\ell_1}{2}}{\sqrt{2}} \left(\sqrt{1 + \cosh \ell_1 + \cosh \ell_2 + \cosh \ell_3 + 4 \cosh \frac{\ell_1}{2} \cosh \frac{\ell_2}{2} \cosh \frac{\ell_3}{2}} \right.$$
$$\left. + \sqrt{2 + \cosh \ell_2 + \cosh \ell_3 + 4 \cosh \frac{\ell_1}{2} \cosh \frac{\ell_2}{2} \cosh \frac{\ell_3}{2}} \right). \tag{3.4.15}$$

The entanglement entropy when the $\mathcal{W}$ geodesic is minimal is then

$$S_{\mathcal{W}} = \frac{\ell_{\mathcal{W}}}{4G} = \frac{\ell_S}{4G} + 2 \ln \mathfrak{g}, \tag{3.4.16}$$

where $\ln \mathfrak{g} = \tanh^{-1}(T)/4G$ is the boundary entropy of the end of the world brane. As in the simpler Poincaré-AdS solution discussed in section 3.2, the $2 \ln \mathfrak{g}$ contribution can be seen from the brane gravity perspective as the boundary contribution to the generalized entropy from the boundaries of the island on the brane (there is a factor of 2 here compared to the discussion in section 3.2 because the island here has two boundaries).

If we also consider the limit of large horizon lengths, $\ell_{1,2,3} \gg 1$, then ℓ_S will typically also be large. In the large horizon length limit, ℓ_S can be interpreted as the portion of the $\mathcal{W}$ geodesic in the "shadow region" beyond the horizon, running over the pair of pants between H_2 and H_3, while the $\ln \mathfrak{g}$ term comes from the portion of the geodesic between the brane and H_1.

There are three distinct cases in the large horizon length limit:

- If $\ell_1 > \ell_2 + \ell_3$, the dominant contribution to $\ell_{\mathcal{W}}$ comes from the $\cosh \ell_1$ in the

first square root; then

$$\cosh\frac{1}{2}\ell_{\mathcal{W}} \approx \frac{1}{\sqrt{1-T^2}}, \tag{3.4.17}$$

or

$$\ell_{\mathcal{W}} \approx 2\cosh^{-1}\left(\frac{1}{\sqrt{1-T^2}}\right) = 2\tanh^{-1}T. \tag{3.4.18}$$

That is, in this case ℓ_S is small, as part of H_1 lies along another portion of H_1, so the minimal geodesic over the pair of pants is short. In this regime the $\mathcal{W}$ geodesic is minimal as soon as $\ell_2 > 2\tanh^{-1}T$.

- If $\ell_3 > \ell_1 + \ell_2$, the dominant contribution to $\ell_{\mathcal{W}}$ comes from the $\cosh\ell_3$ in both square roots; then

$$\cosh\frac{1}{2}\ell_{\mathcal{W}} \approx e^{\frac{\ell_3-\ell_1}{2}}\frac{\sqrt{1+T}}{\sqrt{1-T}}, \tag{3.4.19}$$

that is

$$\ell_{\mathcal{W}} \approx \ell_3 - \ell_1 + 2\ln\left(\frac{2\sqrt{1+T}}{\sqrt{1-T}}\right) \approx \ell_3 - \ell_1 + 2\tanh^{-1}T, \tag{3.4.20}$$

where we again drop an order one term. That is, $\ell_S = \ell_3 - \ell_1$: the $\mathcal{W}$ geodesic follows the part of H_3 that is not along H_1. In this regime the $\mathcal{W}$ geodesic is never minimal, as the first term on the RHS is already bigger than ℓ_2 by assumption.

- Otherwise, the dominant contribution to $\ell_{\mathcal{W}}$ comes from the final term in both square roots; then

$$\cosh\frac{1}{2}\ell_{\mathcal{W}} \approx e^{\frac{\ell_3-\ell_1-\ell_2}{4}}\frac{\sqrt{1+T}}{\sqrt{1-T}}, \tag{3.4.21}$$

that is

$$\ell_{\mathcal{W}} \approx \frac{1}{2}(\ell_3+\ell_2-\ell_1)+2\ln\left(\frac{2\sqrt{1+T}}{\sqrt{1-T}}\right) \approx \frac{1}{2}(\ell_3+\ell_2-\ell_1)+2\tanh^{-1}T, \tag{3.4.22}$$

again dropping order one terms. That is, $\ell_S = \frac{1}{2}(\ell_3+\ell_2-\ell_1)$. The $\mathcal{W}$ geodesic lies along the section where H_2 and H_3 lie along each other, as pictured in figure 3.3. In this regime the $\mathcal{W}$ geodesic is minimal if

$$\ell_2 > \ell_3 - \ell_1 + 4\tanh^{-1}T. \tag{3.4.23}$$

Note that we have not assumed that $\ell_3 - \ell_1$ is positive, but we have assumed $\ell_3 + \ell_2 - \ell_1$ is positive, so this is a stronger condition than the general condition $\ell_2 > 2\tanh^{-1} T$.

We now have a full picture of the behaviour of the entanglement structure as a function of ℓ_i, T, at least in the region where all geodesics are long. To illustrate this, let's consider what happens as we change ℓ_2 at fixed ℓ_1, ℓ_3, T. There are two different cases: $\ell_3 > \ell_1$ and $\ell_1 > \ell_3$.

If $\ell_1 > \ell_3$, at small ℓ_2 some of the degrees of freedom on the brane are actually entangled with other regions on the brane, as we are in an "eyeglass" situation. The reference system boundary 2 is entirely entangled with the brane in the semi-classical state, and tracing over it gives us a mixed state on the brane of entropy $S_{brane} = \frac{\ell_2}{4G}$. This gives a model of the encoding of a mixed state in a closed universe. As we increase ℓ_2, we will eventually make a transition to $\mathcal{W}$ being minimal, and there is an island on the brane associated to boundary 2. If $\ell_1 - \ell_3 > 2\tanh^{-1} T$, we make the transition at $\ell_2 = 2\tanh^{-1} T$, before we get out of the "eyeglass" situation; otherwise, we first enter a regime where boundary 2 is partially entangled with boundary 3, and the entropy due to entanglement with the brane is $S_{brane} = \frac{1}{8G}(\ell_1 + \ell_2 - \ell_3)$. If $\ell_1 > 4\tanh^{-1} T$, we make a transition to $\mathcal{W}$ being minimal at $\ell_2 = \ell_3 - \ell_1 + 4\tanh^{-1} T$. Otherwise, we reach $\ell_2 = \ell_3$ and make a transition to H_3 being minimal, and the brane gets entirely encoded in boundary 2.

If $\ell_3 > \ell_1$, at small ℓ_2 we are in an "eyeglass" situation where horizon 3 is long, so initially boundary 2 is entangled only with boundary 3, and the effective semi-classical state on the brane is entangled only with boundary 3. Microscopically, $\mathcal{H}_3$ factors into a piece which encodes the brane state and a piece which carries the entanglement with boundary 2. H_2 remains the minimal geodesic until we reach a regime with non-zero $S_{brane} = \frac{1}{8G}(\ell_1 + \ell_2 - \ell_3)$, and the transition to $\mathcal{W}$ being minimal is again at $\ell_2 = \ell_3 - \ell_1 + 4\tanh^{-1} T$ for $\ell_1 > 4\tanh^{-1} T$.

In all cases, when there is a transition to $\mathcal{W}$ being minimal the transition is at $S_{brane} = \frac{1}{2G}\tanh^{-1} T = 2\ln \mathfrak{g}$. Thus, we learn that the entropy of the effective state

on the brane is bounded by $S_{brane} < \frac{1}{2} S_{coarse}$ (otherwise it would be favourable to have the brane entirely encoded in the reference system rather than boundary 3) and $S_{brane} < 2 \ln \mathfrak{g}$ (otherwise it would be favourable to have an island on the brane). The simplicity of the latter bound is due to our model describing a particular kind of mixed state, where the reference system is entangled with a particular local region on the brane. We could certainly imagine entangling the brane with the reference system in more complicated ways, which could relax this bound. The first bound seems more universal.

3.5 Discussion

We have shown that entangled or mixed states of closed universes can be described in the context of the island formula, if we consider a closed universe entangled with a non-gravitating system with multiple components. We can have situations where the closed universe is encoded in one system, but still has some entanglement with another, which corresponds microscopically to a part of the entanglement between the two systems. We studied a simple model in three dimensions, based on multiboundary wormholes, and found that the portion of the entropy that could be assigned to the state on the brane was bounded by half of the coarse-grained entropy of the effective theory on the brane, and also bounded by the gravitational entropy of an island on the brane.

The relation to the gravitational entropy on the brane is interesting, and deserves further exploration; it would be interesting if this could shed some light on the interpretation of horizon entropy in closed universes. However, the simple relationship obtained in our model depends on the assumption that the degrees of freedom on the brane that are entangled with the CFT are localised in a particular region of the brane. We would expect that the semi-classical theory would include more general mixed states on the brane with less localised entanglement, by considering more abstract reference systems or systems with more components.

Another interesting way to use this model is to take ℓ_2 and ℓ_3 much smaller than ℓ_1; the brane then has a large coarse-grained entropy, but the fundamental microscopic description has a much smaller entropy, reminiscent of a 'bag-of-gold' spacetime [129]. This could be an interesting avenue to explore the reconstruction of states on the brane, using the Petz map [26, 130] or the tensor network ideas of [131]. It would also be interesting to explore the relation of the model we used here to the somewhat different model in [132]. Finally, if we take all the horizon lengths small, the system should also have a non-trivial phase structure; it would also be interesting to explore the description of the brane universe in cases where it's not connected to the conformal boundaries in the bulk spacetime.

It would be interesting to carry out similar calculations in higher dimensions. There is no simple higher-dimensional version of the multiboundary wormholes, but we could consider working in the original model of [43], where we introduce a brane in an eternal black hole spacetime. The brane is then encoded in the CFT on the asymptotic AdS boundary, and we can consider dividing this boundary into two regions. There are similarly two candidate RT surfaces for this case, one which remains outside the black hole horizon (analogous to H_2 in our discussion) and one which crosses the horizon and ends on the brane (analogous to $\mathcal{W}$ in our discussion) as pictured in figure 3.5. In the first case the brane is entirely described in the larger boundary region, while in the latter case it is divided into two regions, described in the two parts of the boundary.

Because the two regions interact, the entanglement entropy is no longer time independent in this case. The discussion in [43] focused on this time dependence; focusing on the entanglement at $t = 0$ should be similar to our previous discussion. To clearly identify the portion of the entanglement entropy that is associated with the mixed state on the brane, we would like to work with a solution where the horizon area is large compared to the AdS scale $r_h \gg \ell$, so the entanglement between the brane and the boundary in the semi-classical state is local, as in our discussion. Then to have a large enough region where the surface outside the horizon is minimal, we

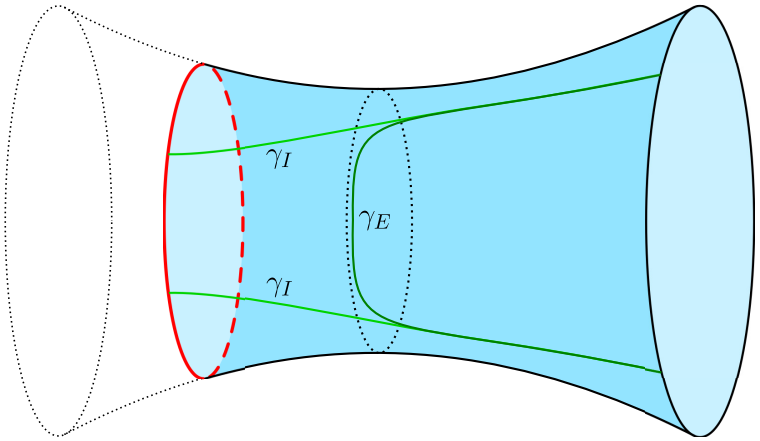

Figure 3.5: For a brane in an eternal black hole spacetime, when we consider a subregion of the CFT on the boundary, the RT surface is either outside the horizon or crosses the horizon and ends on the brane. For large black holes, the surface outside the horizon has a portion which lies along the horizon, whose area can be interpreted as entropy of the mixed state on the brane.

need the brane to lie far from the horizon, $r_0 \gg r_h$. In [43], it was found that the brane can't be taken arbitrarily far from the horizon in uncharged black holes, but this is possible if we consider charged black holes close to extremality [44].

In this context, of large black holes with the brane far from the horizon, we would expect qualitatively similar results to our analysis: the RT surface which stays outside the horizon will have a portion which lies along the horizon, which we can interpret as giving the entropy S_{brane} of the mixed state on the brane. This will never be more than half the horizon area, and the transition to the RT surface that ends on the brane should occur when S_{brane} is bigger than the area of the surface extending from the horizon to the brane, which should correspond to the boundary term in the island formula from the perspective of the induced gravity theory on the brane.

Chapter 4

Constraints on Cosmologies Inside Black Holes

An approach to understanding closed universes with big-bang/big-crunch cosmologies holographically was proposed in [43] (and further developed in [44–47]). The idea is to consider an asymptotically AdS_{d+1} black hole spacetime with a d-dimensional dynamical end of the world (ETW) brane behind the horizon providing an inner boundary of the spacetime, as depicted in figure 4.1. Starting from the $t = 0$ surface, the ETW brane falls into the black hole and terminates at the singularity, so its worldvolume geometry is a big-bang/big-crunch cosmology. The state in the bulk on the $t = 0$ surface is dual to some state in the dual d-dimensional CFT on the asymptotic boundary on the right in figure 4.1, which therefore includes a description of the cosmology on the ETW brane worldvolume.

An appealing feature of this model is that the state in the bulk on the $t = 0$ surface can be constructed from a Euclidean path integral, as depicted on the left in figure 4.2. In the Euclidean section, the ETW brane moves outward away from $t = 0$, and eventually meets the asymptotic boundary. Such solutions were proposed in [65, 117] as duals of boundary conformal field theories (BCFTs). The state in the d-dimensional CFT dual to the $t = 0$ slice in the bulk is then constructed by starting with a $(d - 1)$-dimensional boundary state specified by the BCFT and evolving

through some period of Euclidean time. Such states have been extensively discussed in recent investigations of black holes, see e.g. [25, 26, 40, 92].

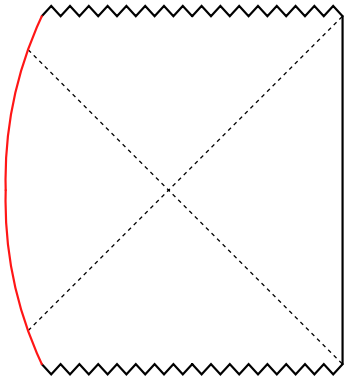

Figure 4.1: Penrose diagram of an AdS black hole with the left asymptotic region terminating in an ETW brane (shown in red). The worldvolume geometry of the ETW brane is a big-bang/big-crunch cosmology.

To have a controlled description of the cosmology on the ETW brane, we want to have a separation of scales between the scale that controls the curvature of the ETW brane and the bulk curvature, such that there is a good effective description of the dynamics in terms of ordinary Einstein gravity localised on the ETW brane. This can be achieved by taking the radial position r_0^{ETW} of the brane at $t = 0$ to be much larger than the horizon scale r_h, which can be achieved by increasing the tension T of the ETW brane [118–120].

However, in simple examples of this construction this separation of scales is incompatible with the path integral construction described above. If we are in $d > 2$, and we take the bulk solution to be an uncharged black hole, increasing T for fixed bulk black hole geometry, there is a critical value $T = T_*$ at which the ETW brane intersects the asymptotic boundary at $t = 0$; increasing T beyond T_*, the ETW brane will self-intersect before it reaches the asymptotic boundary, as depicted in figure 4.2. Thus, for $T > T_*$, we lose the Euclidean path integral construction of the state dual to the $t = 0$ slice. This would not prevent us from considering the Lorentzian brane solution – the Lorentzian solution remains well-behaved even for $T > T_*$ – but we would lose control of the dual CFT state, limiting our ability to

study the holographic duality in detail.[1] One resolution of this problem, proposed in [44], is to take the bulk solution to be a charged black hole.

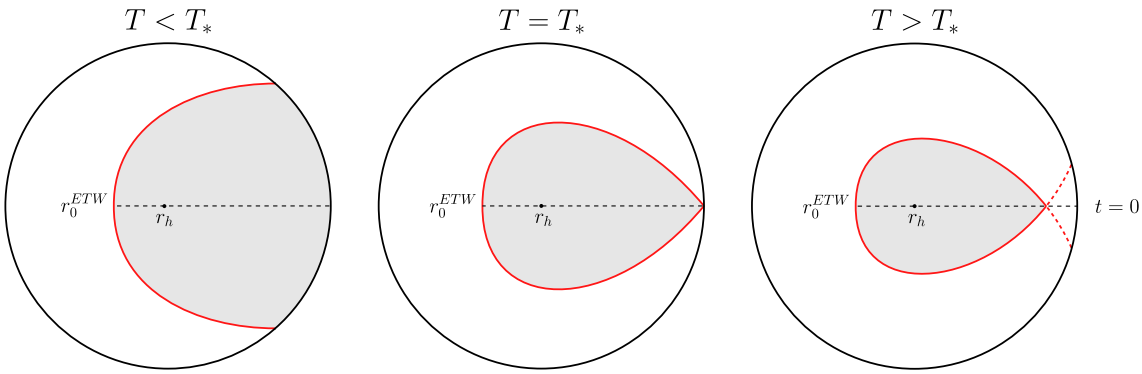

Figure 4.2: Euclidean ETW brane trajectories for different values of the brane tension. The shaded regions are the bulk regions that we keep from the original Euclidean/Schwarzschild geometry without an ETW brane. Below the critical tension, $T < T_*$, there are sensible solutions with the brane intersecting the asymptotic boundary at times $t > 0$; at $T = T_*$ the brane intersects the asymptotic boundary at $t = 0$; for $T > T_*$, the brane intersects itself before reaching the asymptotic boundary and we lose the Euclidean path integral construction of the state dual to the $t = 0$ slice.

In [47], a different perspective on this issue was given. Suppose the spatial directions along the ETW brane are flat. We can then analytically continue the Euclidean solution along one of the spatial directions, to obtain a time-independent Lorentzian solution where the ETW worldvolume has two asymptotically AdS ends. So the geometry on the ETW brane is an example of an eternal traversable wormhole [13]. Thus, these solutions can alternatively be viewed as constructing an eternal traversable wormhole by taking the $(d-1)$-dimensional CFTs at the two ends of the ETW brane and coupling them through the d-dimensional CFT.[2] The construction of traversable wormholes requires violations of the energy conditions, and in $d > 2$ obstructions to the construction of such wormholes were noted in [134]. In [47], the constraints were analysed from the perspective of the ETW brane worldvolume, and shown to obstruct the construction of traversable wormholes with a separation of scales between the brane and bulk AdS scales. This is the same obstruction as the

[1] The situation is somewhat similar to considering a small black hole in AdS with a spherical boundary; this is a perfectly good Lorentzian solution, but we do not understand the precise dual CFT description, unlike for large black holes.

[2] Similar constructions were considered in [133].

self-intersection problem mentioned above, as we will explain below.

In [47], it was proposed that this obstruction could be overcome by considering a more complicated bulk solution with interface branes in addition to the ETW brane. From the bulk self-intersection perspective, the advantage of adding interface branes is that one can allow the time at which the ETW brane reaches the boundary to become negative without necessarily encountering a self-intersection, as pictured in figure 4.3 and explained in more detail below. The aim of this chapter is to explore this construction with interface branes in more detail. Unfortunately, we will find that it does not resolve the self-intersection problem; requiring that the ETW brane remains outside of the interface brane and that the interface brane does not self-intersect limits us to $T < T_*$, just as before. Moreover, in the limit as T approaches T_*, the interface brane tension must go to zero, returning us to the original setup without an interface brane.

It is not clear if this failure is essentially technical, or is indicative of a deeper issue; the connection to eternal traversable wormholes suggests that it may be the latter. As we will comment on later, the charged black hole solution of [44] provides an example where we obtain a good ETW brane solution and can construct its state by a Euclidean path integral, but this does not define an eternal traversable wormhole, as the analytic continuation that gives us the wormhole makes the Maxwell field associated with the charge imaginary (analytically continuing the charge to make the Maxwell field real would instead break the mechanism that avoids self-intersection).

The organisation of the rest of the chapter is: in the next section, we review the models we consider and relate the worldvolume discussion in [47] to the self-intersection picture. In section 4.2, we look at the constraints on the model with interface branes. We give a simple scaling argument to show that no solutions without self-intersection exist in the limit of large r_0^{ETW}, and explore the regions of the parameter space where solutions exist for finite r_0^{ETW} numerically, showing that solutions exist only for $T < T_*$. In section 3.5, we discuss the differences in the charged black hole case and make some brief concluding comments.

Note added: after completing this work, we learned that similar results were obtained independently in [135].

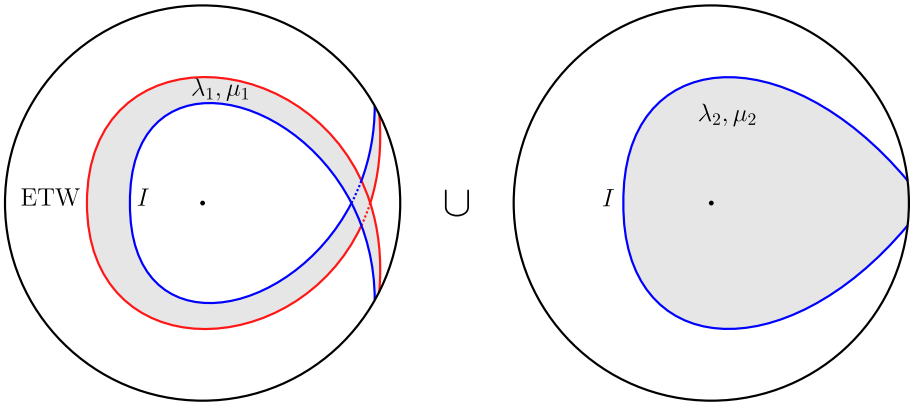

Figure 4.3: The combined model containing both an ETW brane and an interface brane I. The two solutions are glued along the interface brane. Since the Euclidean horizon is not included in the left-hand solution, both branes are multiply wound relative to a single copy of Euclidean/Schwarzschild AdS avoiding self-intersections.

4.1 End of the world brane cosmology

The holographic model of cosmology we consider was first proposed in [43]. The model consists of an AdS black hole bulk with one asymptotic region, with a dynamical constant-tension ETW brane behind the horizon, as pictured in figure 4.1. The induced geometry on the ETW brane worldvolume is that of a closed FRW universe, with the radial position playing the role of the scale factor.

Consider first the original setup with just an ETW brane. The bulk action is

$$I = \frac{1}{16\pi G}\left[\int_{\mathcal{M}} \mathrm{d}^{d+1}x\sqrt{-g}\,(R-2\Lambda) + 2\int_{\partial\mathcal{M}} \mathrm{d}^{d}y\sqrt{-h}\,K - 2(d-1)\int_{\mathcal{Q}} \mathrm{d}^{d}y\sqrt{-h}\,T\right], \tag{4.1.1}$$

where $\Lambda = -\frac{d(d-1)}{2L^2}$ is a cosmological constant, K is the trace of the extrinsic curvature and T is the tension of the ETW brane with worldvolume $\mathcal{Q}$, which we take to be one component of the boundary $\partial\mathcal{M}$ of the spacetime, the other component corresponding to the symptotically AdS conformal boundary. We consider a planar

AdS-Schwarzchild black hole bulk solution

$$\mathrm{d}s^2 = -f(r)\mathrm{d}t^2 + \frac{\mathrm{d}r^2}{f(r)} + \frac{r^2}{L^2}\mathrm{d}x^a\mathrm{d}x_a, \qquad f(r) \equiv \frac{r^2}{L^2} - \frac{\mu}{r^{d-2}}. \tag{4.1.2}$$

This has a horizon at $r = r_h$, where $r_h^d = \mu L^2$. The brane has stress-energy tensor $8\pi G T_{ab} = (1-d)T h_{ab}$, and the action implies that the boundary condition for the bulk metric at $\mathcal{Q}$ is

$$K_{ab} - K h_{ab} = (1-d)T h_{ab} \tag{4.1.3}$$

The tt component of this equation leads to the brane equation of motion

$$\left(\frac{\mathrm{d}r}{\mathrm{d}t}\right)^2 = \frac{f^2(r)}{T^2 r^2}\left(T^2 r^2 - f(r)\right). \tag{4.1.4}$$

In the Lorentzian black hole geometry, the brane will reach a maximum radius r_0^{ETW}, with $(r_0^{ETW})^d = \frac{r_h^d}{1-T^2L^2}$, which we take to occur at $t = 0$. Note $r_0^{ETW} > r_h$ for $T > 0$, and $r_0^{ETW} \to \infty$ as $T \to L^{-1}$. To the future and past of this, $r(t)$ decreases, as pictured in figure 4.1. The brane worldvolume geometry is thus a closed FRW big-bang/big-crunch cosmology, where the brane radius $r(t)$ plays the role of the scale factor, and the brane equation of motion (4.1.4) corresponds to the Friedmann equation in this worldvolume cosmology.

The state on the $t = 0$ slice can be obtained by a Euclidean path integral. In the Euclidean black hole, the motion of the ETW brane is

$$\left(\frac{\mathrm{d}r}{\mathrm{d}\tau}\right)^2 = \frac{f^2(r)}{T^2 r^2}\left(f(r) - T^2 r^2\right). \tag{4.1.5}$$

This now has a minimum at $r = r_0^{ETW}$. Since the ETW brane is inside the black hole in the Lorentzian geometry, it is at its minimum radius in the Euclidean solution at $\tau = \beta/2$, where $\beta = 2\pi L^2/r_h$ is the periodicity in Euclidean time τ. It reaches the AdS boundary at a time

$$\tau^{ETW} = \frac{\beta}{2} - \int_{r_0^{ETW}}^{\infty} \frac{dr}{f(r)} \frac{Tr}{\sqrt{f(r) - T^2 r^2}}. \tag{4.1.6}$$

To avoid self-intersections in the Euclidean solution, we need $\tau^{ETW} > 0$. However,

setting $r = r_0^{ETW} x$, we have

$$\sigma^{ETW} = \frac{2\tau^{ETW}}{\beta} = 1 - \frac{d}{2\pi} TL (y_0^{ETW})^{\frac{d-2}{2}} \int_1^\infty \frac{dx}{x^2(1-(y_0^{ETW})^{-d}x^{-d})\sqrt{1-x^{-d}}}, \tag{4.1.7}$$

where $y_0^{ETW} = r_0^{ETW}/r_h$, so $(y_0^{ETW})^{-d} = 1 - T^2L^2$. It is clear that for $d > 2$ we can't take $r_0^{ETW} \to \infty$ while keeping $\tau^{ETW} > 0$. There must then be some critical value $T = T_* < L^{-1}$ such that $\tau^{ETW} = 0$, and if we consider $T > T_*$ we will have self-intersecting branes in the Euclidean solution.

It is interesting to note in passing that the integral can be computed exactly:

$$\sigma^{ETW} = 1 - \frac{d}{2\sqrt{\pi}} TL(1-T^2L^2)^{\frac{2-d}{2d}} \frac{\Gamma\left(1+\frac{1}{d}\right)}{\Gamma\left(\frac{1}{2}+\frac{1}{d}\right)} {}_2F_1\left(1, \frac{1}{d}; \frac{1}{2}+\frac{1}{d}; 1-T^2L^2\right). \tag{4.1.8}$$

For $d = 2$, the identity ${}_2F_1(b, a; b; z) = (1-z)^{-a}$ reduces this to $\sigma^{ETW} = \frac{1}{2}$, so the brane hits the boundary at $\tau^{ETW} = \frac{\beta}{4}$ independent of the value of r_0^{ETW}, while for $d > 2$ the critical tension T_* is defined implicitly by solving $\sigma^{ETW} = 0$.

4.1.1 Obstruction from worldvolume perspective

As remarked above, if we take the Euclidean solution and analytically continue one of the flat directions x^a, we obtain a solution where the metric on the ETW brane is an eternal traversable wormhole. Thus, the obstruction above can be understood as an obstruction to the existence of such eternal traversable wormholes in the effective induced gravity theory on the brane.

A general analysis of obstructions from the worldvolume perspective was given in [47], in the spirit of [134]. Following [47], we give the discussion for the case $d = 4$. The analysis there is performed in terms of a new coordinate z along the ETW brane, which makes the ETW brane geometry conformally flat,

$$\mathrm{d}s^2 = a^2(z)(\mathrm{d}z^2 + \eta_{ab}\mathrm{d}x^a\mathrm{d}x^b), \tag{4.1.9}$$

where $a(z)$ has simple poles at $z = \pm z_0/2$ and a minimum at $z = 0$. We assume that we have an effective gravity theory on the brane; the zz-component of Einstein's

equation then gives

$$3\left(\frac{a'}{a}\right)^2 - \frac{3a^2}{\ell^2} = 8\pi G_4 T_{zz}, \tag{4.1.10}$$

where G_4 is the effective 4-dimensional Newton's constant on the brane and ℓ is the effective AdS scale on the brane. We take the matter on the brane to be conformal; then $T_{zz} = -3\rho/a^2$. The minimum value of a occurs where $a' = 0$ so we have

$$a_{min} = (8\pi G_4 \rho \ell^2)^{\frac{1}{4}}. \tag{4.1.11}$$

Integrating from this minimum radius to the asymptotically AdS boundary at $z = z_0/2$, we get

$$\frac{z_0}{2} = \int_{a_{min}}^{\infty} \frac{\mathrm{d}a}{\sqrt{\frac{a^4}{\ell^2} - 8\pi G_4 \rho}} = \frac{\ell}{(8\pi G_4 \rho \ell^2)^{\frac{1}{4}}} I, \tag{4.1.12}$$

where

$$I \equiv \int_1^{\infty} \frac{\mathrm{d}x}{\sqrt{x^4 - 1}} \approx 1.311. \tag{4.1.13}$$

Thus we have

$$\rho z_0^4 = \frac{2\ell^2 I^4}{\pi G_4}. \tag{4.1.14}$$

To have an effective gravitational theory on the brane, we want the RHS to be large; we want the brane AdS scale ℓ to be large compared to the brane Planck scale. This ratio can also be interpreted as the central charge c_3 of the 3d CFT dual to the 4d gravity theory on the brane. But the LHS is naturally of order c_4, the number of degrees of freedom of the 4d CFT on the brane. (We get a Casimir energy contribution with $\rho \sim \frac{1}{z_0^4}$ for each species from the finite range of the z coordinate.) We cannot solve this problem by taking the number of species c_4 parametrically large, of order c_3; such a large number of species results in a larger effective UV cutoff on the brane, of order ℓ [134]. Thus, there seems to be a general obstruction to the construction of such traversable wormhole solutions.

For the Schwarzschild-AdS construction considered before, this obstruction is the same as the self-intersection problem. Using (4.1.4), the induced metric on the

brane in Schwarzschild-AdS is

$$\mathrm{d}s^2 = \frac{f(r)^2}{T^2 r^2}\mathrm{d}\tau^2 + \frac{r^2}{L^2}\mathrm{d}x^a \mathrm{d}x_a = \frac{r^2}{L^2}(\mathrm{d}z^2 + \mathrm{d}x^a \mathrm{d}x_a), \tag{4.1.15}$$

so $\mathrm{d}z^2 = \frac{f(r)^2 L^2}{T^2 r^4}\mathrm{d}\tau^2$, and (4.1.4) becomes

$$\frac{L^2}{r^2}\left(\frac{\mathrm{d}r}{\mathrm{d}z}\right)^2 = f(r) - T^2 r^2 = r^2\left(\frac{1}{L^2} - T^2\right) - \frac{\mu}{r^2}. \tag{4.1.16}$$

This maps to equation (4.1.10) with the identifications

$$r^2 \to a^2 L^2, \qquad \left(\frac{1}{L^2} - T^2\right) \to \frac{1}{\ell^2}, \qquad \mu \to 8\pi G_4 \rho L^4. \tag{4.1.17}$$

As stated before, we tune the brane AdS scale ℓ to be large by taking the tension T close to L^{-1}, and as usual, the energy density on boundary (in this case, a dynamical brane) is set by the black hole mass parameter μ in the bulk.

We have $f(r) < \frac{r^2}{L^2}$, so $\mathrm{d}z < \frac{\mathrm{d}\tau}{LT}$, and

$$\rho z_0^4 < \frac{\rho \tau_0^4}{L^4 T^4} = \left(\frac{\tau_0}{\beta}\right)^4 \frac{L^2}{G_4}\frac{8\pi^3}{L^4 T^4}, \tag{4.1.18}$$

so we see that ρz_0^4 is indeed naturally of the order of $L^2/G_4 \sim c_4$, the central charge of the CFT dual to the Schwarzschild-AdS bulk, and the problem of making ρz_0^4 large maps on to the problem of making τ_0 large compared to β, which we can't achieve in this model without self-intersection.

4.1.2 Interface branes

The proposed solution of this problem is to consider adding an interface brane in the bulk [47]. Using results of [136, 137], [47] showed that for extreme values of the interface brane tension, ρz_0^4 could indeed be made large. From the spacetime perspective we will focus on, the idea is that for some choices of the interface tension and bulk parameters, the spacetime on one side of the interface brane doesn't contain a horizon, so both the ETW brane and interface brane can be multiply wound relative to a single copy of the Euclidean Schwarzschild-AdS$_5$ geometry on that side without encountering self-intersections, as pictured in figure 4.3. We find that this setup

doesn't solve the problem however, as the two branes run into each other. In this section we will give a brief overview of interface brane setup; we will discuss the details of the constraints in the next section.

With an interface brane, we have a spacetime region on either side of the brane, so the relevant terms in the action are

$$\begin{aligned} I = \frac{1}{16\pi G}\Big[&\int_{\mathcal{M}_1} \mathrm{d}^{d+1}x\sqrt{-g_1}(R_1 - 2\Lambda_1) + \int_{\mathcal{M}_2} \mathrm{d}^{d+1}x\sqrt{-g_2}(R_2 - 2\Lambda_2) \\ &+ 2\int_{\mathcal{I}} \mathrm{d}^d y\sqrt{-h}(K_1 - K_2) - 2(d-1)\int_{\mathcal{I}} \mathrm{d}^d y\sqrt{-h}\kappa \\ &+ 2\int_{\mathcal{Q}} \mathrm{d}^d y\sqrt{-h}\,K - 2(d-1)\int_{\mathcal{Q}} \mathrm{d}^d y\sqrt{-h}\,T\Big], \end{aligned} \tag{4.1.19}$$

where $\mathcal{I} \equiv \partial\mathcal{M}_1 \cap \partial\mathcal{M}_2$ is the interface brane worldvolume, and $\mathcal{Q}$ is the worldvolume of the ETW brane as before. We assume a constant tension brane with tension parameter κ. The motion of the interface brane is determined by the second Israel junction condition

$$K_{1ab} - K_{2ab} = \kappa h_{ab}. \tag{4.1.20}$$

We consider a bulk solution with either side of the interface brane having the metric of a planar AdS black hole of mass μ_i and AdS scale $L_i \equiv \frac{1}{\sqrt{\lambda_i}}$,

$$\mathrm{d}s_i^2 = f_i(r)\mathrm{d}t^2 + \frac{\mathrm{d}r^2}{f_i(r)} + r^2\mathrm{d}x^a\mathrm{d}x_a, \qquad f_i \equiv \lambda_i r^2 - \frac{\mu_i}{r^{d-2}}. \tag{4.1.21}$$

where $i \in \{1, 2\}$. The black hole horizon radii are $r_{hi}^d = \frac{\mu_i}{\lambda_i}$. We will have an ETW brane in region 1, so in region 1 r lies in a finite range between the ETW brane and the interface brane, while in region 2 r runs from the interface brane to the asymptotic boundary. The second junction condition leads to

$$f_1\frac{dt_1}{ds} - f_2\frac{dt_2}{ds} = \kappa r, \tag{4.1.22}$$

The first junction condition along with the definition of the proper length parameter s leads to

$$f_i\left(\frac{dt_i}{ds}\right) + \frac{1}{f_i}\left(\frac{dt_i}{ds}\right) = 1. \tag{4.1.23}$$

Using these we find

$$\left(\frac{dr}{ds}\right)^2 - V_{eff}(r) = 0, \qquad V_{eff}(r) \equiv \frac{1}{2}(f_1 + f_2) - \frac{(f_1 - f_2)^2 + \kappa^4 r^4}{4\kappa^2 r^2}, \quad (4.1.24)$$

and

$$\frac{dt_1}{dr} = \frac{1}{f_1\sqrt{V_{eff}(r)}}\left(\frac{1}{2\kappa r}(f_1 - f_2) + \frac{1}{2}\kappa r\right), \quad (4.1.25)$$

$$\frac{dt_2}{dr} = -\frac{1}{f_2\sqrt{V_{eff}(r)}}\left(\frac{1}{2\kappa r}(f_2 - f_1) + \frac{1}{2}\kappa r\right). \quad (4.1.26)$$

The minimum radius of the brane, $V_{eff}(r_0^I) = 0$, is found to be

$$(r_0^I)^d = \frac{(\lambda_1 - \lambda_2)(\mu_1 - \mu_2) - \kappa^2(\mu_1 + \mu_2) - 2\kappa\sqrt{\lambda_1\mu_2^2 + \lambda_2\mu_1^2 - (\lambda_1 + \lambda_2 - \kappa^2)\mu_1\mu_2}}{\kappa^4 - 2\kappa^2(\lambda_1 + \lambda_2) + (\lambda_1 - \lambda_2)^2}. \quad (4.1.27)$$

It will be useful to define $\bar{\lambda} = \frac{\lambda_2}{\lambda_1}$, $\bar{\mu} = \frac{\mu_2}{\mu_1}$ and $\bar{\kappa} = \frac{\kappa}{\sqrt{\lambda_1}}$. In terms of these parameters the minimum radius is given by

$$(r_0^I)^d = r_{h1}^d \left(\frac{(1 - \bar{\lambda})(1 - \bar{\mu}) - \bar{\kappa}^2(1 + \bar{\mu}) - 2\bar{\kappa}\sqrt{\bar{\mu}\bar{\kappa}^2 + \left(\bar{\mu} - \bar{\lambda}\right)(\bar{\mu} - 1)}}{\bar{\kappa}^4 - 2\bar{\kappa}^2(1 + \bar{\lambda}) + (1 - \bar{\lambda})^2}\right) \quad (4.1.28)$$

We want solutions that include a horizon in region 2, and don't include the horizon in region 1. The solution will contain a horizon if $\dot{t_2} < 0$ near $r = r_0^I$ or

$$f_2(r_0^I) - f_1(r_0^I) + \kappa^2(r_0^I)^2 > 0. \quad (4.1.29)$$

This condition becomes

$$\frac{(r_0^I)^d}{r_{h1}^d}\left[\bar{\kappa}^2 - (1 - \bar{\lambda})\right] + (1 - \bar{\mu}) > 0. \quad (4.1.30)$$

From (4.1.28), we see that this condition only depends on the three parameters $(\bar{\lambda}, \bar{\mu}, \bar{\kappa})$. From (4.1.30), we find that the t_2 region will contain a horizon if

$$\bar{\kappa} > \sqrt{1 - \frac{\bar{\lambda}}{\bar{\mu}}} \qquad \text{or} \qquad \bar{\mu} < \bar{\lambda}. \quad (4.1.31)$$

Requiring there is no horizon in the t_1 region, $\dot{t_1}(r_0^I) < 0$, leads to

$$\frac{(r_0^I)^d}{r_{h1}^d}\left[\bar{\kappa}^2 - (\bar{\lambda}-1)\right] + (\bar{\mu}-1) > 0. \tag{4.1.32}$$

giving the condition

$$\bar{\kappa} < \sqrt{\bar{\lambda}-\bar{\mu}} \qquad \text{and} \qquad \bar{\mu} < \bar{\lambda}. \tag{4.1.33}$$

Therefore, the desired solution requires we satisfy the second inequality in (4.1.31), $\bar{\mu} < \bar{\lambda}$. From (4.1.33) and $\bar{\kappa}_{min} = |\sqrt{\bar{\lambda}} - 1|$ we get the stronger condition

$$\bar{\lambda} > \frac{1}{4}(1+\bar{\mu})^2. \tag{4.1.34}$$

4.2 Constraints on interface brane models

We now want to consider the constraints we need to satisfy to build well-behaved Euclidean solutions in the interface brane models. Assuming we choose parameters so that the event horizon is not included in region 1, we do not need to impose a periodicity condition on the time coordinate in region 1, so we can have $t^{ETW} < 0$ without a self-intersection problem. However, in the presence of the interface brane, we have new constraints from requiring the ETW brane to not run into the interface brane: we need the minimum radius larger, $r_0^{ETW} > r_0^I$, and we need the time at which the ETW brane meets the boundary to be larger, $t^{ETW} > t_1^I$. To avoid self-intersection of the interface brane in region 2, we also need $t_2^I > 0$. We will find that we can satisfy these constraints simultaneously only for $T < T_*$.

These conditions are conveniently analysed by working in terms of the dimensionless combinations

$$\sigma^{ETW} = \frac{2t^{ETW}}{\beta_1} = 1 - \frac{2}{\beta_1}\int_{r_0^{ETW}}^{\infty} \frac{\mathrm{d}r}{f_1(r)} \frac{Tr}{\sqrt{f_1(r) - T^2r^2}}, \tag{4.2.1}$$

$$\sigma_1^I = \frac{2t_1^I}{\beta_1} = 1 + \frac{2}{\beta_1}\int_{r_0^I}^{\infty} \frac{\mathrm{d}r}{f_1(r)} \left(\frac{f_1(r) - f_2(r) + \kappa^2 r^2}{\kappa r\sqrt{V_{eff}(r)}}\right), \tag{4.2.2}$$

$$\sigma_2^I = \frac{2t_2^I}{\beta_2} = 1 - \frac{2}{\beta_2}\int_{r_0^I}^{\infty} \frac{\mathrm{d}r}{f_2(r)} \left(\frac{f_2(r) - f_1(r) + \kappa^2 r^2}{\kappa r\sqrt{V_{eff}(r)}}\right), \tag{4.2.3}$$

where $\beta_i = \frac{4\pi}{d\lambda_i r_{hi}}$ is the inverse temperature associated to either side of the interface brane.

Let us first consider the region of parameters where both r_0^{ETW} and r_0^I are large compared to r_{hi}. Large r_0^{ETW} is the regime we wanted to reach, where the theory on the ETW brane is approximately d-dimensional Einstein gravity, while we will see that large r_0^I is required to satisfy the constraints; this corresponds to the extreme values of the interface brane tension which were found in [47] to give large ρz_0^4. In this limit we can give a simple scaling argument that no good Euclidean solution exists.

Recall that for the ETW brane, we have

$$\sigma^{ETW} = 1 - \frac{d}{2\pi}\frac{T}{\sqrt{\lambda_1}}(y_0^{ETW})^{\frac{d-2}{2}}\int_1^\infty \frac{\mathrm{d}x}{x^2(1-(y_0^{ETW})^{-d}x^{-d})\sqrt{1-x^{-d}}}. \tag{4.2.4}$$

It is clear that for $d > 2$ we can't take $y_0^{ETW} \to \infty$ while keeping $\sigma^{ETW} > 0$. The interface brane scenario relaxes the condition on σ^{ETW} to $\sigma^{ETW} > \sigma_1^I$ while keeping $\sigma_2^I > 0$. Let us write the integrals in terms of the parameters $(\bar\lambda, \bar\mu, \bar\kappa)$ and scale out r_{h1}, $r = r_{h1}y$,

$$\sigma_1^I = 1 + \frac{d}{4\pi}\int_{y_0^I}^\infty \frac{\mathrm{d}y}{\bar f_1(y)}\left(\frac{\bar f_1(y) - \bar f_2(y) + \bar\kappa^2 y^2}{\bar\kappa y\sqrt{\bar V_{eff}(y)}}\right), \tag{4.2.5}$$

$$\sigma_2^I = 1 - \frac{d\bar\lambda}{4\pi}\frac{r_{h2}}{r_{h1}}\int_{y_0^I}^\infty \frac{\mathrm{d}y}{\bar f_2(y)}\left(\frac{\bar f_2(y) - \bar f_1(y) + \bar\kappa^2 y^2}{\bar\kappa y\sqrt{\bar V_{eff}(y)}}\right), \tag{4.2.6}$$

where $\bar f_1 = y^2(1-y^{-d})$, $\bar f_2 = \bar\lambda y^2(1-\frac{\bar\mu}{\bar\lambda}y^{-d})$,

$$\bar V_{eff} = -\frac{y^2}{4\bar\kappa^2}\left[(\bar\kappa^4 - 2\bar\kappa^2(1+\bar\lambda) + (1-\bar\lambda)^2) + \frac{2}{y^d}(\bar\kappa^2(1+\bar\mu) - (1-\bar\lambda)(1-\bar\mu)) + \frac{1}{y^{2d}}(1-\bar\mu)^2\right]. \tag{4.2.7}$$

To allow $\sigma^{ETW} \to -\infty$, we want to make σ_1^I very negative, by making y_0^I large. For $\bar\kappa$ close to $|1-\sqrt{\bar\lambda}|$, we have

$$(y_0^I)^d \approx \frac{(\bar\mu - \sqrt{\bar\lambda})(1-\sqrt{\bar\lambda}) + |\bar\mu - \sqrt{\bar\lambda}||1-\sqrt{\bar\lambda}|}{2\sqrt{\bar\lambda}[\bar\kappa^2 - (1-\sqrt{\bar\lambda})^2]}. \tag{4.2.8}$$

Thus, for $\sqrt{\bar{\lambda}}$ not between $\bar{\mu}$ and 1, y_0^I blows up as $\bar{\kappa}$ approaches its lower limit $|1-\sqrt{\bar{\lambda}}|$. This is the extremal limit of the interface brane tension introduced in [47].

In this limit, setting $y = y_0^I/w$, we have

$$\bar{V}_{eff} \approx \frac{(\bar{\mu}-\sqrt{\bar{\lambda}})(1-\sqrt{\bar{\lambda}})}{(y_0^I)^{d-2}\bar{\kappa}^2}\left(\frac{1-w^d}{w^2}\right), \tag{4.2.9}$$

and $\bar{f}_1 \approx (y_0^I)^2 w^{-2}$, $\bar{f}_2 \approx (y_0^I)^2\bar{\lambda}w^{-2}$, so

$$\sigma_1^I \approx 1 - \frac{d}{2\pi}(y_0^I)^{\frac{d-2}{2}}\frac{(\sqrt{\bar{\lambda}}-1)}{\sqrt{(\sqrt{\bar{\lambda}}-\bar{\mu})(\sqrt{\bar{\lambda}}-1)}}\int_0^1 \frac{\mathrm{d}w}{\sqrt{1-w^d}} \tag{4.2.10}$$

and

$$\sigma_2^I \approx 1 - \frac{d}{2\pi}(\bar{\lambda})^{\frac{d-2}{2d}}(\bar{\mu})^{\frac{1}{d}}(y_0^I)^{\frac{d-2}{2}}\frac{(\sqrt{\bar{\lambda}}-1)}{\sqrt{(\sqrt{\bar{\lambda}}-\bar{\mu})(\sqrt{\bar{\lambda}}-1)}}\int_0^1 \frac{\mathrm{d}w}{\sqrt{1-w^d}}. \tag{4.2.11}$$

We see from these that $\sigma_1^I < 0$ requires $\bar{\lambda} > 1$. Then to make $\sigma_2^I > 0$, we need to make $\bar{\mu}$ small, so that $(\bar{\mu})^{\frac{1}{d}}(y_0^I)^{\frac{d-2}{2}}$ remains finite as $y_0^I \to \infty$. Note these conditions are consistent with the previous condition on $\bar{\lambda}$, $\bar{\mu}$ given in (4.1.34). In this limit of small $\bar{\mu}$,

$$\sigma_1^I \approx 1 - \frac{d}{2\pi}(y_0^I)^{\frac{d-2}{2}}\sqrt{1-\frac{1}{\sqrt{\bar{\lambda}}}}\int_0^1 \frac{\mathrm{d}w}{\sqrt{1-w^d}}. \tag{4.2.12}$$

Since $y_0^{ETW} > y_0^I \gg 1$, the ETW brane tension is close to its upper bound $T \approx \sqrt{\lambda_1}$ and we have that

$$\sigma^{ETW} - \sigma_1^I \approx \left[(y_0^I)^{\frac{d-2}{2}}\sqrt{1-\frac{1}{\sqrt{\bar{\lambda}}}} - (y_0^{ETW})^{\frac{d-2}{2}}\right]\frac{d}{2\pi}\int_0^1 \frac{\mathrm{d}w}{\sqrt{1-w^d}} < 0. \tag{4.2.13}$$

The requirement that the ETW brane is initially outside the interface brane implies that it will run into the interface brane before reaching the boundary.

Thus, we have shown that our constraints cannot all be satisfied in the region where y_0^{ETW} is large. This is disappointing, as this is the limit of interest. From the perspective of the worldsheet analysis of [47] reviewed in section 4.1.1, increasing y_0^I increases ρ, but at the same time it requires us to increase y_0^{ETW}, which corresponds to increasing c_3. The increasing value of ρz_0^4 never quite catches up with the target value.

However, it looks like the introduction of the interface brane has improved things *somewhat*; while (4.2.13) is always negative, we can make it close to zero if we take $\bar{\lambda}$ large and y_0^I close to y_0^{ETW}. Surprisingly, we will see in the next subsection that this seeming improvement is misleading; there are no values of T where we have good Euclidean solutions with interface branes where we did not already have good solutions without interface branes.

4.2.1 Numerical investigation

In this section, we numerically study the region of the parameter space in which the constraints $\sigma^{ETW} > \sigma_1^I$, $\sigma_2^I > 0$ are satisfied. The relevant parameters are the dimensionless combinations $\bar{\lambda}, \bar{\mu}$ and the brane tensions $\bar{\kappa}, \bar{T} = T/\sqrt{\lambda_1}$. We show that the solutions with interface branes only exist for choices of T that also admit solutions without interface branes.

Due to the constraint on $\bar{\lambda}$ in (4.1.34), we define

$$\bar{\lambda}' \equiv \bar{\lambda} - \bar{\lambda}_{min} = \bar{\lambda} - \frac{1}{4}(1+\bar{\mu})^2. \tag{4.2.14}$$

Plots will be more clear in terms of this shifted variable. The interface tension is constrained to the interval $\bar{\kappa} \in (\bar{\kappa}_{min}, \bar{\kappa}_{max}) = (|\sqrt{\bar{\lambda}}-1|, \sqrt{\bar{\lambda}-\bar{\mu}})$, so we parameterise it as

$$\bar{\kappa} = \bar{\kappa}_{min}(1-x) + \bar{\kappa}_{max}x, \qquad x \in (0,1). \tag{4.2.15}$$

We plot the allowed regions as functions of $\bar{\lambda}', \bar{\mu}$ for a range of values of $\bar{T}$, x. In figure 4.4, we plot this for a value $\bar{T} < \bar{T}_*$, where we see that there is a small allowed range of values of the parameters where all the constraints are satisfied. In figure 4.5, we plot for $\bar{T} = \bar{T}_*$ (to numerical accuracy), seeing that the allowed region shrinks to the single point at $\bar{\lambda}' = 0$, $\bar{\mu} = 1$, for all values of x. This corresponds to the solution with no interface brane, as $\bar{\kappa}_{min} = \bar{\kappa}_{max} = 0$ for $\bar{\lambda}' = 0$, $\bar{\mu} = 1$.

Thus, while there are allowed solutions with interface branes, these only exist for choices of T that also admit solutions without interface branes, and the range of possible values for the interface brane tension shrinks to zero as the critical value is

reached. Allowing the possibility of interface branes has not enlarged the range of possible ETW branes for which we can find eternal wormholes, or good Euclidean solutions describing the initial conditions for our cosmology.

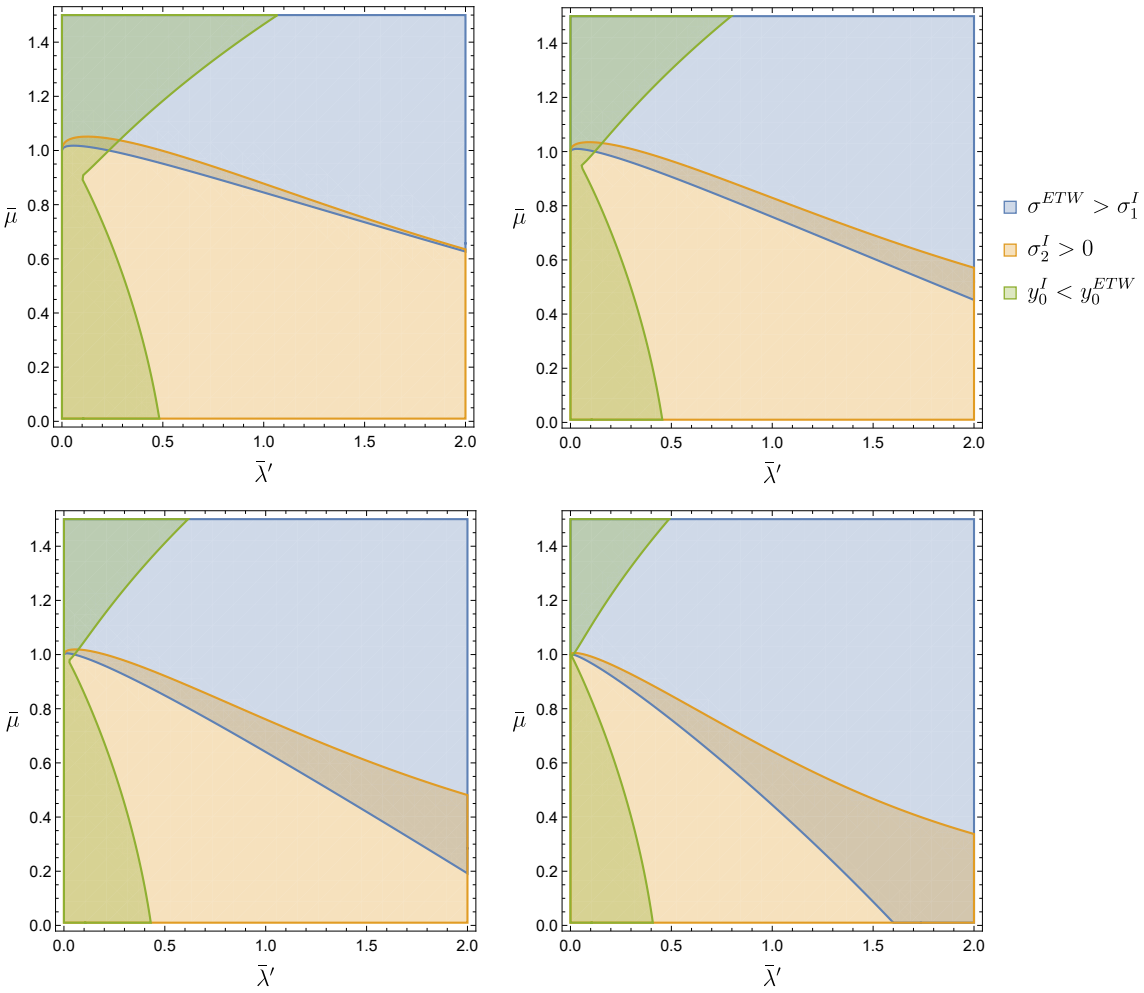

Figure 4.4: Plots of the regions in the parameter space $(\bar{\lambda}', \bar{\mu})$ with $\sigma^{ETW} > \sigma_1^I, \sigma_2^I > 0$, or $y_0^I < y_0^{ETW}$ with $d = 4$, for the sub-critical value $\bar{T} = 0.6 < \bar{T}_*$. Reading from top left to bottom right: $x = 0.16, 0.12, 0.08, 0.04$. We see that there is a small region where all constraints are satisfied. As we decrease x, the constraint that $y_0^I < y_0^{ETW}$ becomes more constraining – this is because, as noted earlier, the interface brane moves towards the boundary as we approach the lower bound on κ.

4.3 Discussion

In this chapter we considered the construction of holographic models for studying closed FRW cosmologies using ETW branes, following [43]. An issue with the

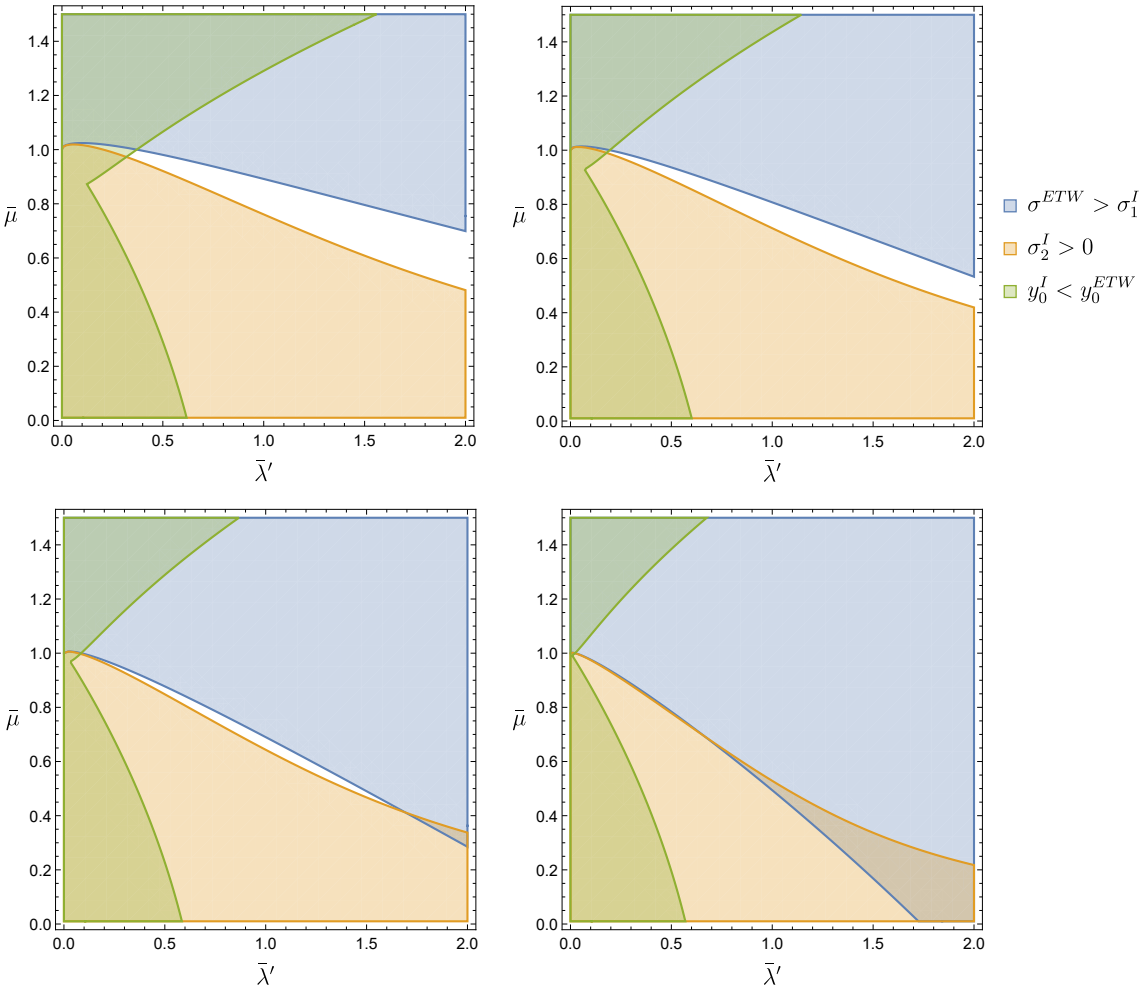

Figure 4.5: Plots of the regions in the parameter space $(\bar{\lambda}', \bar{\mu})$ with $\sigma^{ETW} > \sigma_1^I$, $\sigma_2^I > 0$, or $y_0^I < y_0^{ETW}$ with $d = 4$, $\bar{T} = \bar{T}_* \approx 0.7977$. Reading from top left to bottom right: $x = 0.08, 0.06, 0.04, 0.02$. At this critical value, we see that the only point where all the constraints are satisfied is $\bar{\lambda}' = 0$, $\bar{\mu} = 1$, for all values of x. This corresponds to the solution with no interface brane, as $\bar{\kappa}_{min} = \bar{\kappa}_{max} = 0$ for $\bar{\lambda}' = 0$, $\bar{\mu} = 1$.

construction of such models for $d > 2$ is that the requirements of having a good Euclidean solution and having a separation of scales which gives us Einstein gravity on the ETW brane are difficult to satisfy simultaneously.

We studied a proposed model for satisfying these conditions using interface branes from [47]. We found that the use of interface branes relaxes the constraint in the simple model, but introduces new constraints, from requiring that the ETW brane and the interface brane don't collide. Taking into account all the constraints, we find that adding interface branes doesn't increase the range of values of the ETW brane tension for which we have good solutions.

A key question is whether this failure is essentially technical, or is indicative of a deeper issue. In [47], it was observed that the Euclidean solutions we are trying to construct are related to eternal traversable wormhole solutions, and it has previously been found [134] that it is difficult to construct such solutions in higher dimensions, which might suggest that the problem is deeper. However, we are not aware of any clear physical obstruction to the existence of such eternal traversable wormhole solutions either; see also the discussion of (non-eternal) traversable wormholes in [138].

One hint that the connection to eternal traversable wormholes is relevant to the obstruction we find is that the known way around the obstruction [44] does not give a wormhole solution. By replacing the Schwarzschild-AdS solution we have considered by a charged black hole, we can decouple the period β and the horizon scale r_h. By taking the black hole close to extremality we can make β arbitrarily large, allowing us to keep τ^{ETW} in (4.1.6) positive as r_0^{ETW} grows [44]. However, if we have a real electric or magnetic charge in the Lorentzian black hole solution, after we analytically continue t and one of the x^a, the field will be imaginary, so we do not obtain a good wormhole solution. If we analytically continue the charge parameter, the analytically continued solution does not have an extremal limit, so we can't make β large. It would be very interesting to find some other method for constructing eternal traversable wormholes or brane cosmologies in $d > 2$ to explore these questions further.

Bibliography

[1] L. Susskind, *The world as a hologram*, arXiv:hep-th/9409089.

[2] G. 't Hooft, *Dimensional reduction in quantum gravity*, arXiv:gr-qc/9310026.

[3] J. M. Maldacena, *The large n limit of superconformal field theories and supergravity*, arXiv:hep-th/9711200.

[4] E. Witten, *Anti de sitter space and holography*, arXiv:hep-th/9802150.

[5] D. Z. Freedman, S. D. Mathur, A. Matusis and L. Rastelli, *Correlation functions in the cft(d)/ads(d+1) correpondence*, arXiv:hep-th/9804058.

[6] O. Aharony, S. S. Gubser, J. Maldacena, H. Ooguri and Y. Oz, *Large n field theories, string theory and gravity*, arXiv:hep-th/9905111.

[7] S. Ryu and T. Takayanagi, *Holographic derivation of entanglement entropy from AdS/CFT*, *Phys. Rev. Lett.* **96** (2006) 181602, [hep-th/0603001].

[8] R. Bousso, S. Leichenauer and V. Rosenhaus, *Light-sheets and ads/cft*, arXiv:1203.6619.

[9] B. Czech, J. L. Karczmarek, F. Nogueira and M. V. Raamsdonk, *The gravity dual of a density matrix*, arXiv:1204.1330.

[10] M. Headrick, V. E. Hubeny, A. Lawrence and M. Rangamani, *Causality & holographic entanglement entropy*, arXiv:1408.6300.

[11] A. Almheiri, X. Dong and D. Harlow, *Bulk locality and quantum error correction in ads/cft*, arXiv:1411.7041.

[12] P. Gao, D. L. Jafferis and A. C. Wall, *Traversable Wormholes via a Double Trace Deformation*, *JHEP* **12** (2017) 151, [1608.05687].

[13] J. Maldacena and X.-L. Qi, *Eternal traversable wormhole*, 1804.00491.

[14] J. Maldacena, D. Stanford and Z. Yang, *Diving into traversable wormholes*, *Fortsch. Phys.* **65** (2017) 1700034, [1704.05333].

[15] L. Susskind and Y. Zhao, *Teleportation through the wormhole*, *Phys. Rev. D* **98** (2018) 046016, [1707.04354].

[16] R. van Breukelen and K. Papadodimas, *Quantum teleportation through time-shifted AdS wormholes*, *JHEP* **08** (2018) 142, [1708.09370].

[17] D. Bak, C. Kim and S.-H. Yi, *Bulk view of teleportation and traversable wormholes*, *JHEP* **08** (2018) 140, [1805.12349].

[18] E. Caceres, A. S. Misobuchi and M.-L. Xiao, *Rotating traversable wormholes in AdS*, *JHEP* **12** (2018) 005, [1807.07239].

[19] Z. Fu, B. Grado-White and D. Marolf, *Traversable Asymptotically Flat Wormholes with Short Transit Times*, *Class. Quant. Grav.* **36** (2019) 245018, [1908.03273].

[20] Z. Fu, B. Grado-White and D. Marolf, *A perturbative perspective on self-supporting wormholes*, *Class. Quant. Grav.* **36** (2019) 045006, [1807.07917].

[21] B. Freivogel, D. A. Galante, D. Nikolakopoulou and A. Rotundo, *Traversable wormholes in AdS and bounds on information transfer*, *JHEP* **01** (2020) 050, [1907.13140].

[22] J. Maldacena, A. Milekhin and F. Popov, *Traversable wormholes in four dimensions*, 1807.04726.

[23] G. Penington, *Entanglement Wedge Reconstruction and the Information Paradox*, *JHEP* **09** (2020) 002, [1905.08255].

[24] A. Almheiri, N. Engelhardt, D. Marolf and H. Maxfield, *The entropy of bulk quantum fields and the entanglement wedge of an evaporating black hole*, *JHEP* **12** (2019) 063, [1905.08762].

[25] A. Almheiri, R. Mahajan, J. Maldacena and Y. Zhao, *The Page curve of Hawking radiation from semiclassical geometry*, *JHEP* **03** (2020) 149, [1908.10996].

[26] G. Penington, S. H. Shenker, D. Stanford and Z. Yang, *Replica wormholes and the black hole interior*, 1911.11977.

[27] A. Almheiri, T. Hartman, J. Maldacena, E. Shaghoulian and A. Tajdini, *Replica Wormholes and the Entropy of Hawking Radiation*, *JHEP* **05** (2020) 013, [1911.12333].

[28] A. Almheiri, R. Mahajan and J. Maldacena, *Islands outside the horizon*, 1910.11077.

[29] H. Verlinde, *ER = EPR revisited: On the Entropy of an Einstein-Rosen Bridge*, 2003.13117.

[30] A. Almheiri, R. Mahajan and J. E. Santos, *Entanglement islands in higher dimensions*, arXiv:1911.09666.

[31] H. Geng and A. Karch, *Massive islands*, arXiv:2006.02438.

[32] H. Z. Chen, Z. Fisher, J. Hernandez, R. C. Myers and S.-M. Ruan, *Information flow in black hole evaporation*, arXiv:1911.03402.

[33] T. Hartman, Y. Jiang and E. Shaghoulian, *Islands in cosmology*, *JHEP* **11** (2020) 111, [2008.01022].

[34] T. J. Hollowood and S. P. Kumar, *Islands and Page Curves for Evaporating Black Holes in JT Gravity*, *JHEP* **08** (2020) 094, [2004.14944].

[35] H. Z. Chen, Z. Fisher, J. Hernandez, R. C. Myers and S.-M. Ruan, *Evaporating Black Holes Coupled to a Thermal Bath*, *JHEP* **01** (2021) 065, [2007.11658].

[36] V. Balasubramanian, A. Kar and T. Ugajin, *Islands in de Sitter space*, *JHEP* **02** (2021) 072, [2008.05275].

[37] V. Balasubramanian, A. Kar and T. Ugajin, *Entanglement between two disjoint universes*, 2008.05274.

[38] D. Bak, C. Kim, S.-H. Yi and J. Yoon, *Unitarity of entanglement and islands in two-sided janus black holes*, arXiv:2006.11717.

[39] L. Anderson, O. Parrikar and R. M. Soni, *Islands with gravitating baths: towards ER = EPR*, *JHEP* **21** (2020) 226, [2103.14746].

[40] Y. Chen, V. Gorbenko and J. Maldacena, *Bra-ket wormholes in gravitationally prepared states*, *JHEP* **02** (2021) 009, [2007.16091].

[41] D. N. Page, *Information in black hole radiation*, arXiv:hep-th/9306083.

[42] D. N. Page, *Time dependence of hawking radiation entropy*, arXiv:1301.4995.

[43] S. Cooper, M. Rozali, B. Swingle, M. Van Raamsdonk, C. Waddell and D. Wakeham, *Black Hole Microstate Cosmology*, *JHEP* **07** (2019) 065, [1810.10601].

[44] S. Antonini and B. Swingle, *Cosmology at the end of the world*, *Nature Phys.* **16** (2020) 881–886, [1907.06667].

[45] M. Van Raamsdonk, *Comments on wormholes, ensembles, and cosmology*, 2008.02259.

[46] J. Sully, M. Van Raamsdonk and D. Wakeham, *BCFT entanglement entropy at large central charge and the black hole interior*, 2004.13088.

[47] M. Van Raamsdonk, *Cosmology from confinement?*, 2102.05057.

[48] I. R. Klebanov and E. Witten, *Ads/cft correspondence and symmetry breaking*, arXiv:hep-th/9905104.

[49] D. Marolf and S. Ross, *Boundary conditions and dualities: Vector fields in ads/cft*, arXiv:hep-th/0606113.

[50] M. Van Raamsdonk, *Lectures on Gravity and Entanglement*, in *Theoretical Advanced Study Institute in Elementary Particle Physics: New Frontiers in Fields and Strings*, pp. 297–351, 2017, 1609.00026, DOI.

[51] M. Headrick, *Lectures on entanglement entropy in field theory and holography*, 2019. 10.48550/ARXIV.1907.08126.

[52] M. A. Nielsen and I. L. Chuang, *Quantum Computation and Quantum Information: 10th Anniversary Edition*. Cambridge University Press, 2010, 10.1017/CBO9780511976667.

[53] D. Harlow, *Jerusalem Lectures on Black Holes and Quantum Information*, *Rev. Mod. Phys.* **88** (2016) 015002, [1409.1231].

[54] J. M. Maldacena, *Eternal black holes in anti-de Sitter*, *JHEP* **04** (2003) 021, [hep-th/0106112].

[55] B. S. Kay and R. M. Wald, *Theorems on the uniqueness and thermal properties of stationary, nonsingular, quasifree states on spacetimes with a bifurcate killing horizon*, *Physics Reports* **207** (1991) 49–136.

[56] T. Jacobson, *Note on hartle-hawking vacua*, *Phys. Rev. D* **50** (Nov, 1994) R6031–R6032.

[57] S. F. Ross, *Black hole thermodynamics*, 0502195.

[58] T. Hartman, *Lectures on quantum gravity and black holes*, [http://www.hartmanhep.net/topics2015/gravity-lectures.pdf].

[59] M. Van Raamsdonk, *Comments on quantum gravity and entanglement*, 0907.2939.

[60] M. Van Raamsdonk, *Building up spacetime with quantum entanglement*, *Gen. Rel. Grav.* **42** (2010) 2323–2329, [1005.3035].

[61] J. Maldacena and L. Susskind, *Cool horizons for entangled black holes*, *Fortsch. Phys.* **61** (2013) 781–811, [1306.0533].

[62] T. Andrade, S. Fischetti, D. Marolf, S. F. Ross and M. Rozali, *Entanglement and correlations near extremality: CFTs dual to Reissner-Nordström AdS_5*, *JHEP* **04** (2014) 023, [1312.2839].

[63] A. Chamblin, R. Emparan, C. V. Johnson and R. C. Myers, *Charged AdS black holes and catastrophic holography*, *Phys. Rev. D* **60** (1999) 064018, [hep-th/9902170].

[64] V. E. Hubeny, M. Rangamani and T. Takayanagi, *A Covariant holographic entanglement entropy proposal*, *JHEP* **07** (2007) 062, [0705.0016].

[65] T. Takayanagi, *Holographic Dual of BCFT*, *Phys. Rev. Lett.* **107** (2011) 101602, [1105.5165].

[66] J. D. Brown and M. Henneaux, *Central Charges in the Canonical Realization of Asymptotic Symmetries: An Example from Three-Dimensional Gravity*, *Commun. Math. Phys.* **104** (1986) 207–226.

[67] P. Hayden, M. Headrick and A. Maloney, *Holographic Mutual Information is Monogamous*, *Phys. Rev. D* **87** (2013) 046003, [1107.2940].

[68] A. C. Wall, *Maximin Surfaces, and the Strong Subadditivity of the Covariant Holographic Entanglement Entropy*, *Class. Quant. Grav.* **31** (2014) 225007, [1211.3494].

[69] D. Marolf, A. C. Wall and Z. Wang, *Restricted maximin surfaces and hrt in generic black hole spacetimes*, arXiv:1901.03879.

[70] A. Lewkowycz and J. Maldacena, *Generalized gravitational entropy*, *JHEP* **08** (2013) 090, [1304.4926].

[71] X. Dong, A. Lewkowycz and M. Rangamani, *Deriving covariant holographic entanglement*, arXiv:1607.07506.

[72] R. M. Wald, *Black hole entropy is noether charge*, arXiv:gr-qc/9307038.

[73] V. Iyer and R. M. Wald, *Some properties of noether charge and a proposal for dynamical black hole entropy*, arXiv:gr-qc/9403028.

[74] T. Jacobson, G. Kang and R. C. Myers, *On black hole entropy*, arXiv:gr-qc/9312023.

[75] L.-Y. Hung, R. C. Myers and M. Smolkin, *On holographic entanglement entropy and higher curvature gravity*, arXiv:1101.5813.

[76] X. Dong, *Holographic entanglement entropy for general higher derivative gravity*, arXiv:1310.5713.

[77] R.-X. Miao and W. zhong Guo, *Holographic entanglement entropy for the most general higher derivative gravity*, arXiv:1411.5579.

[78] J. de Boer, M. Kulaxizi and A. Parnachev, *Holographic entanglement entropy in lovelock gravities*, arXiv:1101.5781.

[79] T. Faulkner, A. Lewkowycz and J. Maldacena, *Quantum corrections to holographic entanglement entropy*, *JHEP* **11** (2013) 074, [1307.2892].

[80] N. Engelhardt and A. C. Wall, *Quantum Extremal Surfaces: Holographic Entanglement Entropy beyond the Classical Regime*, *JHEP* **01** (2015) 073, [1408.3203].

[81] X. Dong and A. Lewkowycz, *Entropy, extremality, euclidean variations, and the equations of motion*, arXiv:1705.08453.

[82] X. Dong, D. Harlow and A. C. Wall, *Reconstruction of bulk operators within the entanglement wedge in gauge-gravity duality*, arXiv:1601.05416.

[83] D. Harlow, *The ryu-takayanagi formula from quantum error correction*, arXiv:1607.03901.

[84] J. Cotler, P. Hayden, G. Penington, G. Salton, B. Swingle and M. Walter, *Entanglement wedge reconstruction via universal recovery channels*, arXiv:1704.05839.

[85] A. Almheiri, A. Mousatov and M. Shyani, *Escaping the interiors of pure boundary-state black holes*, 1803.04434.

[86] D. Friedan and A. Konechny, *On the boundary entropy of one-dimensional quantum systems at low temperature*, arXiv:hep-th/0312197.

[87] R.-X. Miao, C.-S. Chu and W.-z. Guo, *A new proposal for holographic bcft*, *Journal of High Energy Physics* **2017** (01, 2017) .

[88] R.-X. Miao, *Holographic BCFT with Dirichlet Boundary Condition*, *JHEP* **02** (2019) 025, [1806.10777].

[89] A. Faraji Astaneh and S. N. Solodukhin, *Holographic calculation of boundary terms in conformal anomaly*, *Phys. Lett. B* **769** (2017) 25–33, [1702.00566].

[90] M. Nozaki, T. Takayanagi and T. Ugajin, *Central Charges for BCFTs and Holography*, *JHEP* **06** (2012) 066, [1205.1573].

[91] G. Hayward, *Gravitational action for spacetimes with nonsmooth boundaries*, *Phys. Rev. D* **47** (Apr, 1993) 3275–3280.

[92] I. Kourkoulou and J. Maldacena, *Pure states in the SYK model and nearly-AdS_2 gravity*, 1707.02325.

[93] S. W. Hawking, *Particle Creation by Black Holes*, *Commun. Math. Phys.* **43** (1975) 199–220.

[94] S. W. Hawking, *Breakdown of predictability in gravitational collapse*, *Phys. Rev. D* **14** (Nov, 1976) 2460–2473.

[95] K. Hashimoto, N. Iizuka and Y. Matsuo, *Islands in schwarzschild black holes*, arXiv:2004.05863.

[96] X. Wang, R. Li and J. Wang, *Islands and page curves of reissner-nordström black holes*, arXiv:2101.06867.

[97] G. K. Karananas, A. Kehagias and J. Taskas, *Islands in linear dilaton black holes*, arXiv:2101.00024.

[98] B. Ahn, S.-E. Bak, H.-S. Jeong, K.-Y. Kim and Y.-W. Sun, *Islands in charged linear dilaton black holes*, arXiv:2107.07444.

[99] W. Kim and M. Nam, *Entanglement entropy of asymptotically flat non-extremal and extremal black holes with an island*, arXiv:2103.16163.

[100] M. Alishahiha, A. F. Astaneh and A. Naseh, *Island in the presence of higher derivative terms*, arXiv:2005.08715.

[101] H. Z. Chen, R. C. Myers, D. Neuenfeld, I. A. Reyes and J. Sandor, *Quantum Extremal Islands Made Easy, Part I: Entanglement on the Brane*, *JHEP* **10** (2020) 166, [2006.04851].

[102] H. Z. Chen, R. C. Myers, D. Neuenfeld, I. A. Reyes and J. Sandor, *Quantum extremal islands made easy, part ii: Black holes on the brane*, *JHEP* **12** (2020) 025, [2010.00018].

[103] J. Hernandez, R. C. Myers and S.-M. Ruan, *Quantum extremal islands made easy, partiii: Complexity on the brane*, arXiv:2010.16398.

[104] G. Grimaldi, J. Hernandez and R. C. Myers, *Quantum extremal islands made easy, part iv: Massive black holes on the brane*, arXiv:2202.00679.

[105] D. Marolf and J. Polchinski, *Gauge/Gravity Duality and the Black Hole Interior*, *Phys. Rev. Lett.* **111** (2013) 171301, [1307.4706].

[106] V. Balasubramanian, M. Berkooz, S. F. Ross and J. Simon, *Black Holes, Entanglement and Random Matrices*, *Class. Quant. Grav.* **31** (2014) 185009, [1404.6198].

[107] T. Faulkner, H. Liu, J. McGreevy and D. Vegh, *Emergent quantum criticality, Fermi surfaces, and AdS(2)*, *Phys. Rev. D* **83** (2011) 125002, [0907.2694].

[108] A. Almheiri and J. Polchinski, *Models of AdS_2 backreaction and holography*, *JHEP* **11** (2015) 014, [1402.6334].

[109] J. Maldacena, D. Stanford and Z. Yang, *Conformal symmetry and its breaking in two dimensional Nearly Anti-de-Sitter space*, *PTEP* **2016** (2016) 12C104, [1606.01857].

[110] J. Engelsöy, T. G. Mertens and H. Verlinde, *An investigation of AdS_2 backreaction and holography*, *JHEP* **07** (2016) 139, [1606.03438].

[111] P. Nayak, A. Shukla, R. M. Soni, S. P. Trivedi and V. Vishal, *On the Dynamics of Near-Extremal Black Holes*, *JHEP* **09** (2018) 048, [1802.09547].

[112] S. S. Gubser, *Breaking an Abelian gauge symmetry near a black hole horizon*, *Phys. Rev. D* **78** (2008) 065034, [0801.2977].

[113] S. A. Hartnoll, C. P. Herzog and G. T. Horowitz, *Building a Holographic Superconductor*, *Phys. Rev. Lett.* **101** (2008) 031601, [0803.3295].

[114] M. Ammon and J. Erdmenger, *Gauge/gravity duality: Foundations and applications*. Cambridge University Press, Cambridge, 4, 2015.

[115] H. W. Lin, J. Maldacena and Y. Zhao, *Symmetries Near the Horizon*, *JHEP* **08** (2019) 049, [1904.12820].

[116] D. Marolf, H. Maxfield, A. Peach and S. F. Ross, *Hot multiboundary wormholes from bipartite entanglement*, *Class. Quant. Grav.* **32** (2015) 215006, [1506.04128].

[117] M. Fujita, T. Takayanagi and E. Tonni, *Aspects of AdS/BCFT*, *JHEP* **11** (2011) 043, [1108.5152].

[118] L. Randall and R. Sundrum, *A Large mass hierarchy from a small extra dimension*, *Phys. Rev. Lett.* **83** (1999) 3370–3373, [hep-ph/9905221].

[119] L. Randall and R. Sundrum, *An Alternative to compactification*, *Phys. Rev. Lett.* **83** (1999) 4690–4693, [hep-th/9906064].

[120] A. Karch and L. Randall, *Locally localized gravity*, *JHEP* **05** (2001) 008, [hep-th/0011156].

[121] K. Skenderis and S. N. Solodukhin, *Quantum effective action from the AdS / CFT correspondence*, *Phys. Lett. B* **472** (2000) 316–322, [hep-th/9910023].

[122] D. R. Brill, *Multi - black hole geometries in (2+1)-dimensional gravity*, *Phys. Rev. D* **53** (1996) 4133–4176, [gr-qc/9511022].

[123] S. Aminneborg, I. Bengtsson, D. Brill, S. Holst and P. Peldan, *Black holes and wormholes in (2+1)-dimensions*, *Class. Quant. Grav.* **15** (1998) 627–644, [gr-qc/9707036].

[124] K. Krasnov, *Holography and Riemann surfaces*, *Adv. Theor. Math. Phys.* **4** (2000) 929–979, [hep-th/0005106].

[125] K. Krasnov, *Black hole thermodynamics and Riemann surfaces*, *Class. Quant. Grav.* **20** (2003) 2235–2250, [gr-qc/0302073].

[126] K. Skenderis and B. C. van Rees, *Holography and wormholes in 2+1 dimensions*, *Commun. Math. Phys.* **301** (2011) 583–626, [0912.2090].

[127] V. Balasubramanian, P. Hayden, A. Maloney, D. Marolf and S. F. Ross, *Multiboundary Wormholes and Holographic Entanglement*, *Class. Quant. Grav.* **31** (2014) 185015, [1406.2663].

[128] H. Maxfield, *Entanglement entropy in three dimensional gravity*, *JHEP* **04** (2015) 031, [1412.0687].

[129] Z. Fu and D. Marolf, *Bag-of-gold spacetimes, Euclidean wormholes, and inflation from domain walls in AdS/CFT*, *JHEP* **11** (2019) 040, [1909.02505].

[130] C.-F. Chen, G. Penington and G. Salton, *Entanglement Wedge Reconstruction using the Petz Map*, *JHEP* **01** (2020) 168, [1902.02844].

[131] A. Almheiri, *Holographic Quantum Error Correction and the Projected Black Hole Interior*, 1810.02055.

[132] V. Balasubramanian, A. Kar, O. Parrikar, G. Sárosi and T. Ugajin, *Geometric secret sharing in a model of Hawking radiation*, *JHEP* **01** (2021) 177, [2003.05448].

[133] P. Betzios, E. Kiritsis and O. Papadoulaki, *Euclidean Wormholes and Holography*, *JHEP* **06** (2019) 042, [1903.05658].

[134] B. Freivogel, V. Godet, E. Morvan, J. F. Pedraza and A. Rotundo, *Lessons on eternal traversable wormholes in AdS*, *JHEP* **07** (2019) 122, [1903.05732].

[135] C. Waddell, *Bottom-up holographic models for cosmology*, 2203.03096.

[136] P. Simidzija and M. Van Raamsdonk, *Holo-ween*, *JHEP* **12** (2020) 028, [2006.13943].

[137] C. Bachas and V. Papadopoulos, *Phases of Holographic Interfaces*, *JHEP* **04** (2021) 262, [2101.12529].

[138] D. Harlow and J.-q. Wu, *Algebra of diffeomorphism-invariant observables in Jackiw-Teitelboim Gravity*, 2108.04841.